NASA TECHNICAL MEMORANDUM

NASA TM X-64948

THE MOTION OF THROW AWAY DETECTORS RELATIVE TO THE SPACE SHUTTLE

By Larry D. Mullins
Systems Analysis and Integration Laboratory

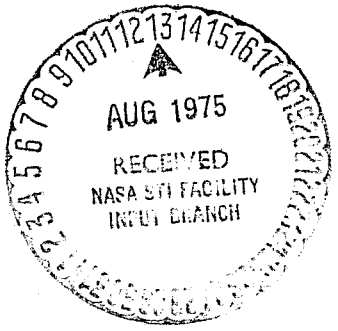

June 30, 1975

NASA

George C. Marshall Space Flight Center
Marshall Space Flight Center, Alabama

TECHNICAL REPORT STANDARD TITLE PAGE

1. REPORT NO.	2. GOVERNMENT ACCESSION NO.	3. RECIPIENT'S CATALOG NO.
NASA TM X-64948		

4. TITLE AND SUBTITLE	5. REPORT DATE
The Motion of Throw Away Detectors Relative to the Space Shuttle	June 30, 1975
	6. PERFORMING ORGANIZATION CODE
7. AUTHOR(S)	8. PERFORMING ORGANIZATION REPORT #
Larry D. Mullins	
9. PERFORMING ORGANIZATION NAME AND ADDRESS	10. WORK UNIT NO.
George C. Marshall Space Flight Center Marshall Space Flight Center, Alabama 35812	11. CONTRACT OR GRANT NO.
	13. TYPE OF REPORT & PERIOD COVERED
12. SPONSORING AGENCY NAME AND ADDRESS	Technical Memorandum
National Aeronautics and Space Administration Washington, D.C. 20546	14. SPONSORING AGENCY CODE

15. SUPPLEMENTARY NOTES

Prepared by Systems Analysis and Integration Laboratory, Science and Engineering

16. ABSTRACT

The motions of Throw Away Detectors (TAD's) are analyzed using the linearized relative motion equations. This work is in support of the AMPS program where the TAD's are to be used as diagnostic instruments for making various measurements near the Shuttle. The TAD's are ejected from the Shuttle in arbitrary directions with small relative velocities (0.1 to 1.0 m/s) and their subsequent trajectories relative to the Shuttle are analyzed. Those initial conditions that are likely to result in recontact between the TAD and the Shuttle are identified. The sensitivity of the motion to variations in the initial conditions, possibly resulting from inaccuracy in the ejection mechanism, are analyzed as are effects of atmospheric drag. A targeting method, a method of giving the TAD correct initial conditions such that it will pass through a given point relative to the Shuttle at a given time, is developed. The results of many specific cases are presented in graphical form.

17. KEY WORDS	18. DISTRIBUTION STATEMENT
TAD's, AMPS, Relative Motion, Free Flyers, Orbital Mechanics	Unclassified – Unlimited for Larry D. Mullins

19. SECURITY CLASSIF. (of this report)	20. SECURITY CLASSIF. (of this page)	21. NO. OF PAGES	22. PRICE
Unclassified	Unclassified	134	NTIS

TABLE OF CONTENTS

LIST OF ILLUSTRATIONS

LIST OF ILLUSTRATIONS (Continued)

LIST OF ILLUSTRATIONS (Continued)

LIST OF ILLUSTRATIONS (Continued)

LIST OF ILLUSTRATIONS (Concluded)

TECHNICAL MEMORANDUM X-64948

THE MOTION OF THROW AWAY DETECTORS RELATIVE TO THE SPACE SHUTTLE

I. INTRODUCTION

This report documents the results of a study of the motion of TAD's relative to the Space Shuttle. It was done in support of the AMPS program. A TAD is a Throw Away Detector – a small, inexpensive, expendable satellite that has no guidance, control, or navigation capability and no propulsive capability. A TAD may be spin stabilized. The TAD's will probably be ejected from the Shuttle by a spring device with a very small impulsive velocity on the order of 1 m/s.

The TAD's may be utilized as diagnostic tools in the AMPS program to examine the electromagnetic interference environment around the Shuttle and to sample the gas contaminants emitted by the Shuttle. They may also be used to measure the perturbations induced by the Shuttle in the ionosphere, i.e., for plasma wake and sheath measurements. There are probably other applications also. The maximum range expected to be utilized by the TAD's will probably be approximately 10 km and in many cases the region of interest may be less than 1 km from the Shuttle.

Once the TAD's are ejected from the Shuttle, the experimenter has no more control over their motion; thus, the only control over their motion is through the ejection conditions. Those conditions must be chosen so as to make the TAD's execute the desired motion to the extent possible. The ejection must also be designed to avoid recontact between the TAD and the Shuttle.

In this report, we shall be concerned with determining: (1) what relative motions are possible with the TAD's, (2) the sensitivity of the motion to the ejection conditions, (3) how to avoid recontact, and (4) how the drag force affects the relative motion. We shall not be concerned with hardware, e.g., with designing a spring ejection device, nor shall we be concerned with communications problems between the TAD's and the Shuttle. These problems must be covered under separate studies.

A method is developed that enables one to target a TAD to a specific point at a given time. A method is also developed that allows one to map specified allowable errors at the target point back into allowable errors in the ejection conditions. This allows one to determine how accurately the ejection mechanism must be built.

It is shown that the motion of a TAD thrown out on the left side of the Shuttle is the "mirror-image" of the motion of a TAD thrown out on the right side; thus, the analysis of the motion has to be made only for ejections on one side.

The targeting capability allows one to examine whatever point or points may be of interest. The only limitation to the number of points examined will be the number of TAD's available because, in general, it will require a separate TAD for each individual point (unless the TAD's are recovered and reused).

Finally, the effects that an uncertainty in the differential drag might have on the targeting problem are examined. It is demonstrated that the effects are small at high altitudes but not at low altitudes.

Most of the results are presented in rather general or parametric form. This was necessary because the AMPS program is still in a formative stage and no specific application has yet been defined. It is believed that the techniques presented here are, for the most part, developed to the extent that they may be directly applied to any specific case.

II. FORMULATION OF THE PROBLEM: THE MOTION OF ONE FREE PARTICLE RELATIVE TO ANOTHER IN AN INVERSE SQUARE GRAVITY FIELD IN THE PRESENCE OF ATMOSPHERIC DRAG

In this section the problem of relative motion, i.e., the motion of one orbiting particle relative to another, is formulated and solved by making certain approximations such as neglecting second-order small quantities. There is nothing new about the development; it has been known for at least 15 years [1]. It is included in this report in order to make it self-contained and to make clear the assumptions made in arriving at the solutions.

Consider a Shuttle orbiting the Earth in a circular orbit of radius R. Establish a local coordinate system at the center of mass of the Shuttle with y positive up along the local vertical, x in the orbit plane with the positive direction opposite the orbital velocity vector, and z perpendicular to the orbit plane and positive in the direction of the orbital angular momentum vector as shown in Figure 1. A TAD may be located at $\vec{\rho}$ relative to the center of the Earth and at $\vec{r}$ relative to the Shuttle.

By definition, the vectors $\vec{r}$, $\vec{R}$, and $\vec{\rho}$ are related by

$$\vec{\rho} = \vec{R} + \vec{r} \quad . \tag{2-1}$$

Clearly, the coordinate system just described is a rotating one, rotating at the orbital rate ω of the Shuttle. The rotational rate ω is related to the orbital radius R by the classical two-body result

$$\omega^2 R^3 = \mu \quad , \tag{2-2}$$

where μ is the product of the universal gravitational constant and the mass of the Earth. This relation will prove useful shortly.

To formulate the equations of motion of a particle, an expression for the acceleration of its position vector must be obtained and then, according to the Newtonian scheme, this must be equated to the forces acting on the particle divided by the mass of the particle. From fundamental considerations [2] the time derivative of a vector in an inertial system is related to the time derivative of the same vector in a rotating system by the relation

$$\dot{\vec{\rho}} = [\dot{\vec{\rho}}] + \vec{\omega} \times \vec{\rho} = \left\{ \left[\frac{d}{dt} \right] + \vec{\omega} \times \right\} \vec{\rho} \quad , \tag{2-3}$$

where $\dot{\vec{\rho}}$ represents the velocity of the particle in the inertial system, $[\dot{\vec{\rho}}]$ represents the velocity of the particle in the rotating system, and $\vec{\omega}$ is the angular velocity of the rotating system. In this application the orbital rate of the Shuttle is given by equation (2-2). A second application of the operator listed in equation (2-3) gives the acceleration of $\vec{\rho}$; namely,

$$\ddot{\vec{\rho}} = [\ddot{\vec{\rho}}] + [\dot{\vec{\omega}}] \times \vec{\rho} + 2\vec{\omega} \times [\dot{\vec{\rho}}] + \vec{\omega} \times (\vec{\omega} \times \vec{\rho}) \quad . \tag{2-4}$$

The second, third, and fourth terms on the right side of equation (2-4) are referred to as the transverse force, the coriolis force, and the centrifugal force, respectively.

If the Shuttle is moving in a circular orbit, $\vec{\omega}$ is constant and $\dot{\vec{\omega}}$ is zero. This makes the second term on the right side of equation (2-4) vanish. We shall make this assumption for this study.

Equation (2-4) is expressed in terms of $\vec{\rho}$. For the relative motion analyses it needs to be expressed in terms of $\vec{r}$. This is easily accomplished by using equation (2-1). Differentiating equation (2-1) with respect to time yields

$$\dot{\vec{\rho}} = \dot{\vec{R}} + \dot{\vec{r}} \quad . \tag{2-5}$$

Applying the operator listed in equation (2-3) to all terms yields

$$[\dot{\vec{\rho}}] + \vec{\omega} \times \vec{\rho} = [\dot{\vec{R}}] + \vec{\omega} \times \vec{R} + [\dot{\vec{r}}] + \vec{\omega} \times \vec{r} \quad . \tag{2-6}$$

Since the Shuttle is in a circular orbit, R is constant so that $[\dot{\vec{R}}]$, the velocity of $\vec{R}$ in the rotating system, is zero. The second and fourth terms on the right side of equation (2-6) can be combined by application of equation (2-1), and the combined term then cancels the second term on the left side to finally yield

$$[\dot{\vec{\rho}}] = [\dot{\vec{r}}] \quad . \tag{2-7}$$

Similarly, it can be shown that

$$[\ddot{\vec{\rho}}] = [\ddot{\vec{r}}] \quad . \tag{2-8}$$

With these results, equation (2-4) can be rewritten as

$$\ddot{\vec{\rho}} = [\ddot{\vec{r}}] + 2\vec{\omega} \times [\dot{\vec{r}}] + \vec{\omega} \times (\vec{\omega} \times \vec{\rho}) \quad . \tag{2-9}$$

By Newton's Second Law, the inertial acceleration of the TAD, $\ddot{\vec{\rho}}$, can be replaced by the force per unit mass acting on the TAD. Two forces are considered, the inverse square Newtonian gravity and the drag due to the atmosphere. Some rather tortuous logic is required to arrive at the next point, which is that the force acting on the TAD is the inverse square gravitational force plus the differential drag force or the difference in the drag force between the TAD and the Shuttle.

Differentiating equation (2-1) twice yields

$$\ddot{\vec{\rho}} = \ddot{\vec{R}} + \ddot{\vec{r}} \tag{2-10}$$

and by Newton's Second Law

$$(\vec{F}/m)_{TAD} = (\vec{F}/m)_{Shuttle} + \Delta(\vec{F}/m) \quad . \tag{2-11}$$

The interpretation of the last term is that if there is an acceleration of the relative position between the TAD and the Shuttle, there must be a differential force between them. Unit masses can be considered for the moment to eliminate m from equation (2-11), and the forces originating from gravity and drag can be written as

$$\vec{F}_{T_g} + \vec{F}_{T_D} = \vec{F}_{S_g} + \vec{F}_{S_D} + \left[\left(\vec{F}_{T_g} - \vec{F}_{S_g}\right) + \left(\vec{F}_{T_D} - \vec{F}_{S_D}\right)\right] \quad . \tag{2-12}$$

Now R and ω can be approximated as constants which means, in effect, that the effects of drag on the Shuttle are ignored; hence, the second term on the right side of equation (2-12) is dropped. It is not, however, ignored in the last term; instead the last two terms are written as

$$\vec{F}_{T_D} - \vec{F}_{S_D} = \Delta\vec{F}_D = \vec{D} \quad . \tag{2-13}$$

The justification for dropping $\vec{F}_{S_D}$ in one place and leaving it in another is that the net result of the drag force on one vehicle for a short time may be small but the result of the difference in drag between two vehicles may be significant.

The first and fourth terms on the right side of equation (2-12) cancel leaving

$$\vec{F}_{T_g} + \vec{F}_{T_D} = \vec{F}_{T_g} + \Delta\vec{F}_D = \vec{F}_{T_g} + \vec{D} \quad . \tag{2-14}$$

This is the desired result; namely, that the force on the TAD is the inverse square gravity force plus the differential drag force. Thus, we can write

$$\ddot{\vec{\rho}} = \vec{F}_{T_g} + \vec{D} = \frac{-\mu\vec{\rho}}{\rho^3} + \vec{D} \quad . \tag{2-15}$$

This is substituted into equation (2-9) which is then solved for $[\ddot{\vec{r}}]$. The result is

$$[\ddot{\vec{r}}] = \frac{-\mu\vec{\rho}}{\rho^3} + \vec{D} - 2\vec{\omega} \times [\dot{\vec{r}}] - \vec{\omega} \times (\vec{\omega} \times \vec{\rho}) \quad . \tag{2-16}$$

It can be verified, by direct multiplication, that the last two terms in equation (2-16) have no z-component. Only the first term on the right side has a z-component (since the differential drag $\vec{D}$ is taken to be opposite the velocity vector and, therefore, along x). This can be equated to the z-component on the left side to obtain

$$\ddot{z} = -\frac{\mu z}{\rho^3} \quad . \tag{2-17}$$

Equation (2-16) can be written again as it stands, but with no z-component in any term; it must now be interpreted as being two dimensional

$$[\ddot{\vec{r}}] = -\frac{\mu\vec{\rho}}{\rho^3} + \vec{D} - 2\vec{\omega} \times [\dot{\vec{r}}] - \vec{\omega} \times (\vec{\omega} \times \vec{\rho}) \quad . \tag{2-18}$$

In two dimensions the last term can be written as $\omega^2\vec{\rho}$. This can be verified by direct multiplication. This can be combined with the first term, where μ can be replaced by equation (2-2), to yield

$$[\ddot{\vec{r}}] = \omega^2\vec{\rho}\left(1 - \frac{R^3}{\rho^3}\right) + \vec{D} - 2\vec{\omega} \times [\dot{\vec{r}}] \quad . \tag{2-19}$$

An expression is now developed for $1/\rho$. By definition

$$\vec{\rho} = \vec{r} + \vec{R} \quad ,$$

so that

$$\rho^2 = \bar{\rho} \cdot \bar{\rho} = (\vec{r} + \bar{R}) \cdot (\bar{r} + \bar{R}) = r^2 + 2rR\cos\theta' + R^2 \quad . \tag{2-20}$$

This last relation can be verified by referring to Figure 1. From equation (2-20) one can get

$$\frac{1}{\rho} = \frac{1}{R}\left[1 - 2\left(\frac{r}{R}\right)(-\cos\theta') + \left(\frac{r}{R}\right)^2\right]^{-1/2} \quad . \tag{2-21}$$

The radical is recognized as the generating function for the Legendre polynomials, $P_n(-\cos\theta')$, so that

$$\frac{1}{\rho} = \frac{1}{R}\sum_{n=0}^{\infty} P_n(-\cos\theta')\left(\frac{r}{R}\right)^n \quad . \tag{2-22}$$

The ratio (r/R) is a small quantity, so to first order in this small quantity,

$$\frac{1}{\rho} = \frac{1}{R}\left[1 - \cos\theta'\left(\frac{r}{R}\right)\right] \quad . \tag{2-23}$$

If the cube of equation (2-23) is taken and first-order small quantities are retained, one then obtains

$$\frac{1}{\rho^3} = \frac{1}{R^3}\left[1 - 3\cos\theta'\left(\frac{r}{R}\right)\right] \quad . \tag{2-24}$$

This result substituted into equation (2-19) will yield

$$\ddot{\vec{r}} = \omega^2\vec{\rho}\left(3\cos\theta'\cdot\frac{r}{R}\right) + \vec{D} - 2\vec{\omega} \times [\dot{\vec{r}}] \quad . \tag{2-25}$$

By inspection of Figure 1 it can be seen that

$$r\cos\theta' = y \quad ,$$

so that equation (2-25) becomes

$$\ddot{\vec{r}} = 3\omega^2 y\frac{\vec{\rho}}{R} + \vec{D} - 2\vec{\omega} \times [\dot{\vec{r}}] \quad . \tag{2-26}$$

Since $\vec{\rho}$ is now two-dimensional, as it has been since equation (2-18), one can write

$$\frac{\vec{\rho}}{R} = \frac{\hat{i}x + \hat{j}(y + R)}{R} = \hat{i}\left(\frac{x}{R}\right) + \hat{j}\left(1 + \frac{y}{R}\right) \quad . \tag{2-27}$$

Again x/R and y/R are very small quantities compared to 1 (about 10^{-3}) so one can approximate $\vec{\rho}/R$ by $\hat{j}$ so that equation (2-26) becomes [this approximation is very important to the further development of the equations since it linearizes them]

$$[\ddot{\vec{r}}] = 3\omega^2 y(\hat{j}) + \vec{D} - 2\vec{\omega} \times [\dot{\vec{r}}] \quad . \tag{2-28}$$

D can be taken to be of constant magnitude and opposite the velocity vector, i.e., in the +x direction. Multiplying out the last term yields

$$\hat{i}\ddot{x} + \hat{j}\ddot{y} = (3\omega^2 y)\hat{j} + (D)\hat{i} + (2\omega\dot{y})\hat{i} + (-2\omega\dot{x})\hat{j} \quad . \tag{2-29}$$

Equating components of the unit vectors yields

$$\begin{aligned} \ddot{x} &= D + 2\omega\dot{y} \\ \ddot{y} &= 3\omega^2 y - 2\omega\dot{x} \quad . \end{aligned} \tag{2-30}$$

These are two second-order linear differential equations with constant coefficients that can be solved with relative ease. They are coupled in the sense that the x-motion affects the y-motion and vice versa.

In the z-equation (2-17) one can replace μ by $\omega^2 R^3$ from equation (2-2) and then approximate $(R/\rho)^3$ by 1 to get

$$\ddot{z} + \omega^2 z = 0 \quad . \tag{2-31}$$

The z-motion is simply that of a harmonic oscillator with the frequency equal to the orbital rate; i.e., it completes one oscillation in one orbital period. In arriving at the z-equation a first-order small quantity (y/R) was ignored. The same was done in equation (2-27). These made possible the linearization of the differential equations that are then solvable in closed form.

A great deal of experience with these equations indicates that they are quite good at least for short time periods or where the TAD's do not drift too far away from the Shuttle in the vertical direction. Most of the neglected terms are at least 10^{-3} times the terms that were retained.

The great value of these equations is that no numerical integration is required to analyze the motion of the TAD's. In summary, the following assumptions were made to arrive at these equations:

- The Shuttle is in a circular orbit ($\dot{\omega} = 0$).
- The Shuttle orbit is unaffected by drag (ω and R remain constant).
- The differential drag force D is constant and opposite V.

- The gravity field is inverse square (oblateness is neglected).
- Second-order small quantities are neglected in the expansion of $1/\rho$.
- First-order small quantities (10^{-3} compared to 1) are neglected in linearizing the differential equations.

If any of these assumptions should be grossly violated, the resulting equations, i.e. (2-30) and (2-31), most likely would be invalidated. For example, if the Shuttle should be in a highly elliptical orbit, then $\dot{\bar{\omega}}$ would not be zero and could not be ignored in equation (2-4). Other violations of the assumptions can be easily determined.

The solutions of these equations are obtained rather easily. The solution to the z-equation (2-31) can be written as

$$z = A \cos \omega t + B \sin \omega t \tag{2-32}$$

and if at $t = 0$, $z = z_0$ and $\dot{z} = \dot{z}_0$, the constants A and B are $A = z_0$ and $B = \dot{z}_0/\omega$; therefore, the solution is

$$\begin{aligned} z &= z_0 \cos \omega t + \dot{z}_0/\omega \sin \omega t \\ \dot{z} &= -\omega z_0 \sin \omega t + \dot{z}_0 \cos \omega t \quad . \end{aligned} \tag{2-33}$$

Equations (2-30) can be solved in various ways. In the method chosen here they are converted to four first-order equations by the following change of variables:

$$\begin{aligned} x_1 &= x \\ x_2 &= y \\ x_3 &= \dot{x} \\ x_4 &= \dot{y} \quad . \end{aligned} \tag{2-34}$$

The differential equations then become

$$\begin{pmatrix} \dot{x}_1 \\ \dot{x}_2 \\ \dot{x}_3 \\ \dot{x}_4 \end{pmatrix} = \begin{pmatrix} 0 & 0 & 1 & 0 \\ 0 & 0 & 0 & 1 \\ 0 & 0 & 0 & 2\omega \\ 0 & 3\omega^2 & -2\omega^2 & 0 \end{pmatrix} \begin{pmatrix} x_1 \\ x_2 \\ x_3 \\ x_4 \end{pmatrix} + \begin{pmatrix} 0 \\ 0 \\ D \\ 0 \end{pmatrix} , \qquad (2\text{-}35)$$

or compactly as

$$\dot{\vec{x}} = A\vec{x} + B \qquad (2\text{-}36)$$

with the solution [3]

$$\vec{x}(t) = e^{At}\left[\vec{x}(t_0) + \int_{t_0}^{t} e^{-A\tau}B d\tau\right] . \qquad (2\text{-}37)$$

A is, of course, the 4 X 4 matrix defined in equation (2-35) and e^{At} is defined as

$$e^{At} = I + At + \frac{A^2t^2}{2!} + \ldots . \qquad (2\text{-}38)$$

For simple matrices, and in this case in particular, equation (2-38) can be used as a computational technique for e^{At}. By direct multiplication and summing of the elements, e^{At} can be verified to be

$$e^{At} = \begin{pmatrix} 1 & 6\omega t - 6\sin\omega t & 4/\omega \sin\omega t - 3t & 2/\omega(1 - \cos\omega t) \\ 0 & 4 - 3\cos\omega t & -2/\omega(1 - \cos\omega t) & 1/\omega \sin\omega t \\ 0 & 6\omega(1 - \cos\omega t) & 4\cos\omega t - 3 & 2\sin\omega t \\ 0 & 3\omega \sin\omega t & -2\sin\omega t & \cos\omega t \end{pmatrix} . \qquad (2\text{-}39)$$

Then e^{-At} can be obtained simply by replacing t by $-t$. If t_0 is chosen as zero and all of the manipulations implied in equation (2-37) are carried out, the solutions can be verified to be

$$x = x_0 + c_0 t - \frac{3}{2} Dt^2 - 2b_0 \sin \omega t + 2a_0(1 - \cos \omega t)$$

$$y = \frac{2c_0}{3\omega} - \frac{2Dt}{\omega} - b_0 \cos \omega t + a_0 \sin \omega t$$

$$\dot{x} = c_0 - 3Dt - 2\omega b_0 \cos \omega t + 2\omega a_0 \sin \omega t$$

$$\dot{y} = -\frac{2D}{\omega} + \omega b_0 \sin \omega t + \omega a_0 \cos \omega t \quad , \tag{2-40}$$

where

$$a_0 = \frac{\dot{y}_0}{\omega} + \frac{2D}{\omega^2}$$

$$b_0 = 3y_0 - \frac{2\dot{x}_0}{\omega}$$

$$c_0 = 6\omega y_0 - 3\dot{x}_0 \quad . \tag{2-41}$$

Equations (2-33) and (2-40) combined with the initial conditions (x_0, y_0, z_0, $\dot{x}_0$, $\dot{y}_0$, $\dot{z}_0$, ω, and D) completely determine the motion of a TAD relative to the Shuttle.

III. INITIALIZATION OF THE MOTION: THE ORBITAL RATE, THE DIFFERENTIAL DRAG, AND THE EJECTION CONDITIONS

The orbital rate ω appearing in the relative motion equations depends only on the orbital radius R of the Shuttle, which is the radius of the earth R_E plus the altitude of the Shuttle orbit. It is given by equation (2-2) or

$$\omega = \sqrt{\mu/R^3} \quad , \tag{3-1}$$

where $\mu = 3.986012 \times 10^{14}$ m^3/s^2.

The differential drag D appearing in the relative motion equations is the difference in drag between the TAD and the Shuttle and is given by

$$D = \frac{1}{2}\rho v^2 \left[\left(\frac{C_D A}{m} \right)_{TAD} - \left(\frac{C_D A}{m} \right)_{Shuttle} \right] \quad . \tag{3-2}$$

In this equation ρ is the atmospheric density and v is the orbital speed, assumed here to be the same for the Shuttle and TAD since they are in nearly the same orbit. For circular orbits, there exists the simple result

$$v^2 = \frac{\mu}{R} \quad . \tag{3-3}$$

The quantity $(C_D A/m)$ is the ballistic coefficient of the object, C_D is the coefficient of drag with a typical value of approximately 2, A is the effective cross-sectional area presented to the resisting medium, and m is the mass of the object. From equation (3-2), it is seen that a differential drag exists only if there is a difference in the ballistic coefficients of the TAD and the Shuttle.

The speed used in equation (3-2) should be the differential speed between the orbiting vehicle and the rotating atmosphere. The error caused by using the inertial speed however is slight and can be offset if necessary by "fudging" some other parameter, for example C_D or A.

The ballistic coefficient of the Shuttle depends on its attitude and on the altitude of its orbit. At altitudes near 400 km the ballistic coefficient varies in the range

$$0.002 \frac{m^2}{kg} \leqslant \beta_{Shuttle} \leqslant 0.009 \frac{m^2}{kg} \quad . \tag{3-4}$$

because of attitude variations. For this study, the TAD's are represented by 45.7 cm (18 in.) spheres weighing 22.7 kg (50 lb). The effective cross-sectional area is assumed to be a circle of 45.7 cm (18 in.) diameter, giving $A = 0.164\ m^2$. The coefficient of drag is taken to be 2. For the ballistic coefficient, this gives

$$\beta_{TAD} = \left(\frac{C_D A}{m} \right)_{TAD} = 0.0145 \frac{m^2}{kg} \quad . \tag{3-5}$$

An intermediate value of the ballistic coefficient of the Shuttle between the two limits listed in equation (3-4) is taken. The intermediate value is taken as 0.0045 m^2/kg so that the difference is a convenient number for computations,

$$\left[\left(\frac{C_D A}{m}\right)_{TAD} - \left(\frac{C_D A}{m}\right)_{Shuttle}\right] = \left[0.0145 \frac{m^2}{kg} - 0.0045 \frac{m^2}{kg}\right] = 0.01 \frac{m^2}{kg} \quad . \tag{3-6}$$

At 400 km the atmospheric density, according to the 1962 U. S. Standard Atmosphere, is

$$\rho_{400} \simeq 6.5 \times 10^{-12} \frac{kg}{m^3} \quad . \tag{3-7}$$

The square of the orbital speed at 400 km altitude is

$$v^2 = \frac{\mu}{R} = \frac{3.986012 \times 10^{14} \frac{m^3}{s^2}}{6.778160 \times 10^{6} \text{ m}} = 5.88067 \times 10^{7} \frac{m^2}{s^2} \quad . \tag{3-8}$$

With these values, the differential drag from equation (3-2) is

$$D = 1.9 \times 10^{-6} \frac{m}{s^2} \quad . \tag{3-9}$$

Variations in the attitude of the Shuttle can make this value increase or decrease. Using the maximum and minimum values of the Shuttle ballistic coefficient gives

$$1.05 \times 10^{-6} \frac{m}{s^2} \leqslant D \leqslant 2.4 \times 10^{-6} \frac{m}{s^2} \quad . \tag{3-10}$$

These values could probably be altered considerably by different designs of the TAD's, i.e., by varying their size, shape, and weight. Operating at different altitudes will also vary D through its dependence on atmospheric density.

If the constant difference of ballistic coefficients of the TAD and Shuttle of 0.01 m^2/kg is assumed, then D varies with altitude in the following way:

Altitude (km)	$\rho(kg/m^3)$	$v^2(m^2/s^2)$	$D(m/s^2)$
200	3.3×10^{-10}	6.05946×10^7	1.0×10^{-4}
300	3.6×10^{-11}	5.96873×10^7	1.07×10^{-5}
400	6.5×10^{-12}	5.88067×10^7	1.91×10^{-6}
500	1.6×10^{-12}	5.79517×10^7	4.6×10^{-7}
600	4.6×10^{-13}	5.71212×10^7	1.3×10^{-7}
700	1.5×10^{-13}	5.63142×10^7	4.2×10^{-8}

A plot of the differential drag versus altitude is shown in Figure 2. These values should be taken as order of magnitude values.

It is assumed that the TAD's are carried in the Shuttle bay until some point in the mission, at which time they are ejected impulsively with arbitrary speed and in an arbitrary direction relative to the coordinate system shown in Figure 1. Because of a lack of knowledge of precisely where the TAD's may be located in the Shuttle, it is assumed for this study that they are at the center of mass of the Shuttle, i.e., at the origin of the relative coordinate system. This defines the initial position for the relative motion studies as

$$x_0 = 0$$

$$y_0 = 0$$

$$z_0 = 0 \qquad (3\text{-}11)$$

The direction and magnitude of the initial velocity can be arbitrary. Consider Figure 3 to initialize the velocities.

If the TAD's are ejected from the Shuttle in an arbitrary direction with an arbitrary impulse, then from Figure 3 it can be seen that the initial velocities are given by

$$\dot{x}_0 = \Delta V \cos\theta \sin\varphi$$

$$\dot{y}_0 = \Delta V \sin\theta$$

$$\dot{z}_0 = \Delta V \cos\theta \cos\varphi \qquad (3\text{-}12)$$

These quantities (ω, D, x_0, y_0, z_0, $\dot{x}_0$, $\dot{y}_0$, and $\dot{z}_0$) completely determine the relative motion.

IV. ANALYSIS OF THE MOTION

The equations of motion (2-33) and (2-40) with the initial conditions defined in Section III are

$$x = -3(\Delta V \cos\theta \sin\varphi)t - \frac{3}{2}Dt^2 + \frac{4}{\omega}(\Delta V \cos\theta \sin\varphi)\sin\omega t + 2\left(\frac{\Delta V \sin\theta}{\omega} + \frac{2D}{\omega^2}\right)(1 - \cos\omega t)$$

$$y = -\frac{2}{\omega}(\Delta V \cos\theta \sin\varphi)(1 - \cos\omega t) - \frac{2Dt}{\omega} + \left(\frac{\Delta V \sin\theta}{\omega} + \frac{2D}{\omega^2}\right)\sin\omega t$$

$$z = \frac{1}{\omega}(\Delta V \cos\theta \cos\varphi)\sin\omega t \quad . \tag{4-1}$$

For purposes of discussion a 400 km altitude circular orbit is assumed with

$$\omega = \sqrt{\frac{\mu}{R^3}} = 1.13 \times 10^{-3} \text{ (radians/s)}$$

and

$$\frac{1}{\omega} = 884 \text{ s} \quad .$$

The differential drag D is taken to be

$$D = 1 \times 10^{-6} \text{ m/s}^2 \quad .$$

The z-motion is that of a simple harmonic oscillator with a period equal to the orbital period. The amplitude of the motion is

$$z_{max} = \frac{\Delta V}{\omega}\cos\theta \cos\varphi \quad .$$

If the TAD was kicked out in the z-direction (θ = 0 degree, φ = 0 degree) with an impulse of 1 m/s, the maximum amplitude would be 884 m; if the impulse was 10 m/s, the amplitude would be 8.84 km; and if the impulse was 0.1 m/s, the amplitude would be 88.4 m, etc. If the TAD was kicked striaght up or straight down (θ = 90 degrees or 270 degrees) there would be no z-motion. If the TAD was ejected anywhere in the x-y plane (Fig. 3) where φ = 90 degrees or 270 degrees there would be no z-motion.

The y-equation, the one determining the vertical motion, has a secular term in it, $-2Dt/\omega$. At the altitude considered here, the value of $2D/\omega$ is approximately 2×10^{-3} m/s. This gives a decay rate for the TAD relative to the Shuttle of about 7 m/hour. At an altitude of about 300 km where the drag is an order of magnitude higher, the decay rate would be about 70 m/hour; and at an altitude of 200 km, the decay rate would be about 700 m/hour.

The first and third terms in the y-equation are periodic terms giving rise to an oscillatory motion in the vertical direction. The amplitude of the first term at one-half period is $(4/\omega)\Delta V \cos\theta \sin\varphi$. If θ = 0 degree, φ = 90 degrees, and ΔV = 1 m/s, this term would be approximately 4 km. This amplitude can be suppressed by choosing proper values of θ and φ. The amplitude of the last term is $(\Delta V/\omega) \sin\theta$ which for θ = 90 degrees and ΔV = 1 m/s is approximately 1 km. This too can be suppressed by keeping θ sufficiently far away from 90 degrees or 270 degrees.

The first two terms in the x-equation are secular terms that will monotonically increase or decrease the x-coordinate, i.e., the coordinate in the direction of orbital travel. This will make the TAD get progressively further in front or progressively further behind the Shuttle with increasing time. For small values of t the first term completely dominates the second. Equating the terms enables one to find the approximate time at which they become of the same order of magnitude. This gives

$$t = \frac{2\Delta V \cos\theta \sin\varphi}{D} .$$

For ΔV = 1 m/s, D = 10^{-6} m/s^2, and $2 \cos\theta \sin\varphi = 1$, the above equation gives about 10 days. This means that for most applications, where we are interested in the motion for at most a few hours, the first term is completely dominant. The second term is always in the -x direction or in the direction of the velocity vector. Thus, after it begins to dominate the first term, the x-coordinate will become progressively more negative and the TAD will move out in front of the Shuttle.

The sign of the first term depends on the ejection conditions and can be positive or negative. Thus for the first few days of the motion the x-coordinate can be made positive or negative by proper choice of the initial conditions. The magnitude of the first

term can vary between $\pm 3\Delta V$ which, for a separation velocity of 1 m/s, is ±3 m/s. In 1 min (60 s), this term can be as large as ±180 m. In one orbital period (90 min or 5400 s) this term can be as large as ±16 km. Thus, this term can lead to "run-away" motion in the x-direction if the ejection conditions are not carefully controlled.

If it is desired to keep the TAD within a certain distance of the Shuttle for a certain length of time, for example keep x less than x_{max} for a period of time t_{max}, the following conditions must be imposed on the ejection velocity

$$\Delta V \cos\theta \sin\varphi \leqslant \frac{x_{max}}{3t_{max}} \quad .$$

As a numerical application, suppose that it was desired to keep x less than 1 km for one orbital period. The above relation would yield the maximum value for $\Delta V \cos\theta \sin\varphi$ to be 0.061 m/s. If the ejection velocity was 1 m/s, the product $\cos\theta \sin\varphi$ would have to be 0.061. For φ near 90 degrees or 270 degrees (in-plane ejection), θ must be near 90 degrees or 270 degrees (vertical ejection). For φ near 0 degree or 180 degrees (sidewise ejection), θ could be arbitrary in value.

In summary, to keep the x secular motion in bounds the ejection velocity must be approximately perpendicular to the orbital velocity direction. This is in any direction in or near the y-z plane. If it was required to keep $\cos\theta \sin\varphi \leqslant 0.061$ and if $\theta = 0$ degree, the maximum value of φ would be 3.5 degrees.

The third and fourth terms in the x-equation are oscillatory with a period equal to the orbital period and having the following amplitudes, respectively,

$$\frac{4\Delta V \cos\theta \sin\varphi}{\omega}$$

and

$$\frac{4\Delta V \sin\theta}{\omega} \quad .$$

For separation velocities of 1 m/s these amplitudes can be as large as 4 km. The ejection conditions must be designed to keep them to whatever magnitude is desirable. If the product $\Delta V \cos\theta \sin\varphi$ was kept small to limit the x secular motion, the first amplitude would also be small. Using the previous example where the product $\Delta V \cos\theta \sin\varphi$ was limited to 0.061, the first amplitude listed above would be limited to less than 250 m.

The product $\Delta V \cos\theta \sin\varphi$ could be kept small by choosing φ small. However, θ could still be near 90 degrees and the second amplitude could be as large as 4 km (for separation velocity of 1 m/s). If it is likewise desirable to keep the amplitude of the second term below a certain value x_{max}, the following condition is imposed on θ

$$\theta \leqslant \sin^{-1}\left(\frac{\omega x_{max}}{4\Delta V}\right) \quad .$$

For $x_{max} = 1$ km and $\Delta V = 1$ m/s this gives

$$\theta \leqslant \sin^{-1}\left(\frac{10^{-3} \cdot 10^{+3}}{4 \cdot 1}\right) \leqslant \sin^{-1}(0.25)$$

or

$$\theta \leqslant 15^\circ \quad .$$

To satisfy all of these conditions means that the ejection must be nearly sidewise; φ within ±3.5 degrees of 0 degree or 180 degrees and not far above the local horizontal, $\theta \leqslant \pm 15$ degrees. This condition results from a separation velocity of 1 m/s with the restriction of limiting the motion of the TAD to within a radius of 1 km of the Shuttle for a time of at least one orbital period (90 min).

The first term in the x-equation determines whether the TAD gets progressively in front of or behind the Shuttle. If x is negative, the TAD is in front of the Shuttle; if x is positive, the TAD is behind the Shuttle. If the ejection is in the positive z-direction, then θ is small, for example $\theta \leqslant \pm 15$ degrees, and cos θ is a positive number near 1. φ can be a small positive or negative angle, $\varphi \leqslant \pm 3.5$ degrees, and sin φ will likewise be a small number, positive if φ is positive and negative if φ is negative. If φ is positive (backward ejection), the whole first term is negative and if φ is negative (forward ejection), the whole first term is positive. Thus, if it is desired to put the TAD behind the Spacelab, the ejection must be forward and if it is desired to put the TAD in front of the Spacelab the ejection must be backward.

The coefficients in the y-equation are the same as those in the x-equation so that if the x-motion is kept small, the y-motion will likewise be kept small. The coefficient in the z-equation, however, is different so that it is large for small θ and small φ. The only way then to keep the z-motion small would be to reduce the impulse (ΔV) given to the TAD. An impulse of 1 m/s, however, keeps the z-motion to less than 1 km. If it is desired to keep it to approximately 100 m, the impulse would have to be reduced to about 0.1 m/s.

Another very important aspect to consider in the analysis of the motion of the TAD's is collision or recontact with the Space Shuttle at some time after the ejection. It would seem that these should be avoided even though recontact would be at a relatively slow velocity, i.e., at about whatever velocity the TAD was ejected. A collision is defined as the condition where all of the coordinates (x, y, and z) become simultaneously zero or near zero at some time after ejection. Collisions are avoided by avoiding the ejection conditions that result in this occurrence.

To avoid "run-away" x secular motion or large amplitude x and y oscillatory motion, the ejection will have to be in the sidewise direction as described earlier. For sidewise ejections there is always a z-motion and it has zeroes only at $t = T/2, T, 3T/2, 2T, \ldots$ etc. Thus, to examine the collision possibilities, it is necessary to examine the x and y motions only at half and whole integral periods.

At half-integral periods, $\omega t = \pi, 3\pi, \ldots$ etc., and

$$t = n\frac{T}{2} = \frac{n\pi}{\omega} \quad ; \quad \cos \omega t = -1 \quad ; \quad \sin \omega t = 0 \quad .$$

At these times the x, y, and z coordinates from equations (4-1) are:

$$x\left(\frac{nT}{2}\right) = -3(\Delta V \cos\theta \sin\varphi)\frac{n\pi}{\omega} - \frac{3}{2} D \frac{n^2\pi^2}{\omega^2} + 4\left(\frac{\Delta V \sin\theta}{\omega} + \frac{2D}{\omega^2}\right)$$

$$y\left(\frac{nT}{2}\right) = -\frac{4}{\omega}(\Delta V \cos\theta \sin\varphi) - \frac{2D}{\omega} \cdot \frac{n\pi}{\omega}$$

$$z\left(\frac{nT}{2}\right) = 0 \qquad n = 1, 2, 3 \ldots \quad . \tag{4-2}$$

To find the collision possibilities, these expressions are simultaneously equated to zero. This, then, places certain requirements on the ejection conditions. At a half-integral period y equal to zero requires

$$\Delta V \cos\theta \sin\varphi = -\frac{n\pi D}{2\omega} \qquad n = 1, 3, 5, \ldots \quad . \tag{4-3}$$

For small n (for example 1, 3, or 5) and for altitudes around 400 km where $D \sim 10^{-6}$ m/s^2, the order of magnitude of the right side ranges from 10^{-3} to 10^{-2}. For ΔV's of approximately 1 m/s, the product $\cos\theta \sin\varphi$ must range from 10^{-3} to 10^{-2}. Since

we are dealing with nearly sidewise ejections where $\theta \leqslant 15$ degrees, cos θ is near 1, so that for the product to be small sin φ must be small. If sin φ ranges from 10^{-3} to 10^{-2}, φ ranges from 0.05 degree to 0.5 degree. Thus, φ should be kept larger than 0.5 degree to keep y from becoming zero at half-integral periods.

If the condition (4-3) is substituted into the x-equation of (4-2), the first two terms cancel exactly. If the remaining expression is equated to zero, the resulting condition is

$$\Delta V \sin \theta = -\frac{2D}{\omega} \quad . \tag{4-4}$$

The right side here is of the order of magnitude 10^{-3}. For a ΔV of 1 m/s this requires that θ be very near 0 degree or 180 degrees (horizontal ejection).

Thus, to avoid collisions at half-integral periods, one must avoid exactly sidewise ejections, i.e., straight out the z or -z directions. The direction of the ejection should be at least 0.5 degree from the z-axis, i.e., one should have $|\varphi| \geqslant 0.5$ degree.

At whole integral periods, $\omega t = 2\pi, 4\pi, \ldots$ etc., and

$$t = nT = \frac{2n\pi}{\omega} \quad ; \quad \cos \omega t = +1 \quad ; \quad \sin \omega t = 0 \quad .$$

At these times the x, y, and z coordinates from equations (4-1) are

$$x(nT) = -3(\Delta V \cos \theta \sin \varphi) \cdot \frac{2n\pi}{\omega} - \frac{3}{2} D \frac{4n^2\pi^2}{\omega^2}$$

$$y(nT) = -\frac{2D}{\omega} \cdot \frac{2n\pi}{\omega}$$

$$z(nT) = 0 \qquad n = 1, 2, 3, \ldots \quad . \tag{4-5}$$

The y-equation shows that there is no control, through the ejection conditions, over the y-coordinate at whole orbital periods. In fact, if there is no differential drag, the y-coordinate comes back exactly to zero at every orbital period. At one whole orbital period (n = 1) at an altitude of approximately 400 km where $D \sim 10^{-6}$ m/s^2, y is approximately -10 m. This is uncomfortably close to zero. Collisions will have to be avoided by control of the x-motion. Equating x to zero gives the following condition for the ejection

$$\Delta V \cos\theta \sin\varphi = -\frac{n\pi D}{\omega} \quad . \tag{4-6}$$

This condition is almost the same as that in equation (4-3), certainly of the same order of magnitude. Thus, collisions are avoided at whole integral periods by the same method as they are avoided at half-integral periods; namely, by making the angle φ equal to or larger than 0.5 degree.

If it is desired, at whole integral periods, to keep x larger than some minimum value, equation (4-5) yields

$$x(nT) = -3(\Delta V \cos\theta \sin\varphi) \cdot \frac{2n\pi}{\omega} - \frac{3}{2} D \cdot \frac{4n^2\pi^2}{\omega^2} \geqslant x_{min} \quad .$$

For horizontal ejections, $\theta = 0$ degree and $\cos\theta = 1$; thus, the condition on φ is

$$-\Delta V \sin\varphi \geqslant \frac{\omega x_{min}}{6n\pi} + \frac{n\pi D}{\omega}$$

or

$$\varphi \geqslant \sin^{-1}\left(\frac{\omega^2 x_{min} + 6n^2\pi^2 D}{6n\pi\omega\Delta V}\right) \quad . \tag{4-7}$$

Using typical values of $\omega = 10^{-3}$, $n = 1$, $D = 10^{-6}$, and $\Delta V = 1$ m/s and choosing $x_{min} = 100$ m gives

$$\varphi \geqslant \sin^{-1}(0.01) = 0.5° \quad .$$

The same considerations for a minimum x-value at one-half an orbital period would yield

$$\varphi \geqslant \sin^{-1}\left(\frac{2\omega^2 x_{min} + 3n^2\pi^2 D - 16D}{6n\pi\omega\Delta V}\right) \quad . \tag{4-8}$$

Using approximately the same values gives the same order of magnitude for φ, i.e., approximately 0.5 degree.

The results, so far, can be summarized as follows:

1. To keep the TAD's reasonably close to the Shuttle, within 1 km for example, for at least one orbital period, they must be ejected out the side approximately perpendicular to the orbital velocity vector and within approximately 15 degrees of the local horizontal.

2. To avoid recontact, or collision, exactly sidewise ejections $\varphi = 0$ degree or 180 degrees must be avoided. To keep the TAD's at least 100 m away from the Shuttle on subsequent passes, the value of φ should not be less than 0.5 degree.

Thus, for separation velocities of 1 m/s, the ejection conditions shown in Figure 4 are permissible.

Some examples of relative motions are now presented. Several variations in the initial conditions will be made to show how the motions may be varied or how they may be controlled through proper selection of the initial conditions. All of the motions are shown in the relative coordinate system with origin at the Shuttle: +y is along the local vertical, +x is opposite the velocity vector, and +z is along the orbital angular momentum vector. The motion is three-dimensional. Some two-dimensional cross sections of the motion and a three-dimensional plot are presented.

As a first case four different motions are shown, those of TAD's ejected into each of the quadrants shown in Figure 4. The initial conditions for the four cases are:

Case	θ	φ	ΔV (m/s)
a	+5°	+3.5°	1
b	+5°	-3.5°	1
c	-5°	+3.5°	1
d	-5°	-3.5°	1

Figure 5 shows the x-y projection of the motion for these four cases. The solid portions of the trajectory correspond to $z > 0$, and the dotted portions correspond to $z < 0$. Cases b and d, which are forward ejections (negative φ), have motions which carry the TAD behind the Shuttle, while cases a and c go in front of the Shuttle. This confirms the previous statements. The motions are shown for slightly more than one orbital period. The maximum y-displacement during this time is approximately 200 m and occurs at approximately one-half an orbital period. At the end of one orbital period, y is back to its initial value of zero. x has a secular motion which increases to slightly more than

1 km in one orbital period. In another orbital period the x secular motion would double, in another it would triple, etc. The y-motion however would remain periodic except for a very slight secular decrease caused by the differential drag. At the orbital altitude of this example, 400 km, the differential drag is very small, only about 10^{-6} m/s^2. The motion shown in this projection is what an observer traveling parallel with, but at some distance off to the side of, the Shuttle would see as the TAD's were ejected from the Shuttle in his direction.

Figure 6 shows the x-z projection of the relative motion for the same four cases. This motion is what an observer traveling parallel with, but above, the Shuttle would see as he looked down at the Shuttle as the TAD's were ejected. The solid portions of the trajectories correspond to $y \geq 0$, and the dotted portions correspond to $y < 0$. Again, cases b and d are observed to go behind the Shuttle, while cases a and c go in front of the Shuttle. Case d, which is ejected forward and down (θ = -5 degrees, φ = -3.5 degrees), at first goes down below the Shuttle ($y < 0$) and in front of it. At one-quarter of an orbital period it is about 100 m in front of the Shuttle and approximately 900 m off to the left side (of an observer looking in the direction of orbital travel). At this point it reverses its x-direction of travel and starts in the direction opposite the Shuttle's direction of travel. At the same time y has become positive and comes up above the horizontal plane of the Shuttle's travel. At one-half an orbital period it crosses behind the Shuttle at a distance of about 200 m and, as can be seen from Figure 5, about 200 m above the Shuttle. This TAD continues traveling in the positive x-direction (opposite the Shuttle's direction of travel). At three-fourths of an orbital period, it is behind the Shuttle about 800 m and approximately 900 m off to the right side. At the same time its height above the horizontal plane is about 200 m, as can be verified from Figure 5. At that point its z-motion reverses and it again crosses behind the Shuttle in one orbital period at a distance of about 950 m and at the same altitude as the Shuttle ($y = 0$), as verified by Figure 5. If this plot was continued for another orbital period, the motion would repeat that of the first orbital period except it would be translated behind the Shuttle about 1 km.

The details of the other cases can be determined by inspection of the figures. The maximum z-displacement always occurs at one-quarter of an orbital period, the minimum z-displacement at three-quarters of an orbital period, and the Shuttle orbital plane ($z = 0$) is crossed at half and whole periods. The oscillatory period of the TAD back and forth accross the Shuttle's orbit plane is equal to the orbital period of the Shuttle (approximately 90 min). There is no way to alter this.

Figure 7 shows the y-z projection of the relative motion. This is what an observer traveling at some distance behind the Shuttle would see as the TAD's were ejected from the Shuttle. The solid portions of the trajectories correspond to $x > 0$, and the dotted portions correspond to $x < 0$. The symmetric oscillations back and forth across the orbit plane are obvious from Figure 7, from which it can be seen that the oscillations in y slightly exceed 200 m while those in z are nearly 900 m. The magnitude of these oscillations can be controlled (increased or decreased) by changing the magnitude of the ejection velocity.

The general three-dimensional motion is that of a spiral, although not a very symmetric one. The motion generally spirals away from the Shuttle along the x-axis in either the positive or negative direction, depending on the ejection conditions. The three-dimensional plots make this quite clear. The plots of cases a, b, c, and d above are presented in Figures 8 through 11, respectively. The letter code on these plots indicates in which octant of the relative coordinate system the TAD is located. The dotted line is the projection of the three-dimensional motion onto the x-z plane, i.e., the local horizontal plane.

To illustrate the effect produced by changing the ejection velocity, Figures 12, 13, and 14 are presented. These correspond to Figures 5, 6, and 7 except that the ejection velocity has been reduced to one-tenth its initial value, i.e., from 1 m/s to 0.1 m/s. By comparing the figures, it can be seen that the motions in each case are similar except that the magnitudes have been reduced by approximately a factor of ten. The maximum x-displacement in one orbital period is of the order of 100 m rather than 1 km, the maximum y-value is of the the order of 20 m rather than 200 m, and the maximum z-displacement is about 90 m rather than 900 m.

To illustrate the effect produced by changing the ejection direction Figures 15, 16, and 17 are presented. These correspond to Figures 5, 6, and 7 except that the angle φ has been reduced in magnitude from 3.5 degrees to 1 degree. By comparing the x-y projections, it can be seen that the maximum y-displacement has been reduced from 200 m to 100 m and the maximum x-displacement has been reduced from approximately 1 km to approximately 500 m. The maximum z-displacement is approximately the same, however, at approximately 900 m. Comparing the x-z projections, it can be seen that the net effect produced by reducing φ is to produce tighter spirals in the x-direction.

Figures 18, 19, and 20 correspond to Figures 5, 6, and 7 except that the angle θ has been reduced in magnitude from 5 degrees to 1 degree. The maximum values of x, y, and z are about the same as for the first case. The net result is that cases b and d are moved closer together in space and cases a and c are moved closer together.

To provide more insight into the relative motions, several more variations in the initial conditions are shown. Figures 21, 22, and 23 show the x-y, x-z, and y-z projections for $\Delta V = 1$ m/s and $(\theta, \varphi) = (+10°, +1°), (+10°, -1°), (-10°, +1°), (-10°, -1°)$. These conditions open the spirals considerably, as can be seen, for example, by comparing Figure 22 to Figure 16. φ is the same in both cases, but θ has been doubled in the latter instance. Figures 24, 25, and 26 present similiar cases except that θ has been increased even further to 15 degrees and the spirals continue to open further.

Figures 27, 28, and 29 show cases where φ is held constant at -1 degree and θ is varied at 1, 5, 10, and 15 degrees. This distributes the TAD's at varying distances behind the Shuttle. The four cases cross behind the Shuttle at one-half an orbital period at distances of 200 m, 450 m, 750 m, and 1050 m, respectively. At one orbital period they all sweep behind the Shuttle at the common distance of approximately 250 m providing a good opportunity for contact between two or more of the TAD's. This contact probably would not cause any damage, however, since they all have common velocities such that relative velocities between them would be near zero.

Figures 30, 31, and 32 show cases where θ is held constant at +5 degrees and φ is varied at -3, -1, +1, and +3 degrees. This distributes the TAD's both in front of and behind the Shuttle, although not in a uniform manner. At one-half an orbital period the first three cases cross behind the Shuttle at distances of 750 m, 450 m, and 150 m, respectively, and the fourth case crosses in front of the Shuttle at a distance of slightly more than 100 m. At one orbital period the first two cases cross behind the Shuttle at distances of 800 m and 250 m, respectively, while the last two cases cross in front of the Shuttle at distances of 350 m and 900 m, respectively.

Some interest has been expressed in trying to keep the TAD's exactly in the horizontal plane, i.e., no y-component to the motion. Figures 33, 34, and 35 show cases where the TAD's are ejected in the horizontal plane θ = 0 degree with φ varied at -3, -1, +1, and +3 degrees. Figure 33 shows that although the TAD's were ejected horizontally, the subsequent motion is not constrained to the horizontal plane. It is not possible to constrain the motion to the horizontal plane because of the coupling of the x- and y-motions, i.e., any x-motion will induce a y-motion.

It is also of interest to determine the effect of increasing atmospheric drag on the relative motions of the TAD's. Figures 36, 37, and 38 show this effect, where the altitude has been reduced from 400 km to 300 km and the differential drag has increased by an order of magnitude from 1×10^{-6} m/s^2 to 1×10^{-5} m/s^2. These figures are similar to Figures 12, 13, and 14 except for the change in drag. The effect produced by the increased drag is very pronounced in all the figures. All cases, regardless of variations in the initial conditions, show similiar behavior. They quickly decay below the Shuttle and rapidly move out in front of it. At one orbital period after ejection, all cases are more than 400 m in front of the Shuttle and rapidly moving away. It is doubtful that TAD's would be of much use as a diagnostic instrument for differential drags this high. If it is necessary to use them at this altitude (300 km), they probably could be designed small and heavy to reduce the differential drag to more acceptable levels.

Figures 39, 40, and 41 show the same cases at an altitude of 200 km where the differential drag has increased another order of magnitude to 1×10^{-4} m/s^2. It appears that the TAD's would be completely unuseable at this altitude because of the enormity of the differential drag. The TAD's get 5 km in front of the Shuttle and decay by about 1 km in altitude in just one orbital period.

All of the motions shown so far have been for only one orbital period. Figures 42, 43, and 44 show one case (ΔV = 1 m/s, θ = +5 degrees, φ = 1 degree at 400 km altitude) for two orbital periods. These figures show the repetitive nature of the motion with a slow secular increase in the x-direction. For example at one-half and one and one-half orbital periods, the TAD crosses behind the Shuttle at 450 m and 650 m, respectively, while at one and two orbital periods it crosses at 250 m and 400 m, respectively.

By proper selection of the initial conditions, it appears that, with a number of TAD's, the region around the Shuttle could be examined closely. The choice of the initial conditions would depend on the specific application that one had in mind.

V. "MIRROR-IMAGE" MOTION

If a TAD is ejected with a certain ΔV, θ, and φ, it has a certain motion relative to the Shuttle. If the TAD should then be ejected in the opposite direction (i.e., with the same ΔV but with $\theta = -\theta$ and $\varphi = \varphi + \pi$), the resultant motion would be the above motion reflected through the origin, i.e., $x \rightarrow -x$, $y \rightarrow -y$, and $z \rightarrow -z$. This is more properly termed a coordinate inversion. This can be demonstrated from the equations of motion (2-33) and (2-40) with the initial conditions of Section III,

$$x = -(\Delta V \cos\theta \sin\varphi)\left(3t - \frac{4}{\omega}\sin\omega t\right) - \frac{3}{2}Dt^2 + 2\left(\frac{\Delta V \sin\theta}{\omega} + \frac{2D}{\omega^2}\right)(1 - \cos\omega t)$$

$$y = -\frac{2}{\omega}(\Delta V \cos\theta \sin\varphi)(1 - \cos\omega t) - \frac{2Dt}{\omega} + \left(\frac{\Delta V \sin\theta}{\omega} + \frac{2D}{\omega^2}\right)\sin\omega t$$

$$z = \frac{1}{\omega}(\Delta V \cos\theta \cos\varphi)\sin\omega t \quad . \tag{5-1}$$

Now, if the replacements $\theta \rightarrow -\theta$ and $\varphi \rightarrow \varphi + \pi$ are made,

$$\sin(\varphi + \pi) = -\sin\varphi \quad , \quad \cos(\varphi + \pi) = -\cos\varphi$$

$$\sin(-\theta) = -\sin\theta \quad , \quad \cos(-\theta) = +\cos\theta \quad .$$

If the terms in equations (5-1) containing D are ignored (since they are small for short time periods) and θ and φ are replaced by $-\theta$ and $\varphi + \pi$, respectively, then it is easily verified that

$$x(-\theta, \varphi + \pi) = -x(\theta, \varphi)$$

$$y(-\theta, \varphi + \pi) = -y(\theta, \varphi)$$

$$z(-\theta, \varphi + \pi) = -z(\theta, \varphi) \quad . \tag{5-2}$$

The implication of this is, of course, that ejections on only one side of the Shuttle, for example the +z side, have to be analyzed. The motions of TAD's ejected on the other side would be merely a reflection of one of these motions.

VI. SENSITIVITY COEFFICIENTS – FIRST ORDER PARTIALS

Frequently it is of interest to know how sensitive the motion of a TAD is to its initial conditions. A practical question arises: Suppose the initial conditions are in error by a certain amount because of inaccurate hardware alignment or some other cause, how much then is the resultant motion of the TAD affected? Fortunately, this question can be answered rather simply for the relative motion equations. The expressions for the coordinates are analytic functions of the initial conditions and the time and, hence, can be expanded in Taylor series about the initial conditions; i.e.,

$$x(\theta,\varphi,\Delta V,t) = x(\theta_0,\varphi_0,\Delta V_0,t) + \left(\frac{\partial x}{\partial \theta}\right)_0 (\theta - \theta_0) + \left(\frac{\partial x}{\partial \varphi}\right)_0 (\varphi - \varphi_0) + \left(\frac{\partial x}{\partial \Delta V}\right)_0 (\Delta V - \Delta V_0) + \ldots$$

or (6-1)

$$x = x_0 + \left(\frac{\partial x}{\partial \theta}\right)_0 \Delta\theta + \left(\frac{\partial x}{\partial \varphi}\right)_0 \Delta\varphi + \left(\frac{\partial x}{\partial \Delta V}\right)_0 \Delta(\Delta V) + \ldots$$

and similiarly for the other coordinates.

If it is now assumed that the displacements $\Delta\theta$, $\Delta\varphi$, and $\Delta(\Delta V)$ from the nominal are small, it is justifiable to retain only first-order terms in the Taylor expansions. The resultant variations in the coordinates at any time point resulting from variations in the initial conditions will be

$$\begin{pmatrix} \Delta x \\ \Delta y \\ \Delta z \end{pmatrix} = \begin{pmatrix} \frac{\partial x}{\partial \theta} & \frac{\partial x}{\partial \varphi} & \frac{\partial x}{\partial \Delta V} \\ \frac{\partial y}{\partial \theta} & \frac{\partial y}{\partial \varphi} & \frac{\partial y}{\partial \Delta V} \\ \frac{\partial z}{\partial \theta} & \frac{\partial z}{\partial \varphi} & \frac{\partial z}{\partial \Delta V} \end{pmatrix} \begin{pmatrix} \Delta\theta \\ \Delta\varphi \\ \Delta(\Delta V) \end{pmatrix} . \quad (6\text{-}2)$$

Since the coordinates are given explicitly by equations (5-1), the partials can be taken directly as follows:

$$\frac{\partial x}{\partial \theta} = (\Delta V \sin\theta \sin\varphi)\left(3t - \frac{4}{\omega}\sin\omega t\right) + \frac{2\Delta V \cos\theta}{\omega}(1 - \cos\omega t)$$

$$\frac{\partial x}{\partial \varphi} = -(\Delta V \cos\theta \cos\varphi)\left(3t - \frac{4}{\omega}\sin\omega t\right)$$

$$\frac{\partial x}{\partial \Delta V} = -(\cos\theta \sin\varphi)\left(3t - \frac{4}{\omega}\sin\omega t\right) + \frac{2\sin\theta}{\omega}(1 - \cos\omega t)$$

$$\frac{\partial y}{\partial \theta} = \frac{2}{\omega}(\Delta V \sin\theta \sin\varphi)(1 - \cos\omega t) + \frac{\Delta V \cos\theta}{\omega}\sin\omega t$$

$$\frac{\partial y}{\partial \varphi} = -\frac{2}{\omega}(\Delta V \cos\theta \cos\varphi)(1 - \cos\omega t)$$

$$\frac{\partial y}{\partial \Delta V} = -\frac{2}{\omega}(\cos\theta \sin\varphi)(1 - \cos\omega t) + \frac{\sin\theta}{\omega}\sin\omega t$$

$$\frac{\partial z}{\partial \theta} = -\frac{1}{\omega}(\Delta V \sin\theta \cos\varphi)\sin\omega t$$

$$\frac{\partial z}{\partial \varphi} = -\frac{1}{\omega}(\Delta V \cos\theta \sin\varphi)\sin\omega t$$

$$\frac{\partial z}{\partial \Delta V} = \frac{1}{\omega}(\cos\theta \cos\varphi)\sin\omega t \quad . \qquad (6\text{-}3)$$

These partials are dependent on the nominal values of the initial conditions and, most significantly, they are dependent on the time. At some points along the trajectory the error in the coordinates because of errors in the ejection conditions will be larger than at other points because of time dependence.

The percentage error in z at least can be shown to be independent of time,

$$\frac{\Delta z}{z} = \frac{\frac{\partial z}{\partial \theta}\Delta\theta + \frac{\partial z}{\partial \varphi}\Delta\varphi + \frac{\partial z}{\partial \Delta V}\Delta(\Delta V)}{z}$$

$$\frac{\Delta z}{z} = \frac{\frac{\Delta V}{\omega}\left[(-\sin\theta\cos\varphi\,\Delta\theta - \cos\theta\sin\varphi\,\Delta\varphi) + \frac{\cos\theta\cos\varphi}{\Delta V}\Delta(\Delta V)\right]\sin\omega t}{\frac{\Delta V}{\omega}\cos\theta\cos\varphi\cdot\sin\omega t}$$

$$\frac{\Delta z}{z} = -\tan\theta\,\Delta\theta - \tan\varphi\,\Delta\varphi + \frac{\Delta(\Delta V)}{\Delta V} \quad . \tag{6-4}$$

For side ejections where θ and φ are both small, the percentage error in z is almost equal to the last term, the percentage error in ΔV.

Some plots of these partial derivatives are presented to get an idea of the numerical values they have. Figure 45 shows the partials of the coordinates with respect to θ for one orbital period for the nominal case: $\theta = +5$ degrees, $\varphi = +3.5$ degrees, and $\Delta V = 0.1$ m/s. Both θ and φ are small for this case so the partials of x and y behave like the second terms in equations (6-3). i.e., the $\partial x/\partial\theta$ dependence on time behaves like $(1 - \cos\ \omega t)$ and that for $\partial y/\partial\theta$ behaves like $\sin\ \omega t$. The z-partial remains very small. The partials of the coordinates with respect to φ are presented in Figure 46 for one orbital period for the same nominal case and the partials of the coordinates with respect to the initial impulse ΔV are presented in Figure 47.

The following conclusions may be drawn from these figures:

1. The coordinates are more sensitive to errors in φ than those in θ by a factor of 4 or 5.

2. The coordinates are very sensitive to an error in the initial impulse, ΔV.

3. The largest errors in z occur at one-fourth and three-fourths of an orbital period. No error occurs at half and whole orbital periods.

4. The largest error in y occurs at one-half orbital periods. No error occurs at whole orbital periods.

5. As evidenced by the graphs and the equations, the error in x grows monotonically with time. The errors in y and z are periodic in time.

Figure 48 presents deviations in the coordinates because of "errors" in the ejection conditions for the nominal case just discussed. The "errors" are $\Delta\theta = 0.5$, $\Delta\varphi = 0.5$ degree, and $\Delta(\Delta V) = 0.1$ m/s. It can be observed that these errors in the coordinates

behave exactly like the partials of the coordinates with respect to ΔV that were presented in Figure 47. This is because the coordinates are much more sensitive to errors in ΔV than to errors in θ or φ, at least for the nominal case being considered here and for any nominal case where θ and φ are both small as they are likely to be for many TAD's applications.

VII. TARGETING

There may be applications of the TAD's for which it would be desirable to place them at a certain point in space relative to the Shuttle at a specified time. A specific example would be the case where a balloon had been ejected from the Shuttle and a TAD would then be ejected such that the TAD would pass through the wake of the balloon. We refer to this problem as the targeting problem and formulate it more precisely as follows. The TAD is initially in the Shuttle (coordinates: 0, 0, 0,). It is desired to have the TAD pass through the point x, y, z in a certain time interval t after ejection. What initial velocity $\dot{x}_0$, $\dot{y}_0$, $\dot{z}_0$ (or ΔV, θ, φ) is required to meet these criteria?

The relative motion equations (2-33) and (2-40) can be written as:

$$x(t) = x_0 + 6\omega t y_0 - \frac{3}{2} Dt^2 - 6y_0 \sin \omega t + \frac{4D}{\omega^2} (1 - \cos \omega t) + \left(-3t + \frac{4}{\omega} \sin \omega t \right) \dot{x}_0$$

$$+ \frac{2}{\omega} (1 - \cos \omega t) \dot{y}_0$$

$$y(t) = 4y_0 - \left(\frac{2D}{\omega}\right) t - 3y_0 \cos \omega t + \frac{2D}{\omega^2} \sin \omega t - \frac{2}{\omega} (1 - \cos \omega t) \dot{x}_0 + \frac{\sin \omega t}{\omega} \dot{y}_0$$

$$z(t) = z_0 \cos \omega t + \frac{\dot{z}_0}{\omega} \sin \omega t \quad . \tag{7-1}$$

These equations can be rewritten collecting coefficients of $\dot{x}_0$, $\dot{y}_0$, and $\dot{z}_0$ on the left side with all other terms on the right side. The results are:

$$\frac{1}{\omega} (-3\omega t + 4 \sin \omega t) \dot{x}_0 + \frac{2}{\omega} (1 - \cos \omega t) \dot{y}_0 = x(t) - x_0 - 6y_0 (\omega t - \sin \omega t)$$

$$+ \frac{3}{2} Dt^2 + \frac{4D}{\omega^2} (1 - \cos \omega t) \tag{7-2}$$

$$- \frac{2}{\omega} (1 - \cos \omega t) \dot{x}_0 + \frac{1}{\omega} \sin \omega t \, \dot{y}_0 = y(t) - 4y_0 + \frac{2Dt}{\omega} + 3y_0 \cos \omega t - \frac{2D}{\omega^2} \sin \omega t$$

$$\frac{1}{\omega} \sin \omega t \, \dot{z}_0 = z(t) - z_0 \cos \omega t \quad .$$

This can now be cast in matrix form as

$$\begin{pmatrix} \frac{1}{\omega}(-3\omega t + 4 \sin \omega t) & \frac{2}{\omega}(1 - \cos \omega t) & 0 \\ -\frac{2}{\omega}(1 - \cos \omega t) & \frac{1}{\omega} \sin \omega t & 0 \\ 0 & 0 & \frac{1}{\omega} \sin \omega t \end{pmatrix} \begin{pmatrix} \dot{x}_0 \\ \dot{y}_0 \\ \dot{z}_0 \end{pmatrix}$$

$$= \begin{pmatrix} x(t) - x_0 - 6y_0(\omega t - \sin \omega t) + \frac{3Dt^2}{2} + \frac{4D}{\omega^2}(1 - \cos \omega t) \\ y(t) - 4y_0 + \frac{2D}{\omega} t + 3y_0 \cos \omega t - \frac{2D}{\omega^2} \sin \omega t \\ z(t) - z_0 \cos \omega t \end{pmatrix} \quad . \qquad (7\text{-}3)$$

Equation (7-3) is compactly represented by

$$A\dot{\bar{x}}_0 = \bar{b} \quad , \qquad (7\text{-}4)$$

where A is the 3 X 3 square matrix explicity presented in equation (7-3) and $\dot{\bar{x}}_0$ and $\bar{b}$ are the column matrices in equation (7-3). One inserts the initial position x_0, y_0, z_0 and the desired position at time t, i.e., x(t), y(t), z(t). Equation (7-4) is then solved to determine what initial velocity is required to get from one point to another in the specified time interval. The solution to equation (7-4) is, of course, given by

$$\dot{\bar{x}}_0 = A^{-1} \bar{b} \quad . \qquad (7\text{-}5)$$

The inverse of A in this simple case can be computed by the co-factor method. The determinant of A, required by this method, is

$$\det A = \frac{\sin \omega t}{\omega^3} [-3\omega t \sin \omega t + 8 (1 - \cos \omega t)] \quad . \qquad (7\text{-}6)$$

A^{-1} exists only if or when det $A \neq 0$. It is easily determined from equation (7-6) that the determinant is zero at half and whole orbital periods, so the inverse does not exist there.

A basic reason behind, and the meaning of, the singularity at half and whole orbital periods is that z will be zero at these times regardless of what is done to the initial conditions, and it cannot be forced to be otherwise as long as we are restricted to a single initial impulse.

There are also other times at which the determinant is zero, namely those which satisfy the transcendental equation,

$$f(t) = -3\omega t \sin \omega t + 8(1 - \cos \omega t) = 0 \quad . \tag{7-7}$$

A graph of this function for a few orbital periods will give an estimate of the positions of its zeroes. This is shown in Figure 49. Zeroes of this function occur at whole orbital periods. In addition, after the first orbital period, there is another zero that occurs just prior to a half-orbital period. As t increases this zero more closely approaches one-half orbital period. For large t it approaches the zeroes of sin ωt, i.e., at half and whole orbital periods. This is because the first term in equation (7-7) soon dominates the function.

Thus, det A is zero at half and whole orbital periods and, for the first few orbits after the initial one, it is zero at an isolated point just prior to one-half orbit. To calculate the position of this zero accurately, equation (7-7) would have to be solved iteratively. In practical applications of the targeting procedure, this will cause no difficulty because it is extremely unlikely that one would choose a time to target at precisely the position of this zero. In summary, then, one can target to a point at any time except at half and whole orbital periods.

With these limitations, the inverse of A is:

$$A^{-1} = \frac{\omega}{-3\omega t \sin \omega t + 8(1 - \cos \omega t)} \begin{pmatrix} \sin \omega t & -2(1 - \cos \omega t) & 0 \\ 2(1 - \cos \omega t) & (-3\omega t + 4 \sin \omega t) & 0 \\ 0 & 0 & \dfrac{-3\omega t \sin \omega t + 8(1 - \cos \omega t)}{\sin \omega t} \end{pmatrix} . \tag{7-8}$$

Multiplying A^{-1} by the column matrix $\bar{b}$ will give the required initial velocity $\dot{x}_0$, $\dot{y}_0$, and $\dot{z}_0$. The results of performing this multiplication are:

$$\dot{x}_0 = \frac{\omega}{-3\omega t \sin \omega t + 8(1 - \cos \omega t)} \left[\sin \omega t \left\{ x(t) - x_0 - 6y_0(\omega t - \sin \omega t) + \frac{3}{2} D t^2 + \frac{4D}{\omega}(1 - \cos \omega t) \right\} \right.$$

$$\left. -2(1 - \cos \omega t) \left\{ y(t) - 4y_0 + \frac{2D}{\omega} t + 3y_0 \cos \omega t - \frac{2D}{\omega^2} \sin \omega t \right\} \right]$$

$$\dot{y}_0 = \frac{\omega}{-3\omega t \sin \omega t + 8(1 - \cos \omega t)} \left[2(1 - \cos \omega t) \left\{ x(t) - x_0 - 6y_0(\omega t - \sin \omega t) + \frac{3}{2} D t^2 + \frac{4D}{\omega}(1 - \cos \omega t) \right\} \right.$$

$$\left. +(-3\omega t + 4 \sin \omega t) \left\{ y(t) - 4y_0 + \frac{2D}{\omega} t + 3y_0 \cos \omega t - \frac{2D}{\omega^2} \sin \omega t \right\} \right]$$

$$\dot{z}_0 = \frac{\omega}{\sin \omega t} [z(t) - z_0 \cos \omega t] \quad . \tag{7-9}$$

It can be seen from these equations that x and y are coupled but z is not. If z is required to be other than zero at half and whole orbital periods, the required $\dot{z}_0$ would be infinite, which is an impossibility. If x and y were required to be some arbitrary value at one orbital period, the $\dot{y}_0$ equation, from (7-9), would be

$$\dot{y}_0 = -\frac{6\omega\pi \left[y(t) - y_0 + \frac{4\pi D}{\omega^2} \right]}{0} \quad . \tag{7-10}$$

This is infinite unless the term in brackets is zero; i.e., unless

$$y(t) = y_0 - \frac{4\pi D}{\omega^2} \quad . \tag{7-11}$$

Thus, the only specification that can be made on y at one orbital period is that it returns to its initial value minus the amount that it decays in one orbit because of drag.

The $\dot{x}_0$ equation yields the indeterminant form 0/0 at one orbital period. An application of L'Hospital's rule with subsequent evaluation at one orbital period yields

$$\dot{x}_0 = -\frac{\omega(x - x_0)}{6\pi} + 2\omega y_0 - \frac{\pi D}{\omega} \quad . \tag{7-12}$$

Exactly the same result can be obtained from equations (2-40) and (2-41). Since, in our case, x_0 and y_0 are both zero, equation (7-12) becomes

$$\dot{x}_0 = -\frac{\omega x}{6\pi} - \frac{\pi D}{\omega} \quad . \tag{7-13}$$

Thus, we get the important result that although y and z cannot be specified at one orbital period (they both return to zero), x can be specified at one orbital period and equation (7-13) gives the initial impulse required (the x-component).

It can similiarly be determined that although z cannot be specified at half-orbital periods, both x and y can be. The results can be summarized as follows:

1. One can target to an arbitrary point (x, y, z) at times other than half and whole orbital periods.

2. One can target to an arbitrary (x, y) point (but not z) at half-orbital periods.

3. One can target to an arbitrary x-point (but not y or z) at whole orbital periods.

Once the target point (x, y, z) and the time t are specified, equations (7-9) determine the required velocity. The required ΔV, θ, and φ will be

$$\Delta V = \sqrt{\dot{x}_0^2 + \dot{y}_0^2 + \dot{z}_0^2}$$

$$\theta = \sin^{-1}\left(\frac{\dot{y}_0}{\Delta V}\right)$$

$$\varphi = \tan^{-1}\left(\frac{\dot{x}_0}{\dot{y}_0}\right) \quad . \tag{7-14}$$

These equations are evident from Figure 3.

Two numerical examples of the targeting capability are presented. The two examples are: target to the point x = 200 m, y = 200 m, z = 200 m in (a) one-fourth orbital period and (b) one and one-fourth orbital periods. The required initial conditions from equations (7-14) are:

Case a

$\dot{x}_0 = -0.06844558$ m/s $\qquad \Delta V = 0.253099$ m/s

$\dot{y}_0 = +0.0903975$ m/s $\qquad \theta = 20.926°$

$\dot{z}_0 = +0.22628$ m/s $\qquad \varphi = -16.8296°$

Case b

$\dot{x}_0 = +0.0108422$ m/s $\qquad \Delta V = 0.3449086$ m/s

$\dot{y}_0 = +0.26008036$ m/s $\qquad \theta = 48.9429°$

$\dot{z}_0 = +0.22628$ m/s $\qquad \varphi = 2.7432°$.

The x-y projection of the motion for both cases is presented in Figure 50. Case a is shown for approximately one orbital period and case b is shown for approximately two orbital periods. The x-z projection is presented in Figure 51 and the y-z projection is presented in Figure 52. It can be verified that both cases go through the target point at the specified time.

In order to hit the specified target point within a certain accuracy, it is necessary to determine the accuracy with which the initial velocity must be controlled. This can be determined with the aid of the partials developed in Section VI. For case a the partials of the coordinates with respect to θ are presented in Figure 53 for one orbital period. The partials of the coordinates with respect to φ are presented in Figure 54 and the partials of the coordinates with respect to ΔV are presented in Figure 55. From these figures it can be determined at one-quarter of an orbital period, the time at which we desire to hit the target point, that the partials are approximately

$$\begin{pmatrix} \frac{\partial x}{\partial \theta} & \frac{\partial x}{\partial \varphi} & \frac{\partial x}{\partial \Delta V} \\ \frac{\partial y}{\partial \theta} & \frac{\partial y}{\partial \varphi} & \frac{\partial y}{\partial \Delta V} \\ \frac{\partial z}{\partial \theta} & \frac{\partial z}{\partial \varphi} & \frac{\partial z}{\partial \Delta V} \end{pmatrix}_{\frac{T}{4}} = \begin{pmatrix} 7.7 & -2.5 & 800 \\ 2.85 & -7.0 & 800 \\ -1.35 & +1.0 & 800 \end{pmatrix} . \qquad (7\text{-}15)$$

It seems remarkable that the partials of the coordinates with respect to the initial ΔV are all the same at one-quarter period. If the allowable errors Δx, Δy, and Δz in the position x, y, z are specified, the allowable errors in the ejection conditions can be determined by inverting the matrix in equation (6-2). If equation (6-2) is written as

$$\Delta\vec{x}(t) = B(t)\,\Delta\vec{V}_i \quad , \tag{7-16}$$

then

$$\Delta\vec{V}_i = B^{-1}(t)\,\Delta\vec{x}(t) \quad . \tag{7-17}$$

It can be verified, by much tedious algebra, that the inverse of the partial matrix B, defined by

$$B^{-1} = \frac{1}{|B|}\begin{pmatrix} B_{11} & B_{21} & B_{31} \\ B_{12} & B_{22} & B_{32} \\ B_{13} & B_{23} & B_{33} \end{pmatrix} \quad , \tag{7-18}$$

where

$$|B| = \frac{1}{\Delta V}\left(\frac{\Delta V}{\omega}\right)^3 \cos\theta \sin\omega t\,[3\omega t \sin\omega t - 8(1 - \cos\omega t)] \quad , \tag{7-19}$$

is

$$B_{11} = \frac{1}{\Delta V}\left(\frac{\Delta V}{\omega}\right)^2 \cos\theta \sin\omega t\left\{\sin\theta \sin\varphi \sin\omega t - 2\cos\theta(1 - \cos\omega t)\right\}$$

$$B_{12} = \frac{1}{\Delta V}\left(\frac{\Delta V}{\omega}\right)^2 \cos\theta \sin\omega t\left\{-\frac{\cos\varphi \sin\omega t}{\cos\theta}\right\}$$

$$B_{13} = \left(\frac{\Delta V}{\omega}\right)^2 \cos\theta \sin\omega t\left\{-2\sin\theta(1 - \cos\omega t) - \sin\varphi \cos\theta \sin\omega t\right\}$$

$$B_{21} = \frac{1}{\Delta V}\left(\frac{\Delta V}{\omega}\right)^2 \cos\theta \sin\omega t\left\{(3\omega t - 4\sin\omega t)\cos\theta - 2\sin\theta \sin\varphi(1 - \cos\omega t)\right\}$$

$$B_{22} = \frac{1}{\Delta V}\left(\frac{\Delta V}{\omega}\right)^2 \cos\theta \sin\omega t \left\{(1 - \cos\omega t)\frac{2\cos\varphi}{\cos\theta}\right\}$$

$$B_{23} = \left(\frac{\Delta V}{\omega}\right)^2 \cos\theta \sin\omega t \left\{(3\omega t - 4\sin\omega t)\sin\theta + 2\cos\theta \sin\varphi (1 - \cos\omega t)\right\}$$

$$B_{31} = \frac{1}{\Delta V}\left(\frac{\Delta V}{\omega}\right)^2 \cos\theta \sin\omega t \left\{\frac{-\sin\theta\cos\varphi}{\sin\omega t}[3\omega t \sin\omega t - 8(1 - \cos\omega t)]\right\}$$

$$B_{32} = \frac{1}{\Delta V}\left(\frac{\Delta V}{\omega}\right)^2 \cos\theta \sin\omega t \left\{\frac{-\sin\varphi}{\cos\theta \sin\omega t}[3\omega t \sin\omega t - 8(1 - \cos\omega t)]\right\}$$

$$B_{33} = \left(\frac{\Delta V}{\omega}\right)^2 \cos\theta \sin\omega t \left\{\frac{\cos\theta\cos\varphi}{\sin\omega t}[3\omega t \sin\omega t - 8(1 - \cos\omega t)]\right\} \quad . \qquad (7\text{-}20)$$

The zeroes of the determinant $|B|$ occur at the same places as those for the determinant $|A|$, i.e., at half and whole orbital periods; therefore, B^{-1} does not exist there just as A^{-1} does not. In addition, B^{-1} does not exist for vertical ejections, i.e., for $\theta = \pi/2$ or $\theta = 3\pi/2$.

We divide each element in equation (7-18) by $|B|$ and, for example, rewrite $B_{11}/|B| = b_{11}$. Equation (7-17) then becomes

$$\begin{pmatrix} \Delta\theta \\ \Delta\varphi \\ \Delta(\Delta V) \end{pmatrix} = \begin{pmatrix} b_{11} & b_{21} & b_{31} \\ b_{12} & b_{22} & b_{32} \\ b_{13} & b_{23} & b_{33} \end{pmatrix} \begin{pmatrix} \Delta x \\ \Delta y \\ \Delta z \end{pmatrix} \quad , \qquad (7\text{-}21)$$

where each element can be explicitly determined from equations (7-19) and (7-20). The units on each of the elements in the first two rows are radians/meter. These can be multiplied by 57.29577951 to change them to the more convenient units of degrees/meter. The units on the elements in the last row are $(\text{seconds})^{-1}$. The elements in the first row of equation (7-21) are plotted in Figure 56 for case a for one orbital period. The units are shown as degrees/meter. The elements in the second row are plotted in Figure 57 and the elements in the third row are plotted in Figure 58.

The elements at one-quarter period, reading from these graphs, are approximately

$$\begin{pmatrix} \Delta\theta \\ \Delta\varphi \\ \Delta(\Delta V) \end{pmatrix} = \begin{pmatrix} +0.15 & -0.07 & -0.085 \\ +0.077 & -0.16 & +0.077 \\ +0.16 \times 10^{-3} & +0.09 \times 10^{-3} & +1.0 \times 10^{-3} \end{pmatrix}_{\frac{T}{4}} \begin{pmatrix} \Delta x \\ \Delta y \\ \Delta z \end{pmatrix} \quad . \qquad (7\text{-}22)$$

If we suppose that up to a +10 m error could be tolerated in all of the coordinates at this time, the allowable errors in the ejection conditions would be

$$\Delta\theta = -0.05°$$

$$\Delta\varphi = -0.06°$$

$$\Delta(\Delta V) = 0.0125 \text{ m/s} \quad .$$

If these errors are multiplied by the partial matrix in equation (7-15) it is verified that they will indeed produce approximately a +10 m error in all of the coordinates. If up to a -10 m error in all coordinates could be tolerated, the errors allowed in the ejection conditions would be the negative of those above. If a +10 m error is allowed in x and none in y or z, the allowable errors in the ejection conditions would be $\Delta\theta = +1.5°$, $\Delta\varphi = +0.77°$, and $\Delta(\Delta V) = +0.0016$ m/s.

One aspect becomes clear from this; that is, if an allowed "box" of errors in the coordinates at some point in time is specified, this can be mapped into an allowed volume of errors in the ejection conditions. This provides a method by which one may specify how accurately the ejection conditions θ, φ, and ΔV must be controlled.

The smallness of the coefficients in the third row of equation (7-22), and from Figure 58, indicates that the impulsive velocity will have to be controlled very accurately. For the example quoted above, it cannot have an error of more than 0.01 m/s.

As a concrete example of the mapping capability, a cube of allowed position errors having sides of 20 m in magnitude centered about the nominal point is taken at 20 min after ejection and mapped back into allowed ejection errors in θ, φ, and ΔV. The $\Delta\theta$, $\Delta\varphi$ results are plotted in Figure 59. The allowed error in ΔV, while not shown on Figure 59, is always equal to less than 0.01 m/s in absolute magnitude. It is seen that the allowed "box" of ejection errors is a rectilinear figure. This is because the mapping, being linear, maps straight lines into straight lines. Thus, from this figure, one sees that the allowed error in θ can be up to approximately 3 degrees and that in φ up to approximately 3.5 degrees, and the TAD will still be somewhere in the cube having sides of 20 m defined about the nominal point at 20 min after ejection (provided that the error in ΔV is also less than 0.01 m/s). At various time points along the trajectory this allowed error box will vary some in size and shape. As an example, Figure 60 gives the allowed error box at 25 min. Although they look similiar at first glance, a careful comparison will reveal differences.

Another important point should be emphasized about equation (7-21); that is, the allowed ejection errors are linear functions of the allowable errors in the final position, so the allowable ejection errors scale linearly up or down with the allowable position errors.

The targeting capability can also be used to maximize the amount of space sampled by a given number of TAD's. For example, suppose it was desired to examine the wake behind the Shuttle with four TAD's. These TAD's could be distributed, at one-half an orbital period or at a whole orbital period, at the best distances as determined by the investigators; they could be distributed at 250, 500, 750 and 1000 m or at any other set of desired distances. If it was desired to make them pass through the wake, not simultaneously but in a certain time sequence, this could easily be accomplished by proper time-sequencing of the ejections.

The discussion concerning targeting accuracy thus far has assumed that the differential drag is known perfectly. In fact there could be, and probably will be, some uncertainty about its exact value and this could upset the accuracy estimates. To determine the effects that an uncertainty in drag would produce, it is necessary to look at the partials of the coordinates with respect to the differential drag. From equations (7-1) it is easily determined that these partials are

$$\frac{\partial x(t)}{\partial D} = -\frac{3}{2}t^2 + \frac{4}{\omega^2}(1 - \cos \omega t)$$

$$\frac{\partial y(t)}{\partial D} = -\frac{2t}{\omega} + \frac{2}{\omega^2}\sin \omega t$$

$$\frac{\partial z(t)}{\partial D} = 0 \quad . \tag{7-23}$$

The z-coordinate is not affected at all by drag or by any uncertainty in it. It is seen that these partials are not dependent on initial conditions and only slightly dependent on altitude (through ω). Therefore, they are approximately the same for all orbits. A plot of these partials versus time for one orbital period is given in Figure 61. It is seen that the secular terms quickly dominate the periodic ones, and the partials decrease monotonically with time indicating that the errors introduced by uncertainties in drag would be larger for large times than for small times. This is what one would intuitively expect.

Ignoring other uncertainties for the present, the errors induced in the coordinates because of an uncertainty ΔD in the differential drag would be

$$\Delta x = \frac{\partial x}{\partial D}\Delta D = \left[-\frac{3}{2}t^2 + \frac{4}{\omega^2}(1 - \cos \omega t)\right] \cdot \Delta D$$

$$\Delta y = \frac{\partial y}{\partial D}\Delta D = \left[-\frac{2}{\omega}t + \frac{2}{\omega^2}\sin \omega t\right] \cdot \Delta D$$

$$\Delta z = \frac{\partial z}{\partial D}\Delta D = 0 \quad . \tag{7-24}$$

The uncertainty ΔD in differential drag could be constant or time varying. If it was time varying, however, its exact form would probably be unknown to us. In the simple case where ΔD is taken to be a constant value, the errors in the coordinates at any time point are obtained simply by multiplying the partials at that time point by the uncertainty.

At an altitude of 400 km, the nominal differential drag is of the order of 10^{-6} m/s^2. If the uncertainty is 10 percent of the nominal value, ΔD would be of the order of $\pm 10^{-7}$ m/s^2. In this case the induced errors in the coordinates over one orbital period would be negligible (< 1 m). If the uncertainty is 100 percent of the nominal value, the induced errors in the coordinates could be ± 10 m or more in the first orbital period (and larger in succeeding orbital periods). This may be significant for precise requirements. At an altitude of 300 km where the nominal differential drag is of the order of 10^{-5} m/s^2, one would definitely have to become concerned about uncertainties in differential drag.

VIII. OPTIMUM USE OF TAD's FOR ELECTROMAGNETIC INTERFERENCE AND WAKE STUDIES

One of the desired objectives of this study is to identify trajectories of TAD's that will cover or scan as much volume around the Shuttle as possible. It is desired to maximize the volume coverage while minimizing the number of TAD's used. Since TAD's can be made to go forward and backward and to oscillate in the vertical plane and sweep back and forth in the horizontal plane (although these do not remain in the horizontal plane but have vertical displacements), it would seem at first glance that four TAD's would give reasonably complete coverage of the volume around the Shuttle. The plan is to have two TAD's oscillating in the vertical plane with one in front of the Shuttle and one behind the Shuttle. The other two TAD's would be given horizontal sweeping motion with one in front of the Shuttle and one behind the Shuttle.

With this plan in mind and assuming that 100 m above and below and to each side of the Shuttle is a sufficient distance for electromagnetic interference and wake studies, it is determined from equations (4-1) that an impulse of 0.1 m/s is sufficient to achieve these distances in oscillations. For the vertical oscillations, the angle φ should be 90 degrees (in-plane ejections). For the TAD going behind the Shuttle, it can be determined that a θ angle of 100 degrees (slightly forward of vertical) will produce an acceptable trajectory and for the TAD going in front of the Shuttle, a θ angle of 270 degrees (straight down) will produce an acceptable trajectory.

These two trajectories are shown in Figure 62 for approximately five orbital revolutions. Case a going in front starts with overlapping trajectories but drag starts drawing them out until by the fourth orbit they are no longer overlapping. Drag is also slowly making them decay at a rate of about 10 m per orbit (this is at an altitude of 400 km with a differential drag of 1×10^{-6} m/s^2). This TAD will continue to accelerate away from the Orbiter. Case b going behind the Shuttle starts receding from the Shuttle, but by the third orbit drag has stopped the receding motion at about 800 m

and starts the TAD back toward the Shuttle. In the five orbits shown here, the TAD has not yet gotten back to the Shuttle but will in one or two more orbits. This gives a definite possibility of recontact and is a potential safety problem. The relative velocities between the TAD and Shuttle are so small (approximately 0.1 m/s), however, that even if recontact did occur it is doubtful that it would result in any damage. It might even be possible to recover the TAD if it came close enough. (The continuation of this trajectory is shown later.) These trajectories make it appear that the vertical plane in front of and especially that behind the Shuttle can be sampled quite densely by TAD's for several orbital periods.

For the two TAD's executing horizontal sweeps, the initial angle θ is chosen to be zero. For the TAD going forward, the initial φ is chosen to be 2 degrees and for the TAD going backward, the initial φ is chosen to be -12 degrees. These two cases, labeled c and d, are shown in Figure 63 for approximately five orbits. The vertical plane (x-y) motion for these two cases is shown in Figure 64. Case c going in front of the Shuttle starts off with a compact oscillation, the distance between successive axis crossings being about 100 m. Just as in case a previously, however, the differential drag stretches these oscillations and this TAD is accelerated away from the Shuttle. The TAD in case d going behind the Shuttle is rapidly slowed by drag and its backward motion is halted at about 3.75 orbital periods, at which time it starts forward coming back toward the Shuttle. It is fortuitous that the backward motion in this case ceases at almost exactly 3.75 orbital periods, because this makes the motion coming back toward the Shuttle follow almost the same projected path in the horizontal plane as it took going out. This poses a definite safety problem. (The continuation of this trajectory is also presented in the following.)

The continuation of case b, initially presented in Figure 62, is shown for about nine orbits in Figure 65. The TAD passes back by the Shuttle on the sixth orbit at 630 min after ejection. At this time it is about 130 m below the Shuttle so there is no recontact problem in this case. After the TAD passes the Shuttle, it is then accelerated away and there is no further concern with recontact. The closest approach of this TAD to the Shuttle as it returns occurs at about 565 min, where it crosses the x-axis immediately behind the Shuttle at a distance of about 40 m. Any slight variation in the conditions of this case, such as differential drag or ejection conditions, could critically alter it, changing it from a safe trajectory to an unsafe one from a recontact point of view.

The continuation of case d, initially presented in Figure 63, is shown for about ten orbits in Figure 66, with the vertical motion shown in Figure 67. The horizontally projected oscillations coming back follow the same path as they went out on and go right back through the origin. The vertical projection of the motion coming back is the mirror image of that going out. The projection, too, goes through the origin. This trajectory would definitely be a problem unless a provision was made to "catch" the TAD as it came back or to move the Shuttle to a different position before the TAD got back.

One nice feature about these trajectories is that double coverage of the wake behind the Shuttle is obtained, i.e., going out and coming back. As the TAD passes by coming back, it might be possible to recover and reuse it. Another possibility is to design

the trajectory such that the TAD misses the Shuttle as it comes back and then continues on to map the region in front of the Shuttle. With this possibility, the region behind and in front of the Shuttle could be mapped with one or two TAD's rather than four. For completeness the y-z projection of this motion is shown in Figure 68.

To show that the horizontal projection of the returning motion following that of the outgoing motion was coincidental in the preceding case, we present a similiar case where this does not happen. The ejection conditions are changed slightly. The angle φ is changed from -12 degrees to -14 degrees. All other values remain fixed. The motion in this case is presented in Figures 69 through 71. The projection of the returning motion here clearly does not follow that of the outgoing motion. In this case the returning TAD easily misses the Shuttle. This TAD could give double coverage of the wake behind the Shuttle to about 1 km and then could map some of the region in front of the Shuttle.

The question remains: How does one choose these trajectories optimally? To answer this quantitatively it would be helpful if some specific measure could be chosen to optimize. Then the pertinent parameters can be chosen so as to optimize that measure. As a specific example of this possibility, we might choose to maximize the amount of time that the TAD spent behind the Shuttle. To do this we take the secular terms in the x-equation (4-1) and equate them to zero. (The oscillatory terms will average out to zero and hence can be ignored here.) This yields

$$t = \frac{-3\Delta V \cos\theta \sin\varphi}{1.5\ D} \tag{8-1}$$

as the amount of time spent behind the Shuttle. This can be made as large as desired by choosing ΔV as large as desired. This, however, would not satisfy our desire to remain close to the wake of the Shuttle. Obviously we have constraints on the optimum problem; we must maximize t while remaining close to the wake of the Shuttle. If we want to remain within ±100 m of the wake, ΔV must be constrained to approximately 0.1 m/s. D is generally fixed by the orbital altitude and the configurations and attitudes of the spacecraft involved, so the optimization must be through manipulation of the angles θ and φ. If we hold θ constant at zero and vary φ, we get the result shown in Figure 72. If θ is varied, plus or minus from zero, the result will be lower than that shown. Clearly, then, t is maximized by chosing φ = -90 degrees and θ = 0 degree.

This is one way to optimize the trajectory selection: choose a quantitative measure, and maximize or minimize it. The problem is finding the proper quantity to optimize. There may be undesirable features about maximizing t above. For example, the maximum distance that the TAD goes behind the Shuttle in this case is about 15 km which may be farther than experimental interests dictate. The x-distance behind the Shuttle versus time is shown in Figure 73 with φ parameterized. From this figure one can pick φ such that x does not go beyond a certain distance.

One may be interested in having several wake crossings spaced closely behind the Shuttle rather than extended out over a large distance behind the Shuttle. Figure 74 shows the distances of the first five wake crossings behind the Shuttle versus the ejection angle φ. For φ = -10 degrees, the first five crossings occur within 0.5 km of the Shuttle. For φ = -30 degrees the first five crossings are distributed out to 1.8 km, and for φ = -90 degrees they are distributed out to 4 km. The local altitude (y-coordinate) above or below the wake of the Shuttle at the wake crossings (z = 0) is shown for the first six wake crossings versus φ in Figure 75. The altitudes of the odd-numbered wake crossings (half-orbital periods) increase rapidly with increasing φ from about 50 m at φ = -10 degrees to about 350 m at φ = -90 degrees. This is lowered about 10 m per orbit for each successive odd-numbered wake crossing because of the relative decay of the TAD orbit caused by the differential drag.

The even-numbered wake crossings (whole orbital periods) would all be zero if there was no differential drag. The drag considered here (10^{-6} m/s^2) causes each orbit to decay about 10 m below that of the previous orbit.

Information equivalent to that shown in Figure 74 is presented in a different form in Figure 76. This shows the distance of the wake crossings behind the Shuttle versus wake crossing number with φ parameterized from -10 degrees to -90 degrees.

Figure 77 presents the distance of the TAD in front of the Shuttle versus time with φ parameterized. This figure complements Figure 73. From this figure one can determine, for example, that the TAD ejected at an angle of φ = -10 degrees will stay in front of the Shuttle and within 1 km of the Shuttle for about 4 hours. The TAD ejected at φ = -90 degrees will stay within this region for only 1 hour. This might be a useful criterion for choosing optimum trajectories; i.e., maximize the amount of time that the TAD stays within a certain distance of the Shuttle.

To illustrate the above possibility, the amount of time that the TAD is behind the Shuttle and within a certain distance of the Shuttle versus the ejection angle φ is presented in Figure 78. For example, if we wanted to maximize the amount of time that the TAD is within 2 km of the Shuttle, we would go along the line labeled $x \leqslant 2$ km until we found its maximum point. In this case it occurs at φ = -20 degrees and gives 19.5 hours of time (or about 13 orbits) behind the Shuttle with $x \leqslant 2$ km. Any other ejection angle will give less time in this region. The height at the first wake crossing in this case, from Figure 75, would be about 116 m and that at the second wake crossing would be about -10 m. The wake crossings on each successive orbit would be about 10 m less; so, by the 12th orbit the altitude of the wake crossing on the half-orbit would be slightly negative (-1.7 m from calculations) and the altitude of the wake crossing on the whole orbit would be -118 m. Thus, this orbit starts with nearly all of the vertical displacement above the horizontal plane and ends with all of it below the horizontal plane. This TAD would pass beneath the Shuttle and continue to accelerate down and away from the Shuttle.

In Figure 79 we present the amount of time that the TAD is within a given distance in front of the Shuttle versus the ejection angle φ. These curves all approach a maximum for the smallest possible φ.

Figure 80 gives the amount of time that the TAD is within plus or minus a given distance of the Shuttle versus the ejection angle φ. It is a combination of the two previous figures. The maximums on it occur at the same φ's as the maximums on Figure 78.

From the above discussion it can be seen that the following criteria are among the probable numerous ones available to pick from to optimize the TAD trajectories:

1. Maximize the amount of time behind the Shuttle.

2. Maximize the amount of time within a given distance behind the Shuttle.

3. Maximize the amount of time within plus or minus a given distance of the Shuttle.

4. Do any of the above while limiting the vertical and horizontal oscillations to some given value.

From the discussion in this section it is known that if there are no constraints on maximizing the amount of time behind the Shuttle, that it is practically unlimited. The figures that have been presented enable one to pick optimum values for the remaining possibilities for the single case where ΔV has been limited to 0.1 m/s.

IX. SUMMARY

Hopefully, it has been shown from an operational point of view that TAD's can be useful as diagnostic tools in the AMPS program. Their motions can be controlled to a very significant degree simply through careful control of their ejection conditions. It has been shown that they can be made to go through a specified point at a specified time, and a technique has been developed to determine how accurately the initial conditions must be controlled. Those initial conditions that might result in recontact with the Shuttle have been identified and those which cause the TAD to rapidly leave the vicinity of the Shuttle have been identified. This results in a range of acceptable initial conditions being delineated.

The effect of atmospheric drag on the motion of the TAD's has been demonstrated. It appears doubtful that they can be useful at altitudes as low as 200 km because of the very strong effect of drag there. They probably can be useful at 300 km and most certainly can be useful at 400 km and above.

The targeting capability may prove to be extremely useful because it will allow one to examine whatever point may be of interest to him. The only limitation to examining a large number of points would be the number of TAD's available because, in general, it will require a separate TAD for each discrete point to be examined (unless the TAD's are recovered and reused).

A brief look was taken at what an uncertainty in differential drag might do to targeting accuracy. It was shown that at high altitudes ($\geqslant$ 400 km), it is probably of little consequence. At lower altitudes ($\leqslant$ 300 km), however, it could definitely pose a significant problem.

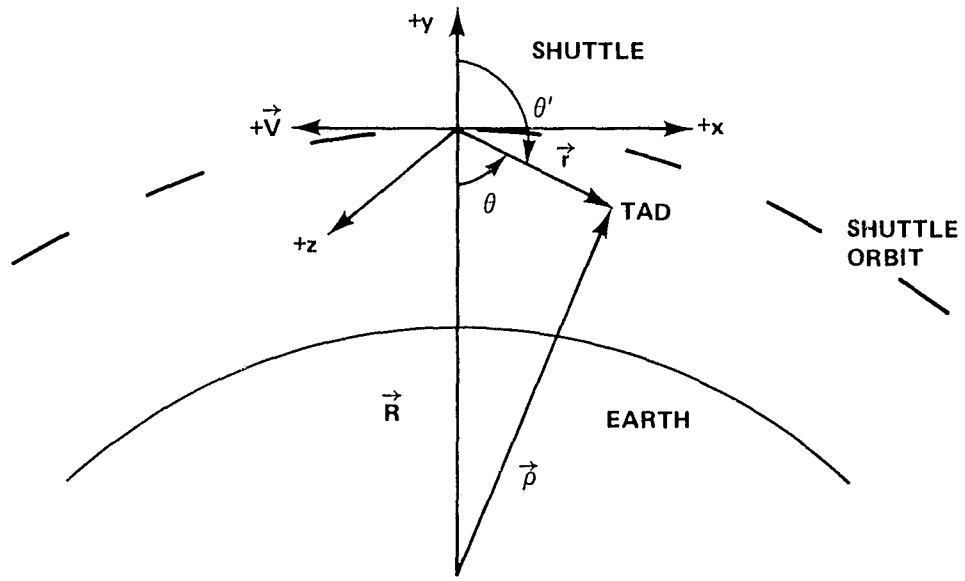

Figure 1. Relative coordinate system.

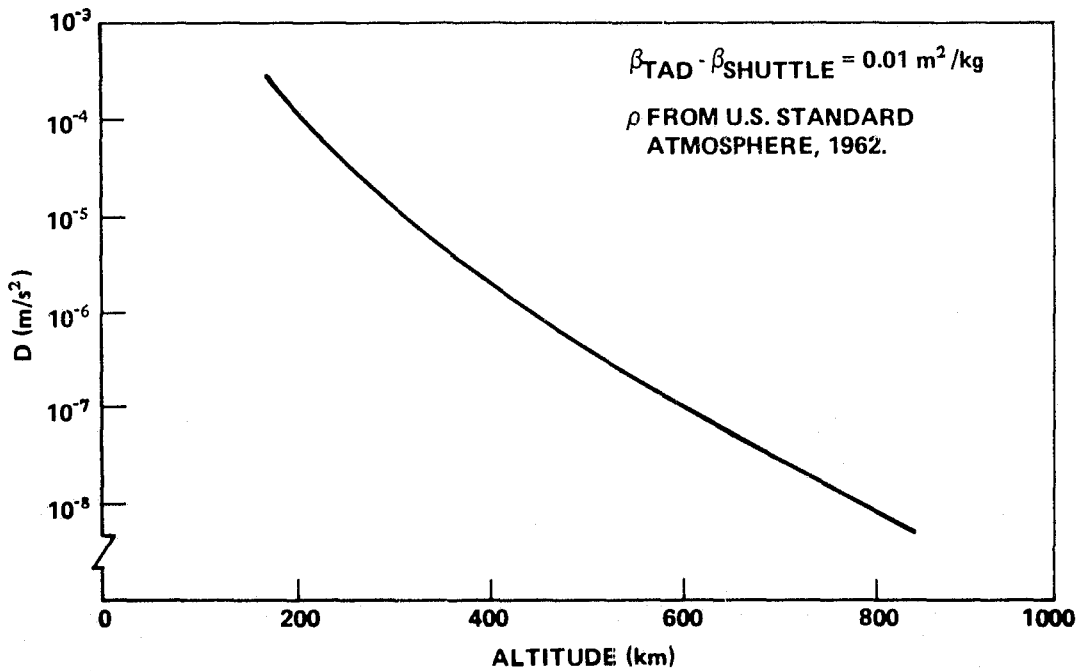

Figure 2. Differential drag D versus altitude for constant ballistic coefficients.

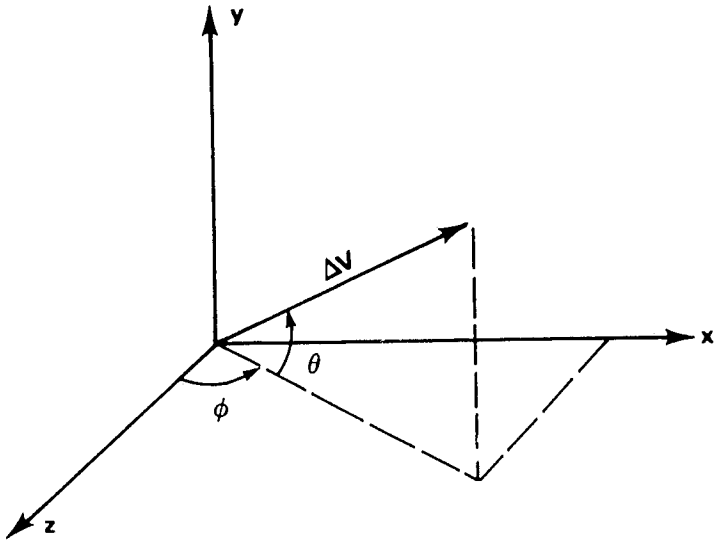

Figure 3. Ejection velocity.

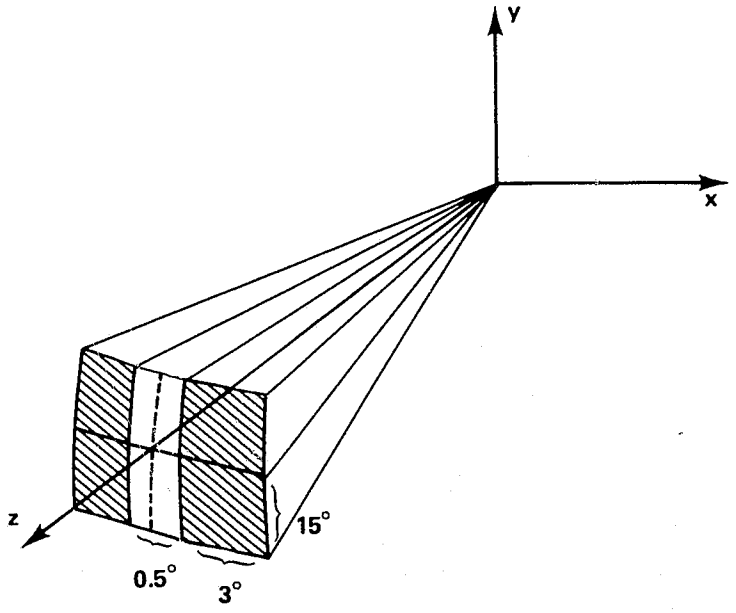

Figure 4. Allowable ejection directions.

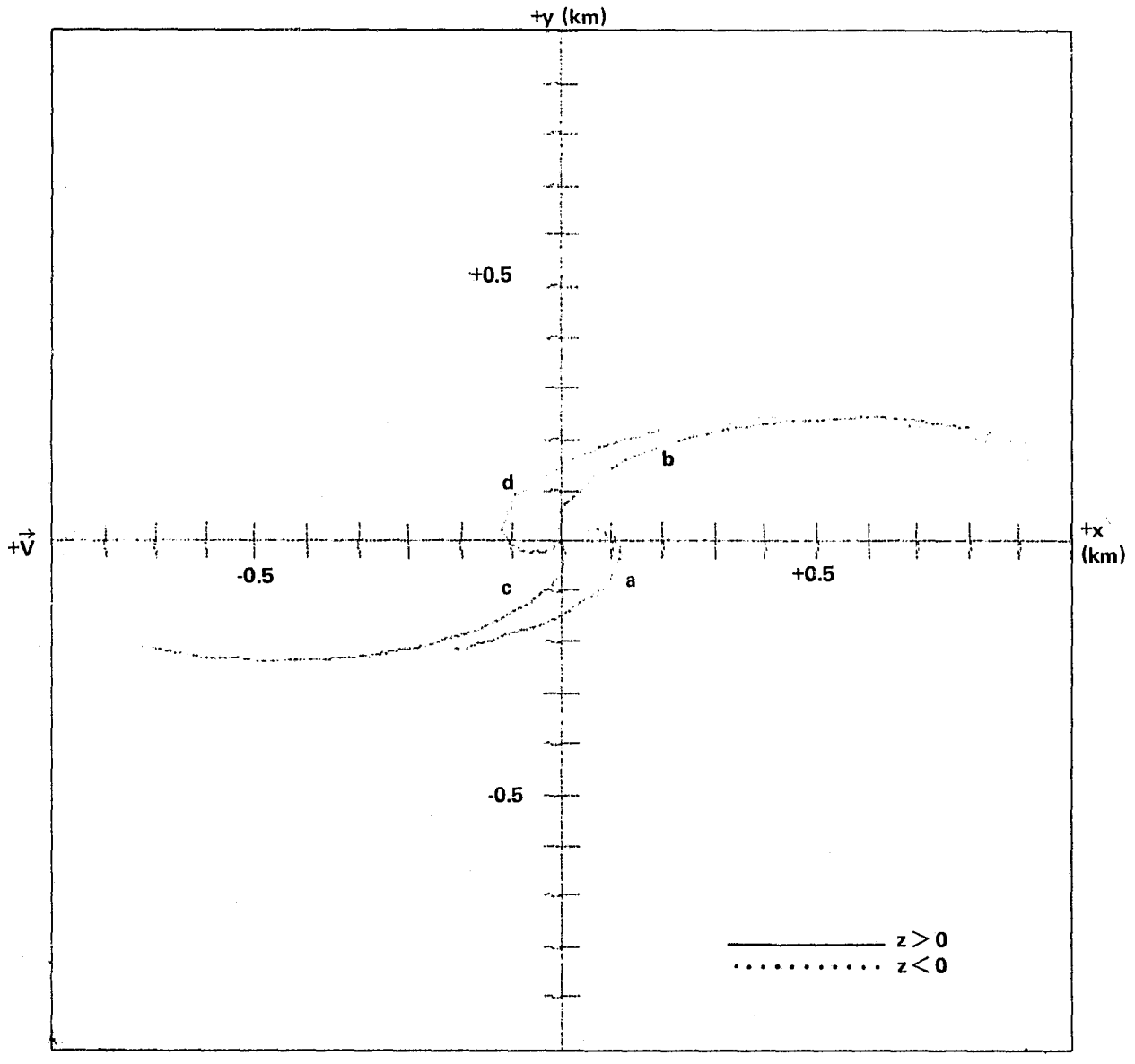

400 km CIRCULAR ORBIT $D = 1 \times 10^{-6}$ m/s^2

CASES	θ (degrees)	φ (degrees)	ΔV (m/s)
a	+5	+3.5	1
b	+5	-3.5	1
c	-5	+3.5	1
d	-5	-3.5	1

DOTS ARE SEPARATED BY 1 min IN TIME.

Figure 5. The x-y projection of the relative motion.

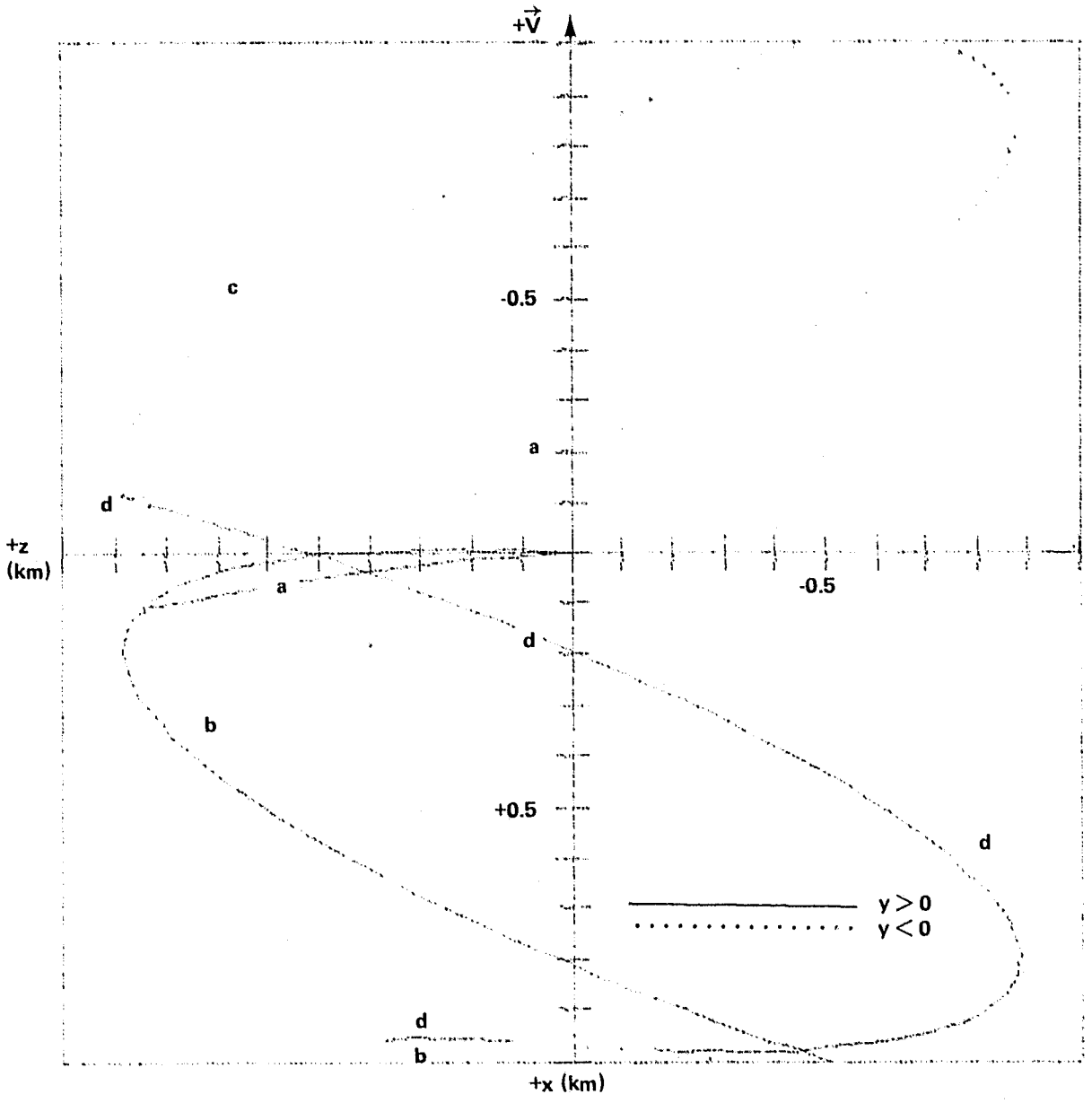

400 km CIRCULAR ORBIT $D = 1 \times 10^{-6}$ m/s^2

CASES	θ (degrees)	φ (degrees)	ΔV (m/s)
a	+5	+3.5	1
b	+5	-3.5	1
c	-5	+3.5	1
d	-5	-3.5	1

DOTS ARE SEPARATED BY 1 min IN TIME.

Figure 6. The x-z projection of the relative motion.

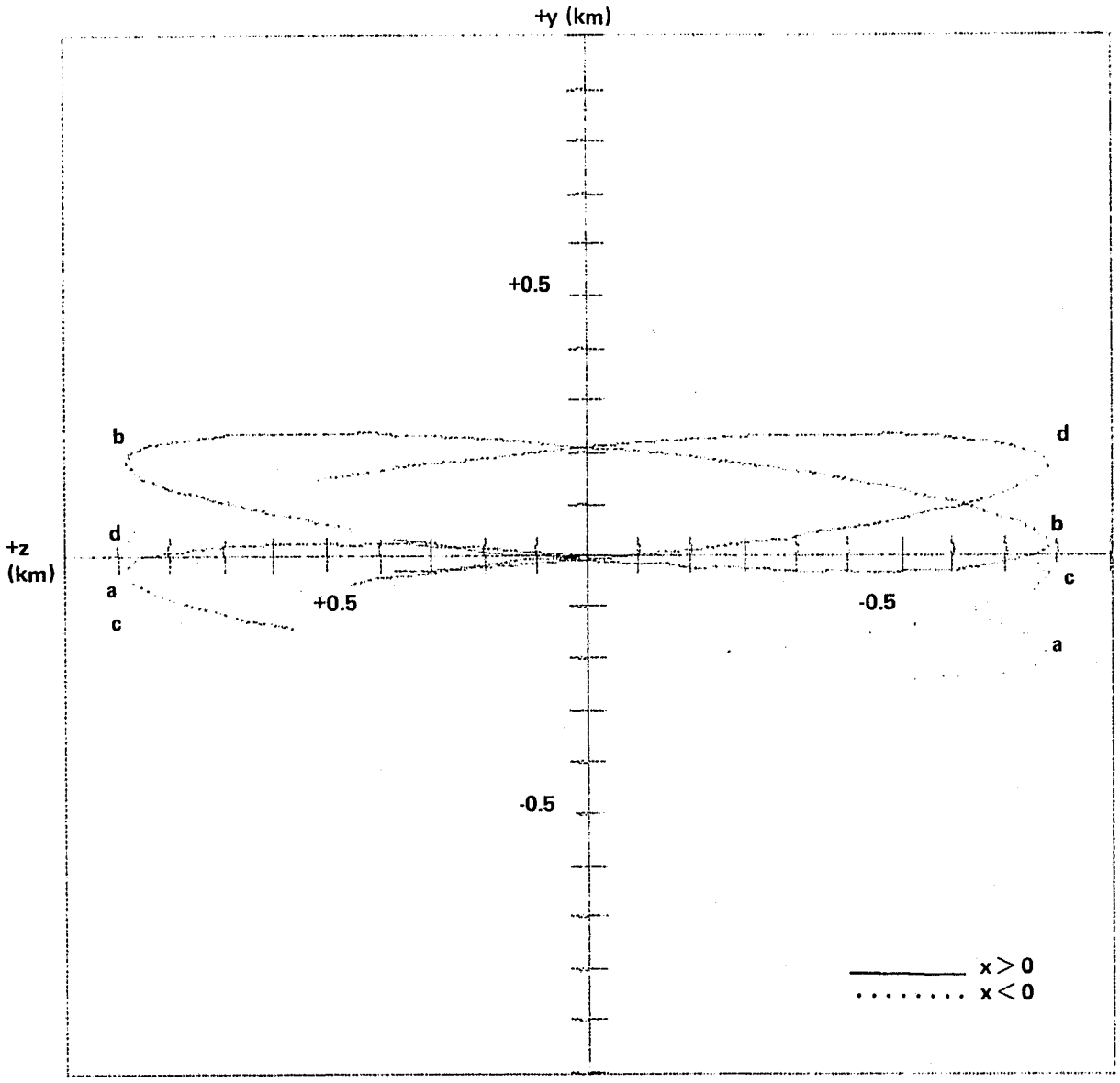

400 km CIRCULAR ORBIT $D = 1 \times 10^{-6}$ m/s^2

CASES	θ (degrees)	φ (degrees)	ΔV (m/s)
a	+5	+3.5	1
b	+5	-3.5	1
c	-5	+3.5	1
d	-5	-3.5	1

DOTS ARE SEPARATED BY 1 min IN TIME. ORBITAL VELOCITY VECTOR INTO PAGE.

Figure 7. The y-z projection of the relative motion.

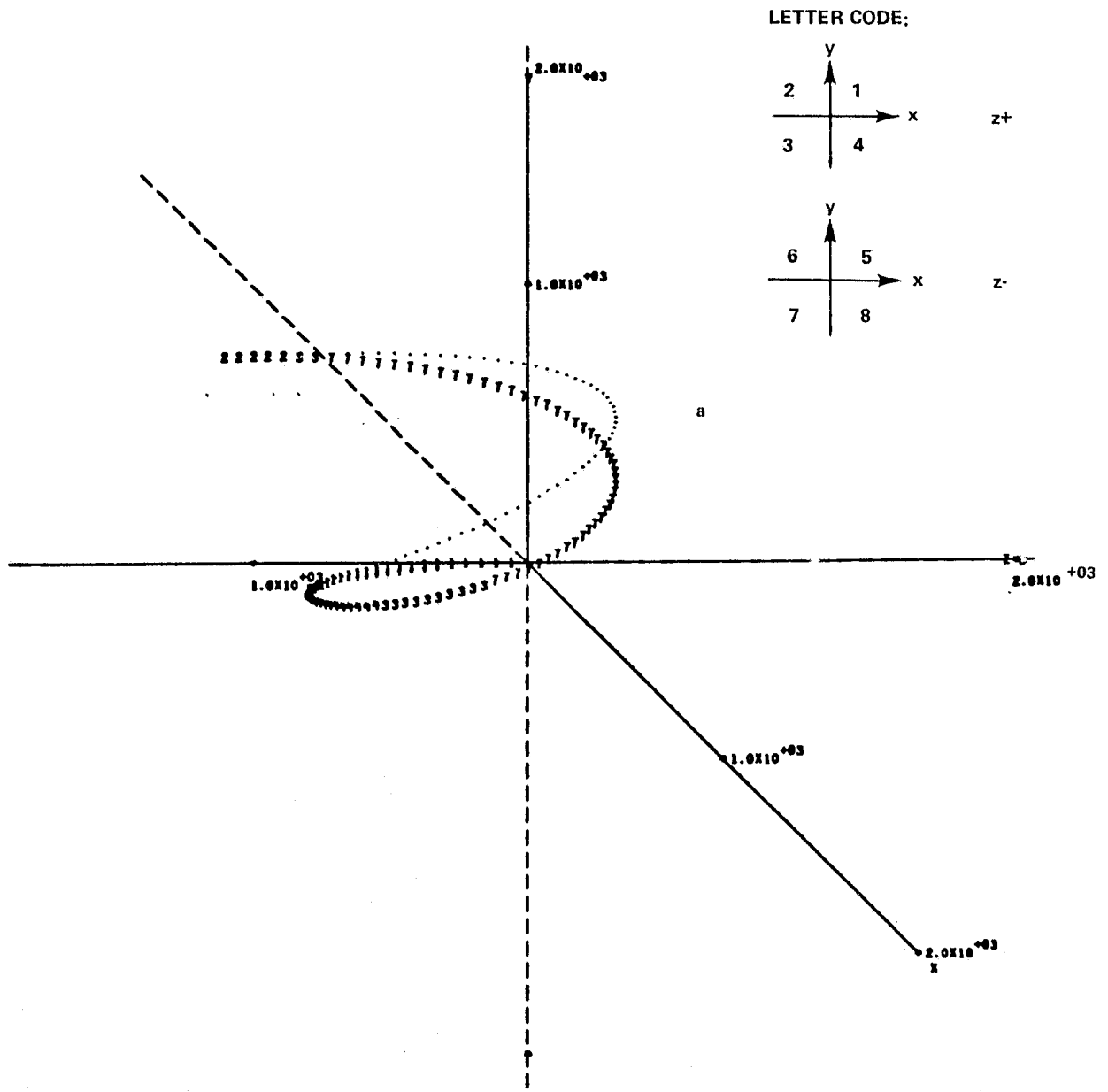

400 km CIRCULAR ORBIT

$D = 1 \times 10^{-6}$ m/s^2

INITIAL CONDITIONS:

CASE a $\theta = +5°$

$\varphi = +3.5°$

$\Delta V = 1$ m/s

Figure 8. Three-dimensional plot of the motion of a TAD relative to the Space Shuttle for approximately one orbit.

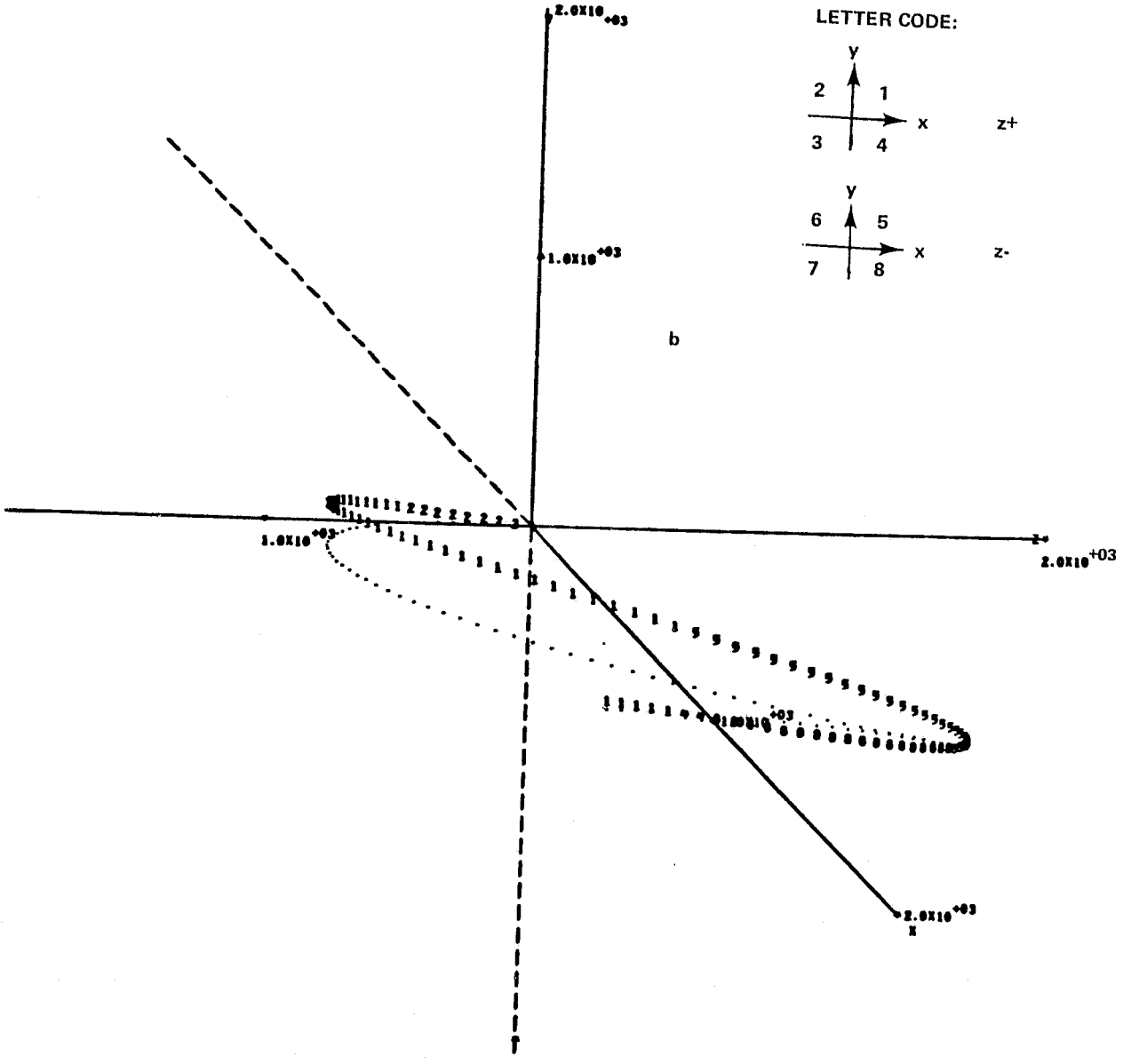

400 km CIRCULAR ORBIT

$D = 1 \times 10^{-6}$ m/s^2

INITIAL CONDITIONS:

CASE b $\theta = +5°$

$\varphi = -3.5°$

$\Delta V = 1$ m/s

Figure 9. Three-dimensional plot of the motion of a TAD relative to the Space Shuttle for approximately one orbit.

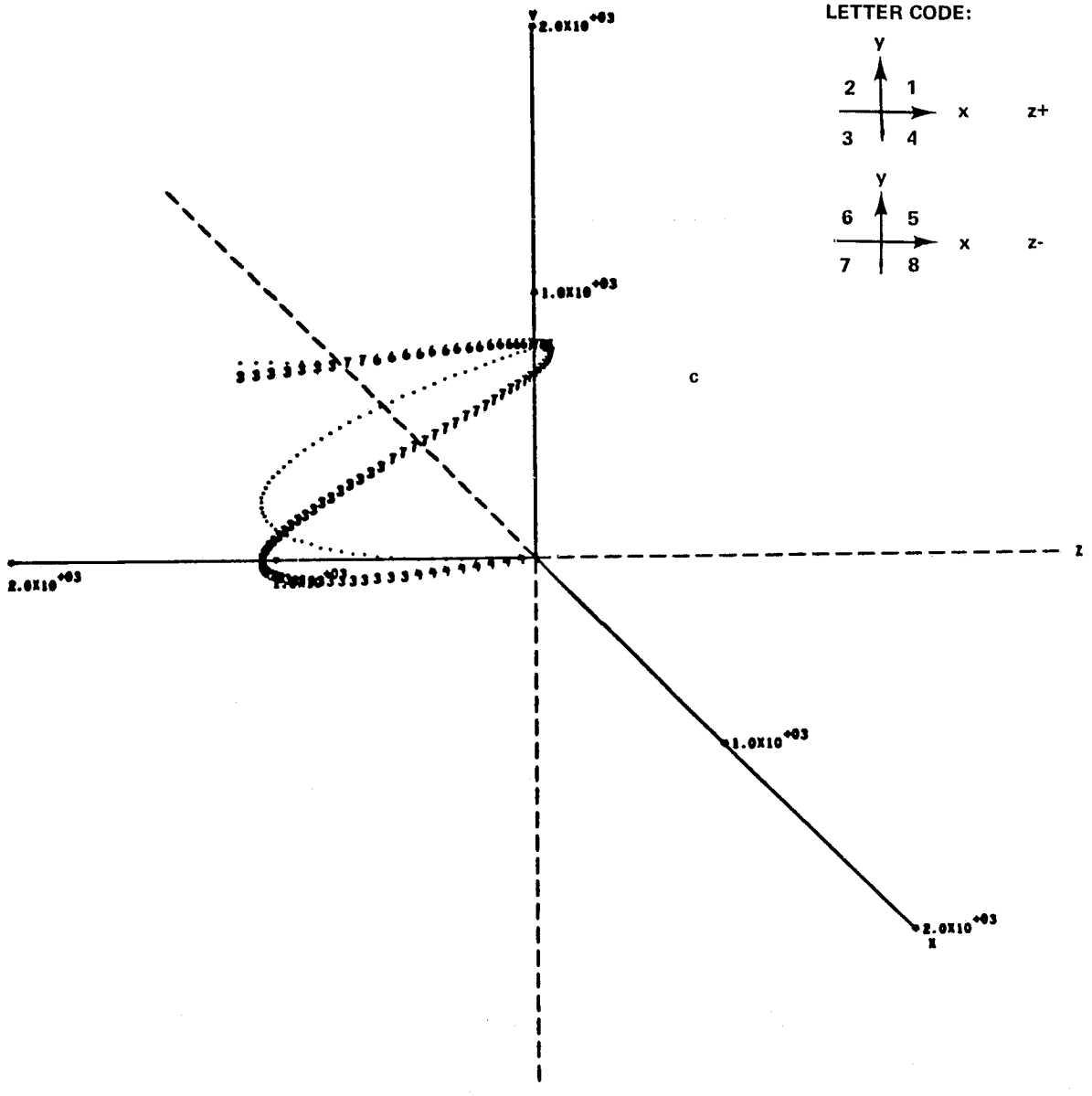

400 km CIRCULAR ORBIT

$D = 1 \times 10^{-6}$ m/s^2

INITIAL CONDITIONS:

CASE c

$\theta = -5^\circ$

$\varphi = +3.5^\circ$

$\Delta V = 1$ m/s

Figure 10. Three-dimensional plot of the motion of a TAD relative to the Space Shuttle for approximately one orbit.

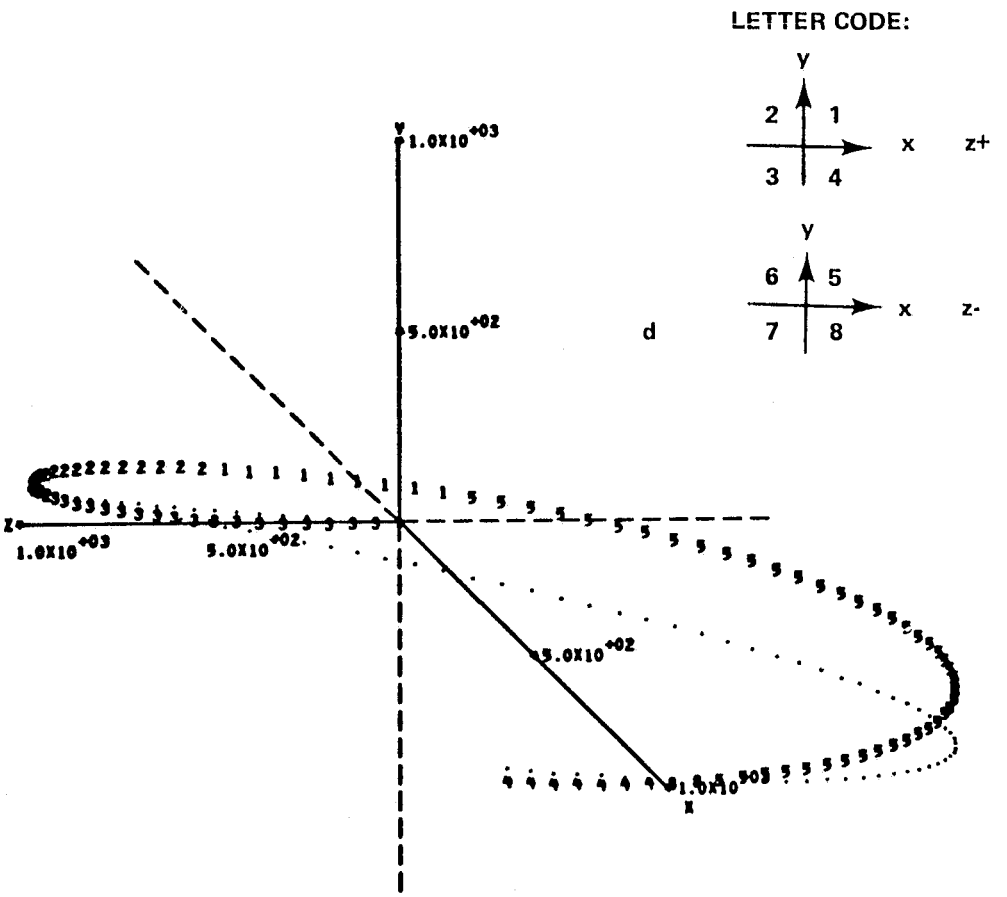

400 km CIRCULAR ORBIT

$D = 1 \times 10^{-6}$ m/s^2

INITIAL CONDITIONS:

CASE d $\theta = -5°$

$\varphi = -3.5°$

$\Delta V = 1$ m/s

Figure 11. Three-dimensional plot of the motion of a TAD relative to the Space Shuttle for approximately one orbit.

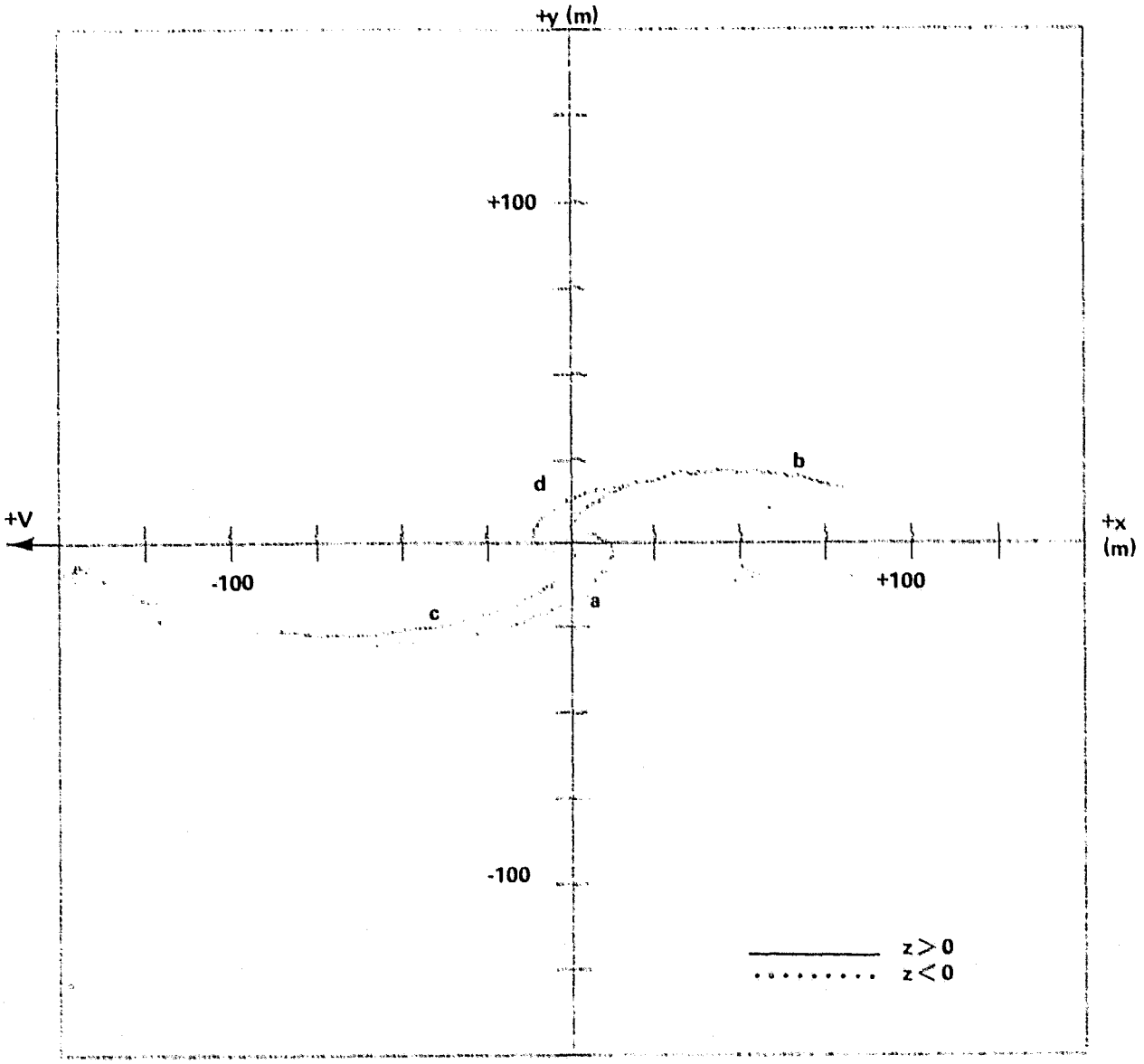

400 km CIRCULAR ORBIT $D = 1 \times 10^{-6}$ m/s^2

CASE	θ (degrees)	φ (degrees)	ΔV (m/s)
a	+5	+3.5	0.1
b	+5	-3.5	0.1
c	-5	+3.5	0.1
d	-5	-3.5	0.1

DOTS ARE SEPARATED BY 1 min IN TIME.

Figure 12. The x-y projection of the relative motion.

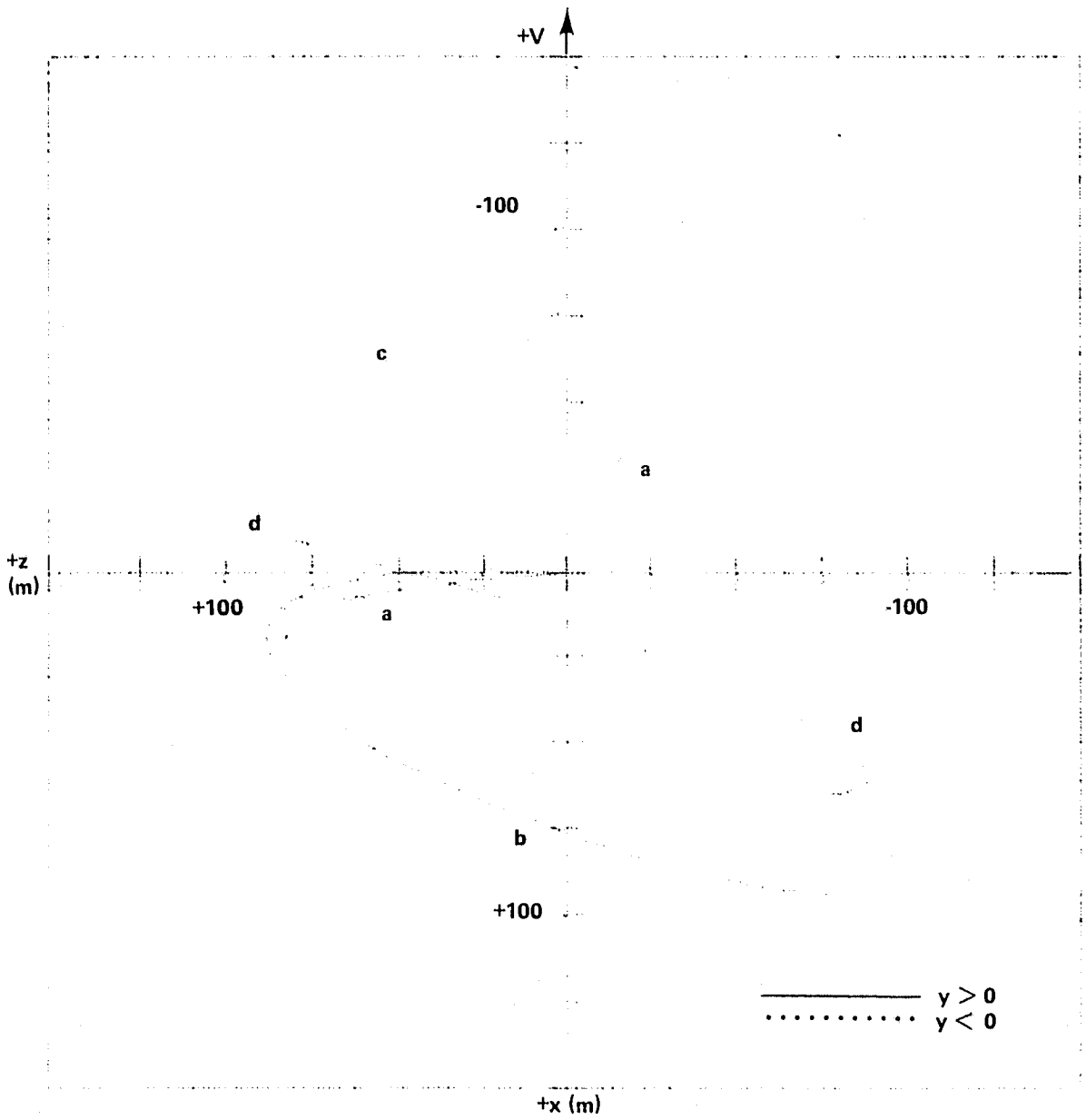

400 km CIRCULAR ORBIT $D = 1 \times 10^{-6}$ m/s^2

CASE	θ (degrees)	φ (degrees)	ΔV (m/s)
a	+5	+3.5	0.1
b	+5	-3.5	0.1
c	-5	+3.5	0.1
d	-5	-3.5	0.1

DOTS ARE SEPARATED BY 1 min IN TIME.

Figure 13. The x-z projection of the relative motion.

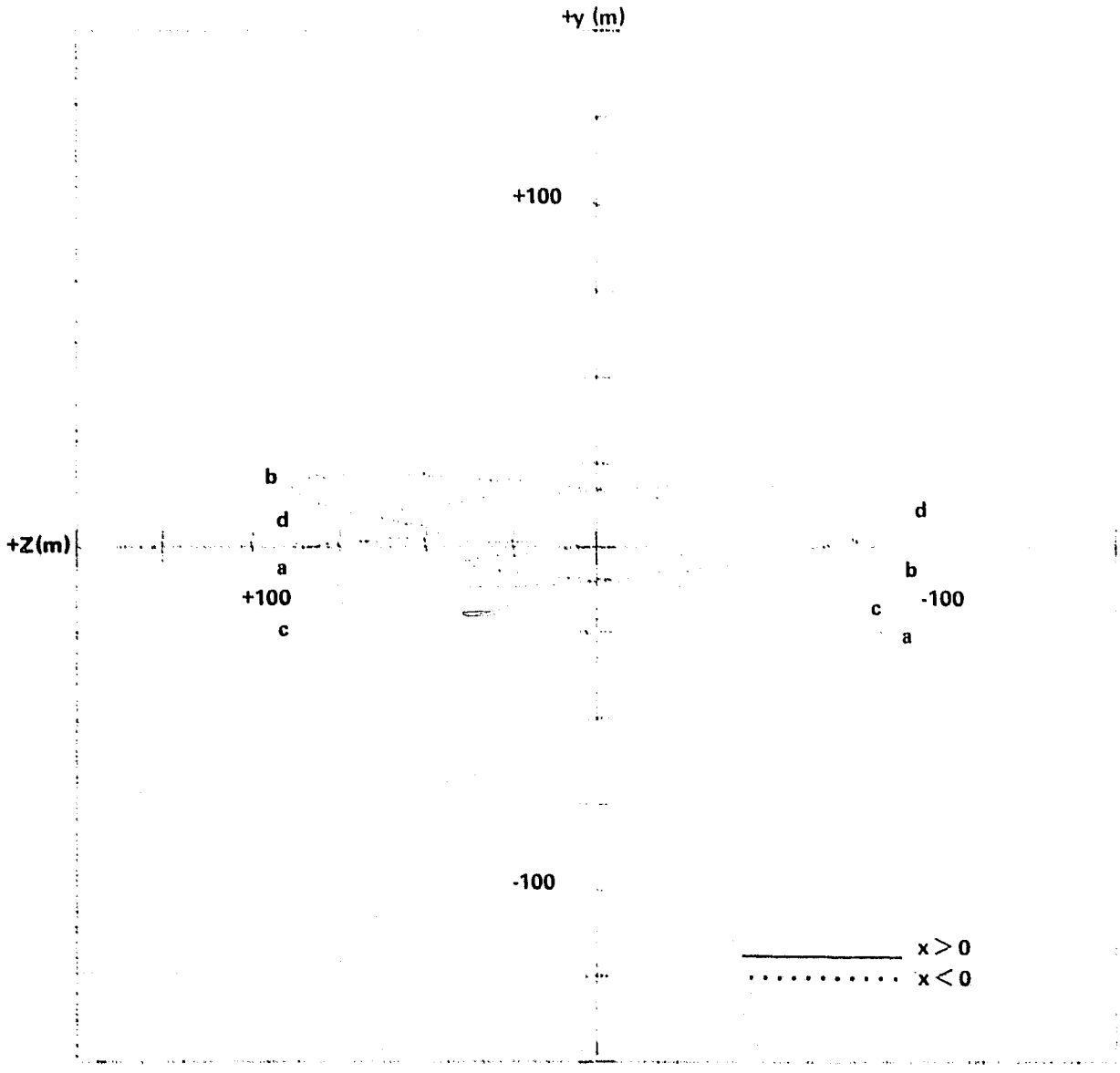

400 km CIRCULAR ORBIT $D = 1 \times 10^{-6}$ m/s^2

CASE	θ (degrees)	φ (degrees)	ΔV (m/s)
a	+5	+3.5	0.1
b	+5	-3.5	0.1
c	-5	+3.5	0.1
d	-5	-3.5	0.1

DOTS ARE SEPARATED BY 1 min IN TIME. ORBITAL VELOCITY VECTOR INTO PAGE.

Figure 14. The y-z projection of the relative motion.

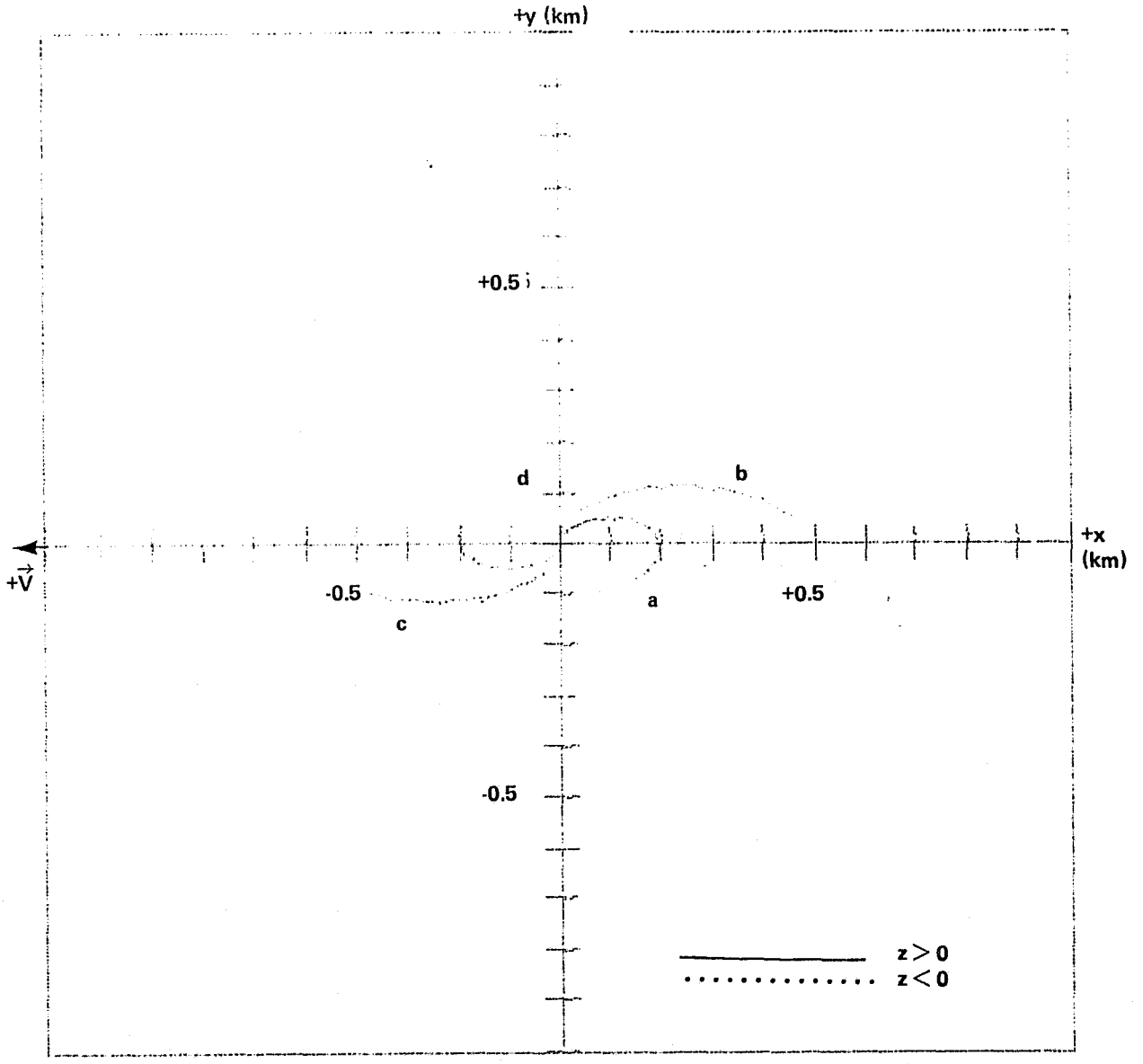

400 km CIRCULAR ORBIT $D = 1 \times 10^{-6}$ m/s^2

CASE	θ (degrees)	φ (degrees)	ΔV (m/s)
a	+5	+1	1
b	+5	-1	1
c	-5	+1	1
d	-5	-1	1

DOTS ARE SEPARATED BY 1 min IN TIME.

Figure 15. The x-y projection of the relative motion.

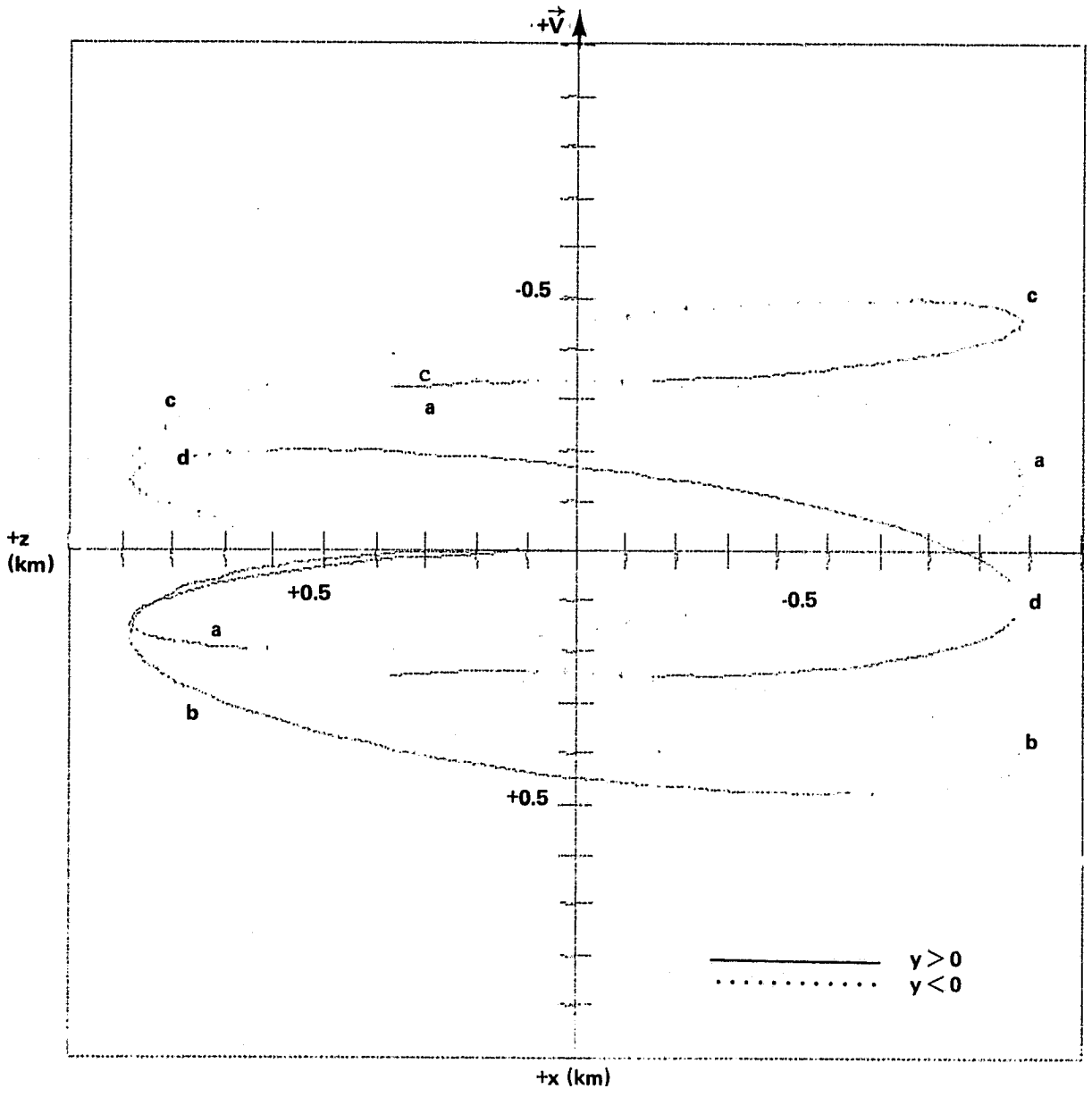

400 km CIRCULAR ORBIT $D = 1 \times 10^{-6}$ m/s^2

CASE	θ (degrees)	φ (degrees)	ΔV (m/s)
a	+5	+1	1
b	+5	-1	1
c	-5	+1	1
d	-5	-1	1

DOTS ARE SEPARATED BY 1 min IN TIME.

Figure 16. The x-z projection of the relative motion.

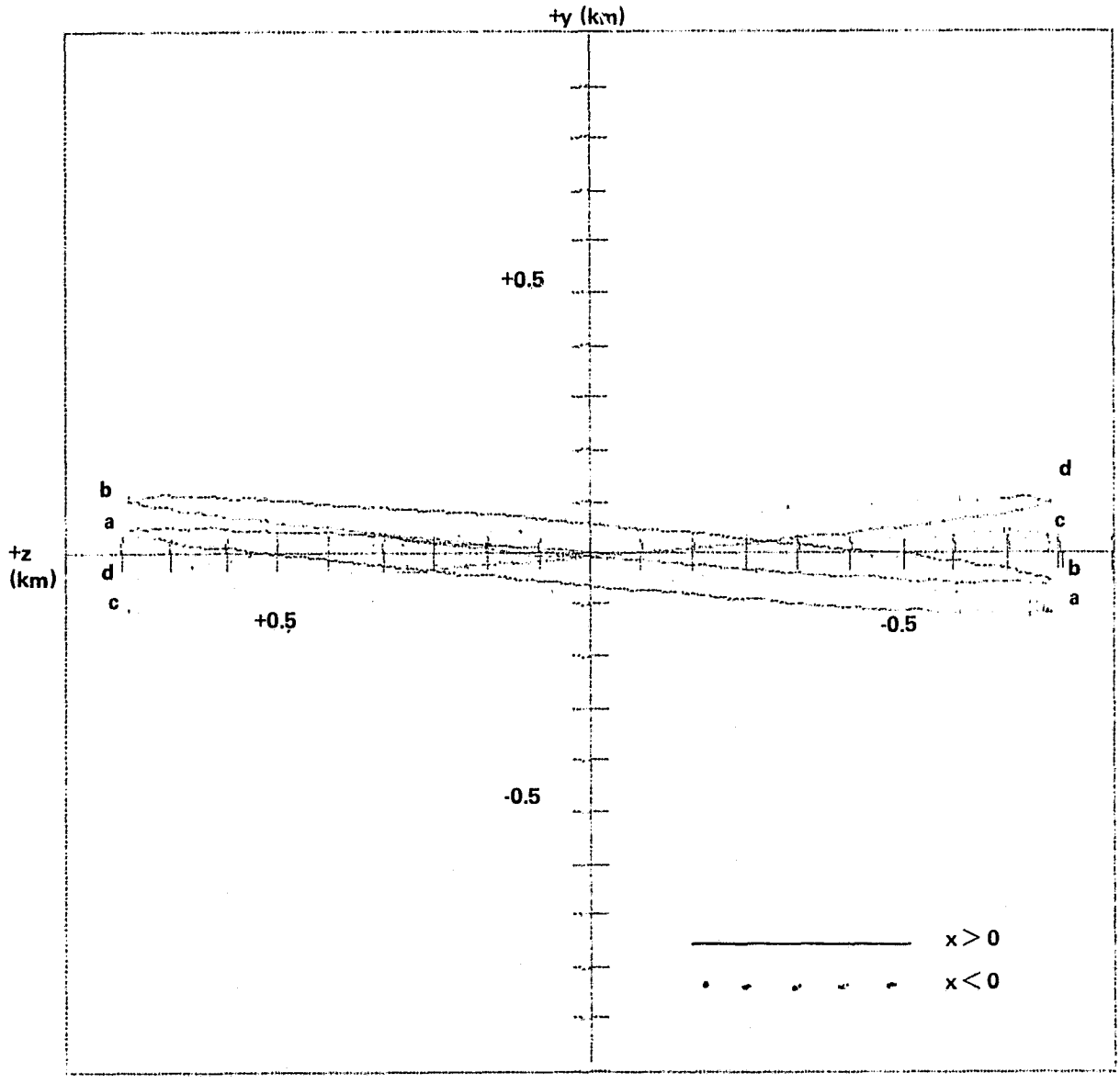

400 km CIRCULAR ORBIT $D = 1 \times 10^{-6}$ m/s^2

CASE	θ (degrees)	φ (degrees)	ΔV (m/s)
a	+5	+1	1
b	+5	-1	1
c	-5	+1	1
d	-5	-1	1

DOTS ARE SEPARATED BY 1 min IN TIME. ORBITAL VELOCITY VECTOR INTO PAGE.

Figure 17. The y-z projection of the relative motion.

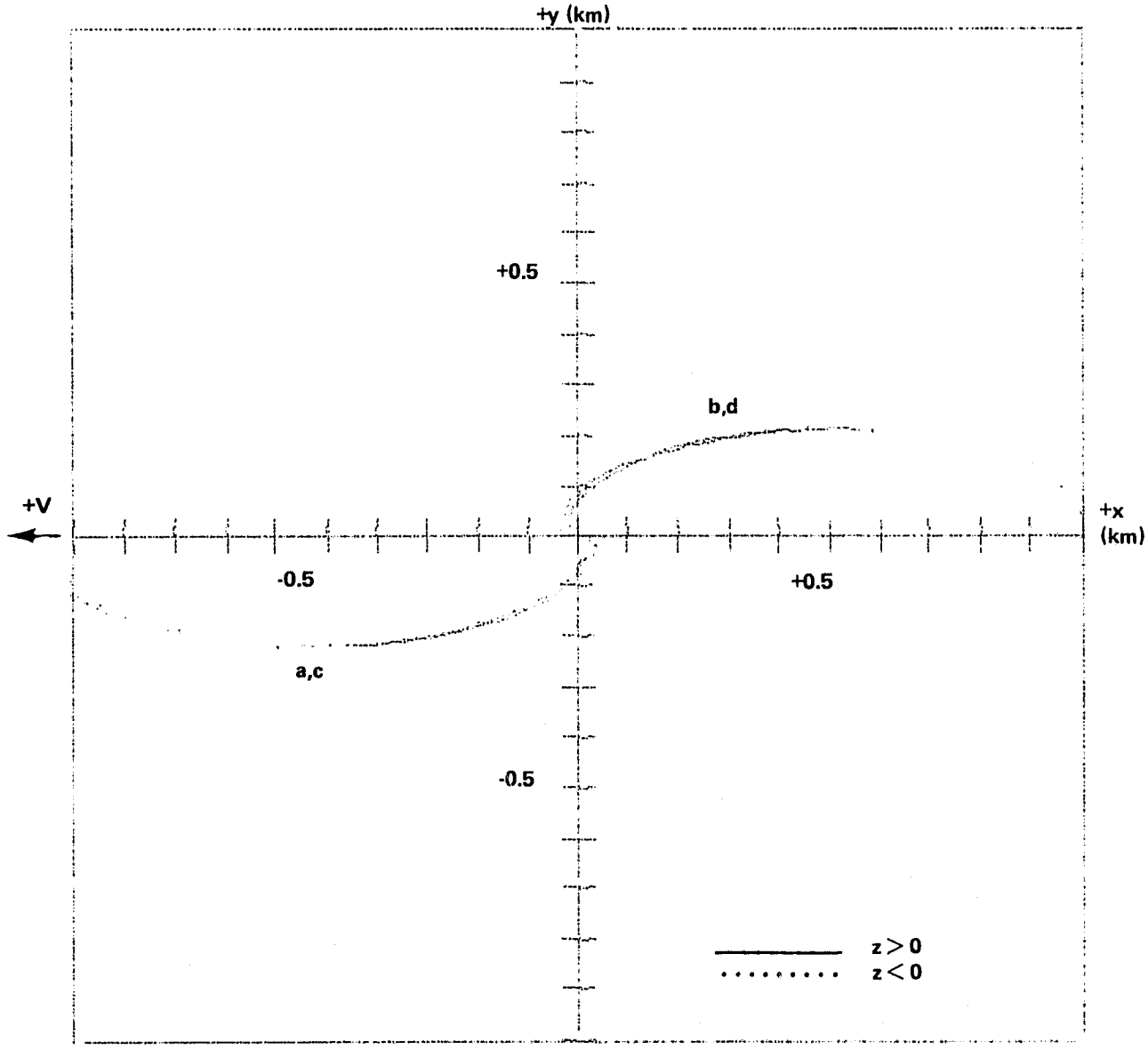

400 km CIRCULAR ORBIT $D = 1 \times 10^{-6}$ m/s^2

CASE	θ (degrees)	φ (degrees)	ΔV (m/s)
a	+1	+3.5	1
b	+1	-3.5	1
c	-1	+3.5	1
d	-1	-3.5	1

DOTS ARE SEPARATED BY 1 min IN TIME.

Figure 18. The x-y projection of the relative motion.

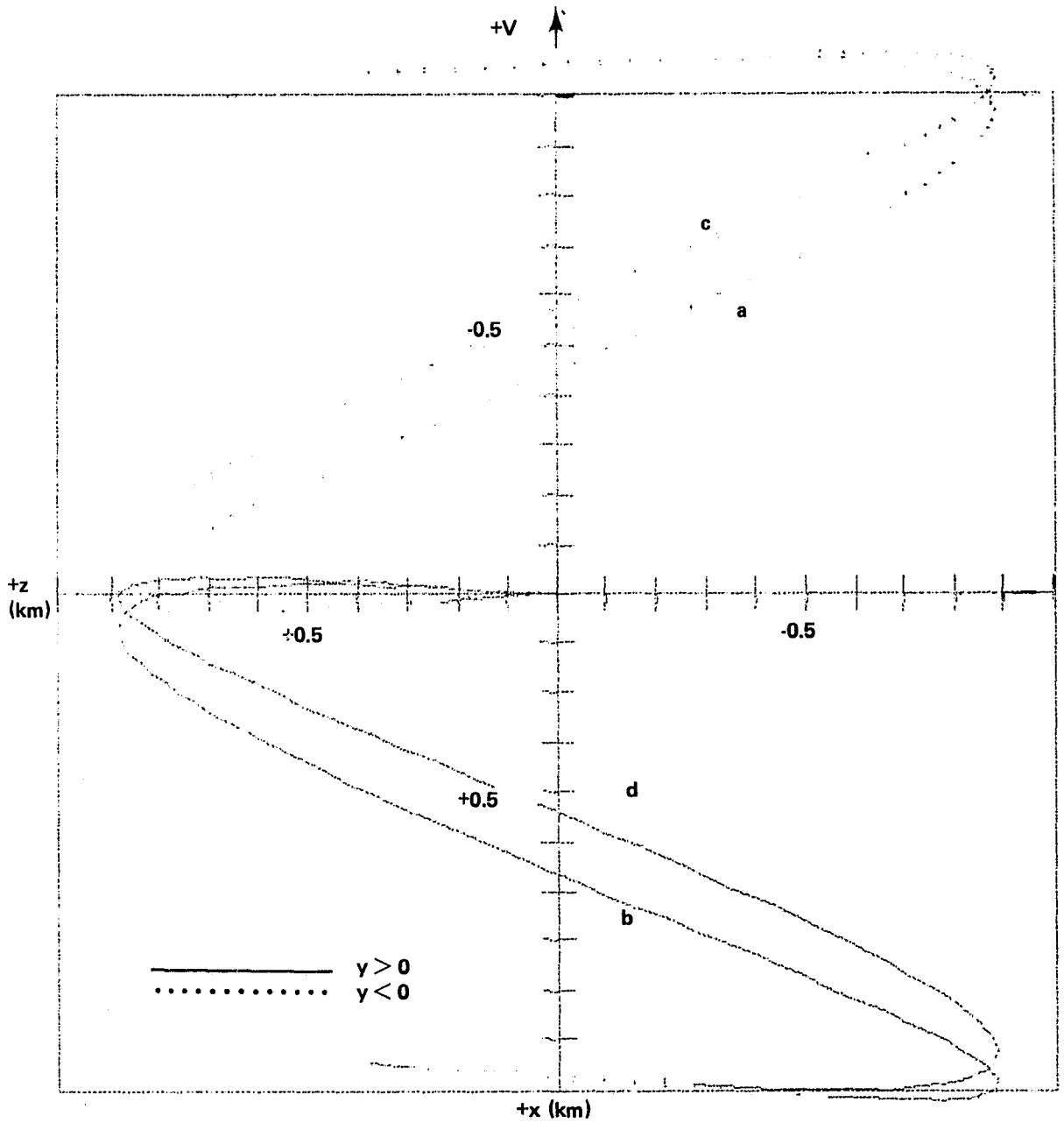

400 km CIRCULAR ORBIT $D = 1 \times 10^{-6}$ m/s^2

CASE	θ (degrees)	φ (degrees)	ΔV (m/s)
a	+1	+3.5	1
b	+1	-3.5	1
c	-1	+3.5	1
d	-1	-3.5	1

DOTS ARE SEPARATED BY 1 min IN TIME.

Figure 19. The x-z projection of the relative motion.

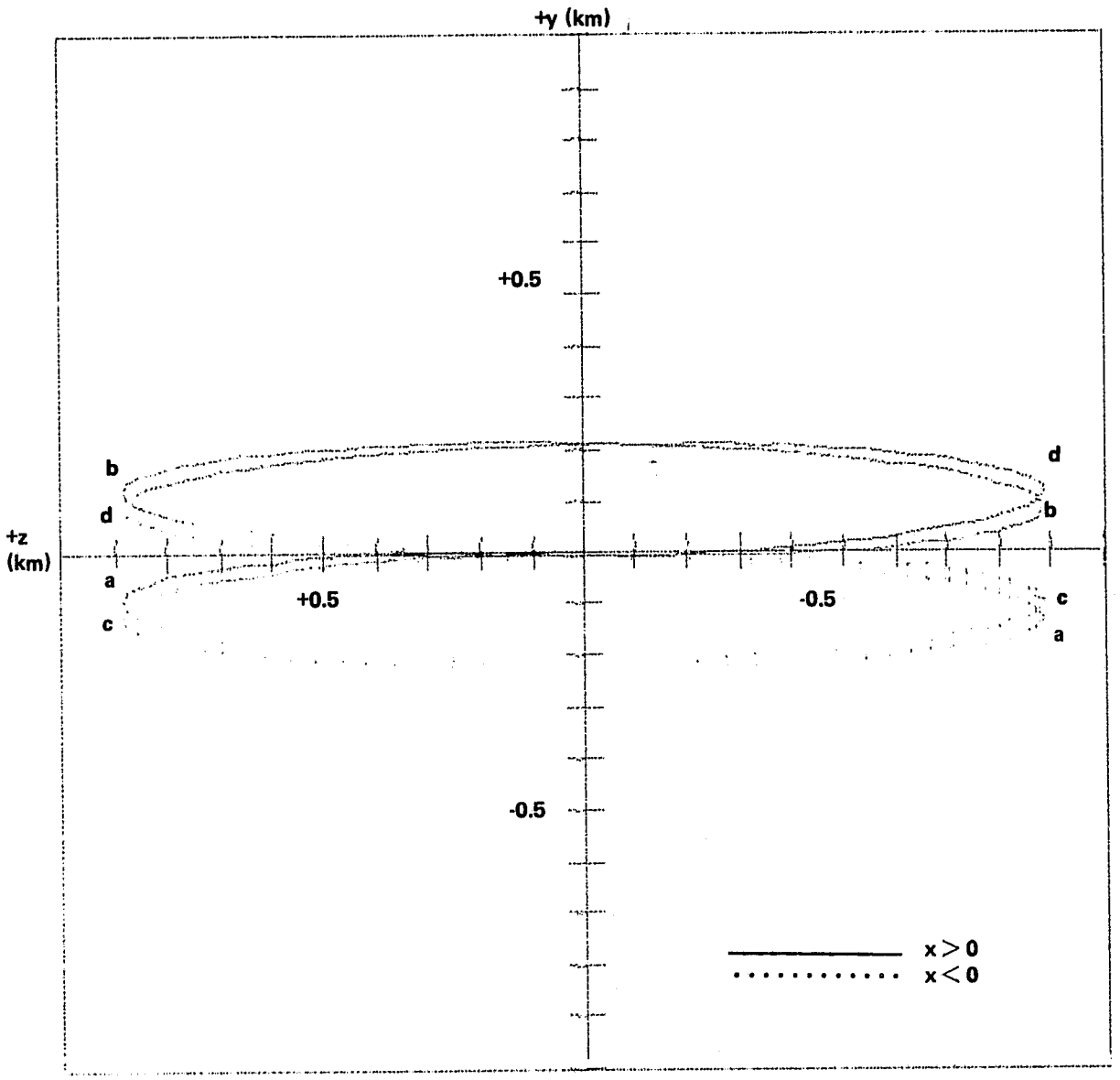

400 km CIRCULAR ORBIT $D = 1 \times 10^{-6}$ m/s^2

CASES	θ (degrees)	φ (degrees)	ΔV (m/s)
a	+1	+3.5	1
b	+1	-3.5	1
c	-1	+3.5	1
d	-1	-3.5	1

DOTS SEPARATED BY 1 min IN TIME. ORBITAL VELOCITY VECTOR INTO PAGE.

Figure 20. The y-z projection of the relative motion.

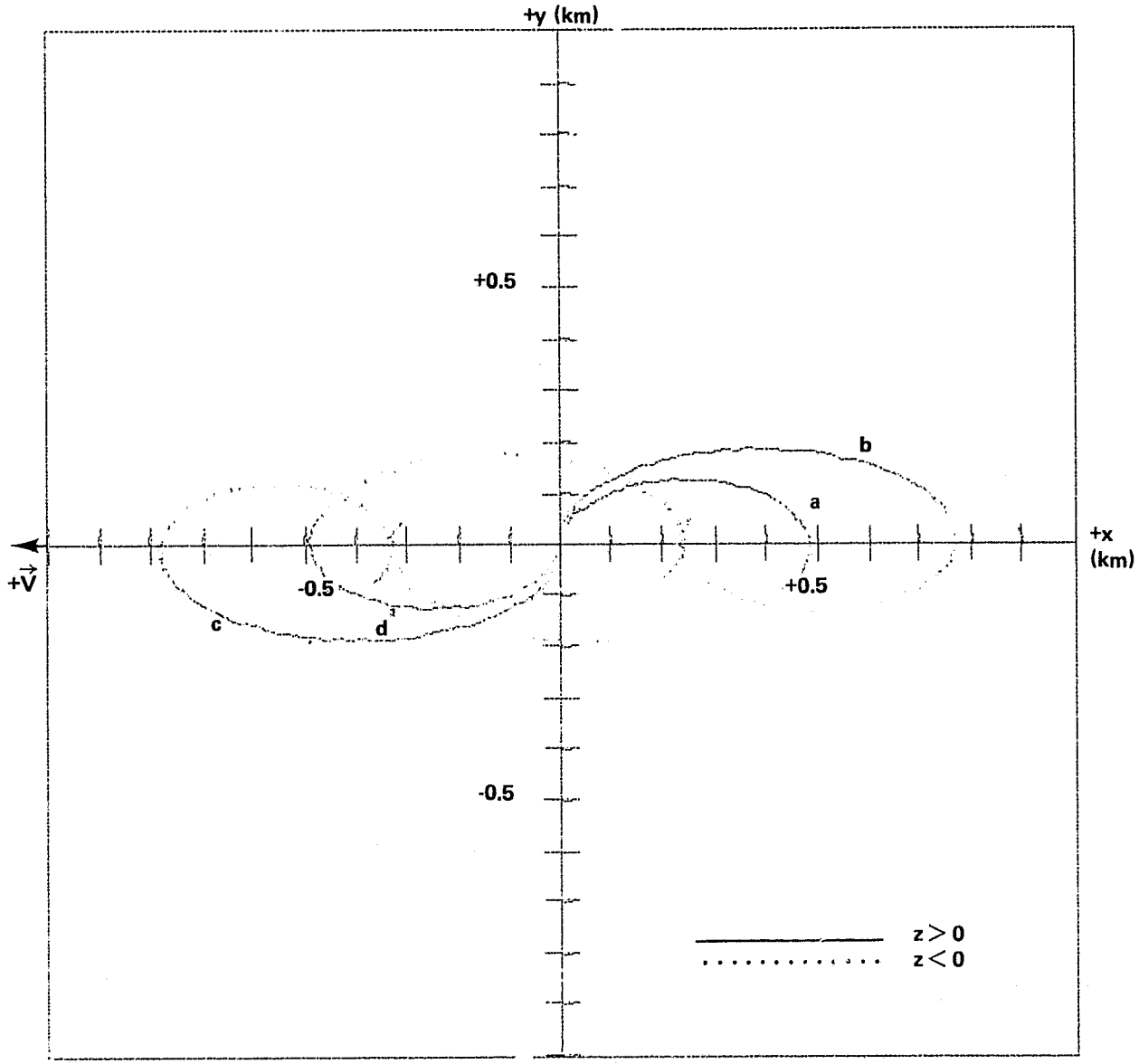

400 km CIRCULAR ORBIT $D = 1 \times 10^{-6}$ m/s^2

CASE	θ (degrees)	φ (degrees)	ΔV (m/s)
a	+10	+1	1
b	+10	-1	1
c	-10	+1	1
d	-10	-1	1

DOTS ARE SEPARATED BY 1 min IN TIME.

Figure 21. The x-y projection of the relative motion.

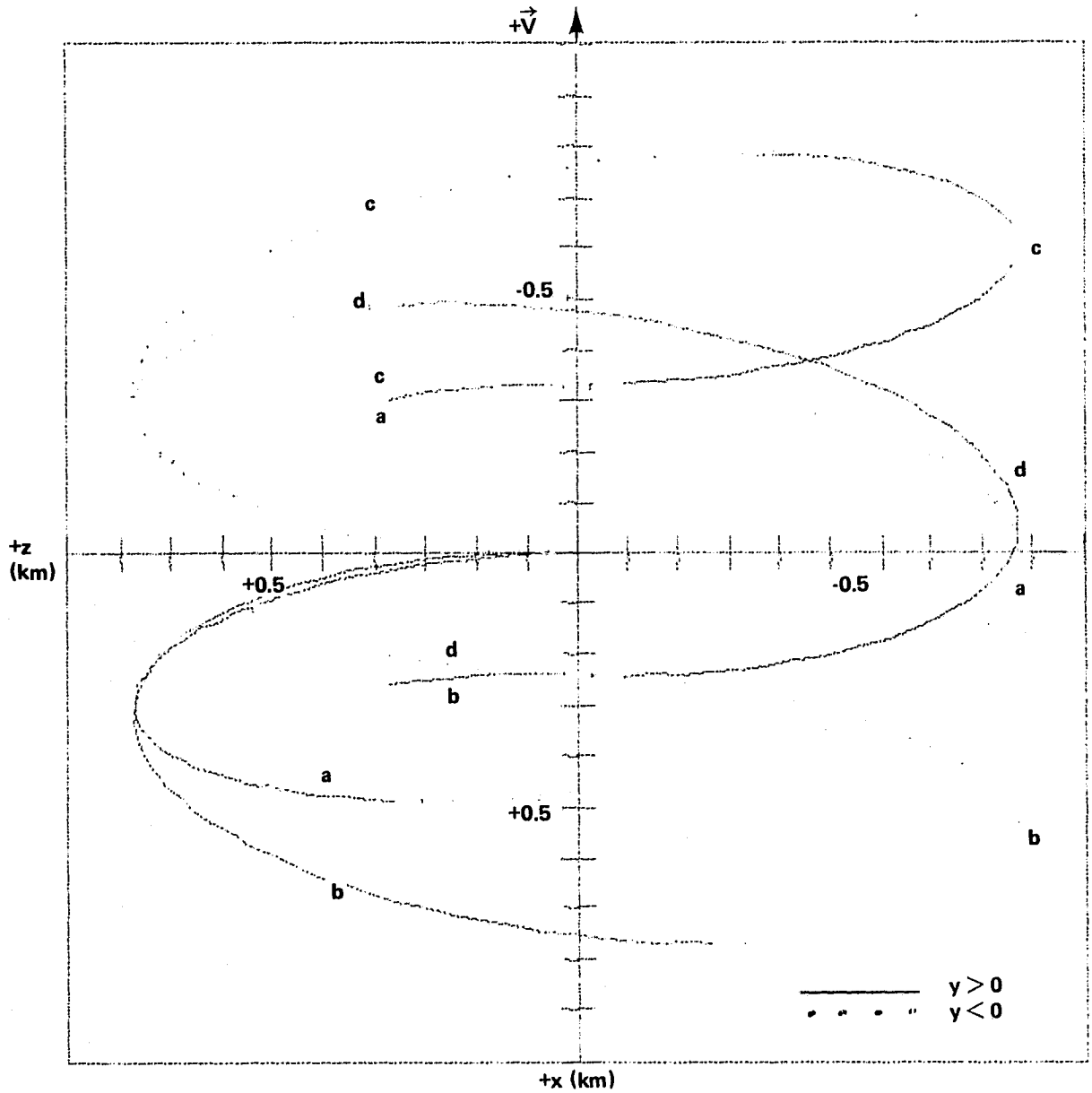

400 km CIRCULAR ORBIT $D = 1 \times 10^{-6}$ m/s^2

CASE	θ (degrees)	φ (degrees)	ΔV (m/s)
a	+10	+1	1
b	+10	-1	1
c	-10	+1	1
d	-10	-1	1

DOTS ARE SEPARATED BY 1 min IN TIME.

Figure 22. The x-z projection of the relative motion.

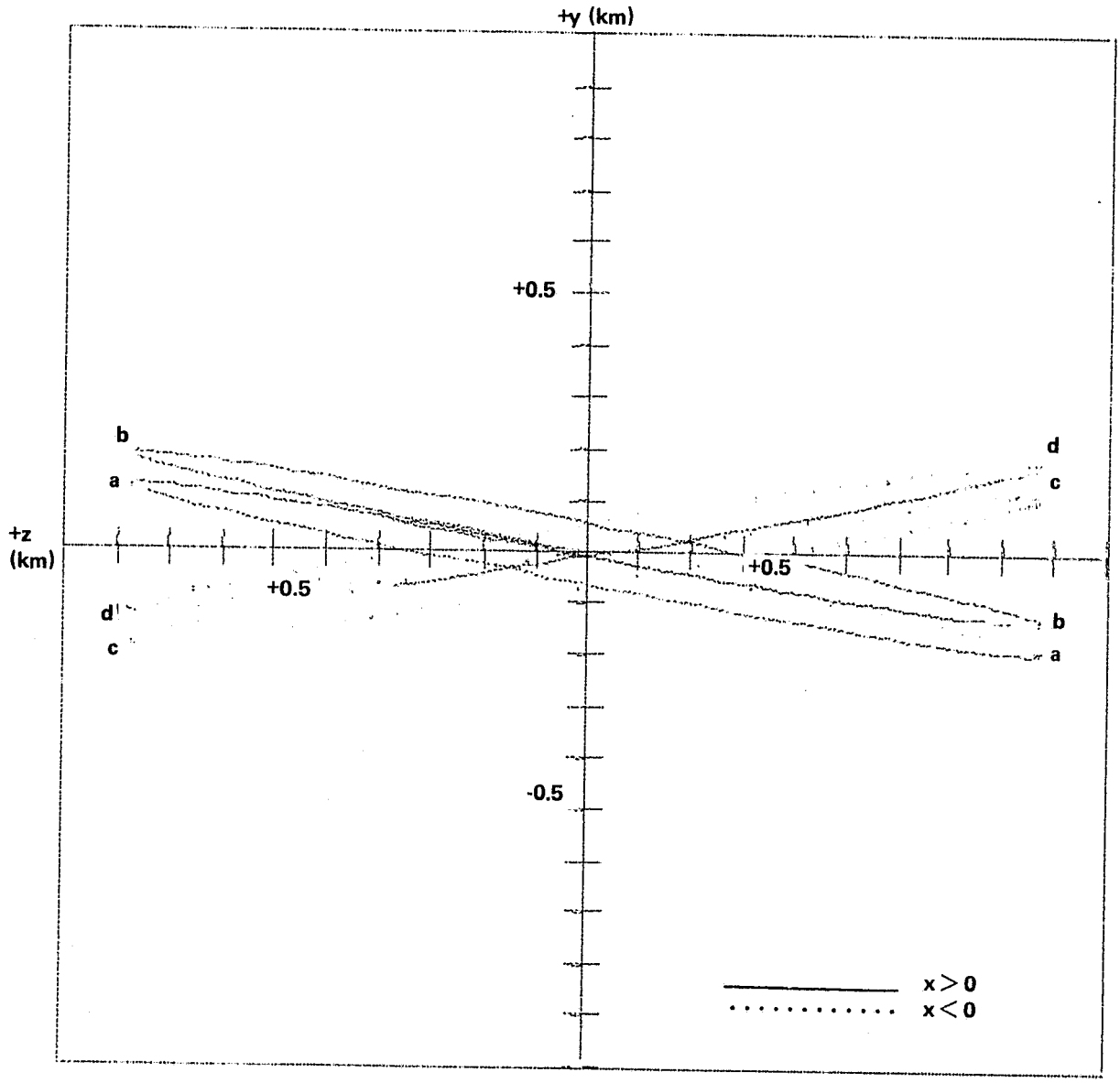

400 km CIRCULAR ORBIT

$D = 1 \times 10^{-6}$ m/s^2

CASE	θ (degrees)	φ (degrees)	ΔV (m/s)
a	+10	+1	1
b	+10	-1	1
c	-10	+1	1
d	-10	-1	1

DOTS ARE SEPARATED BY 1 min IN TIME. ORBITAL VELOCITY VECTOR INTO PAGE.

Figure 23. The y-z projection of the relative motion.

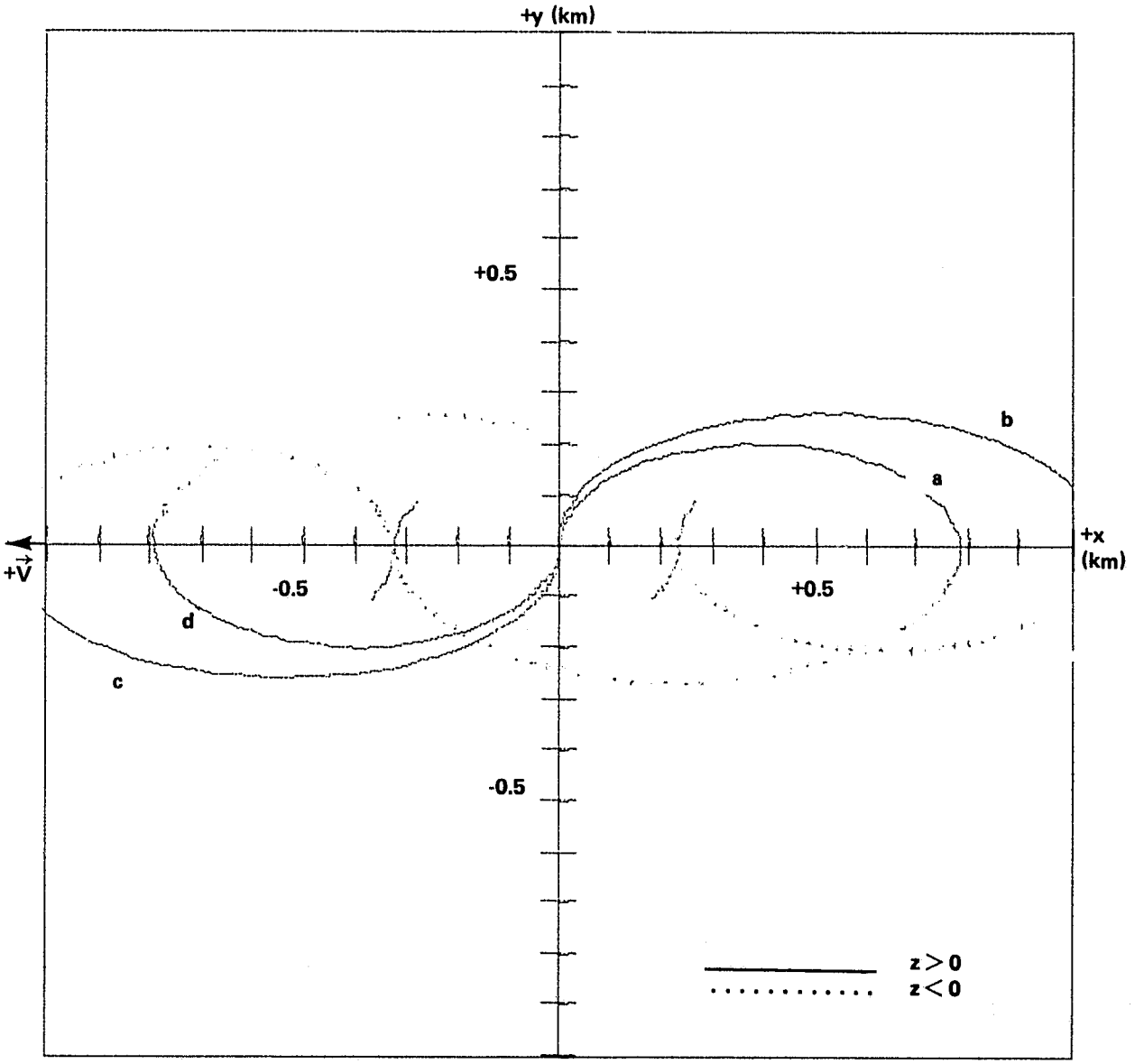

400 km CIRCULAR ORBIT $D = 1 \times 10^{-6}$ m/s^2

CASE	θ (degrees)	φ (degrees)	ΔV (m/s)
a	+15	+1	1
b	+15	-1	1
c	-15	+1	1
d	-15	-1	1

DOTS ARE SEPARATED BY 1 min IN TIME.

Figure 24. The x-y projection of the relative motion.

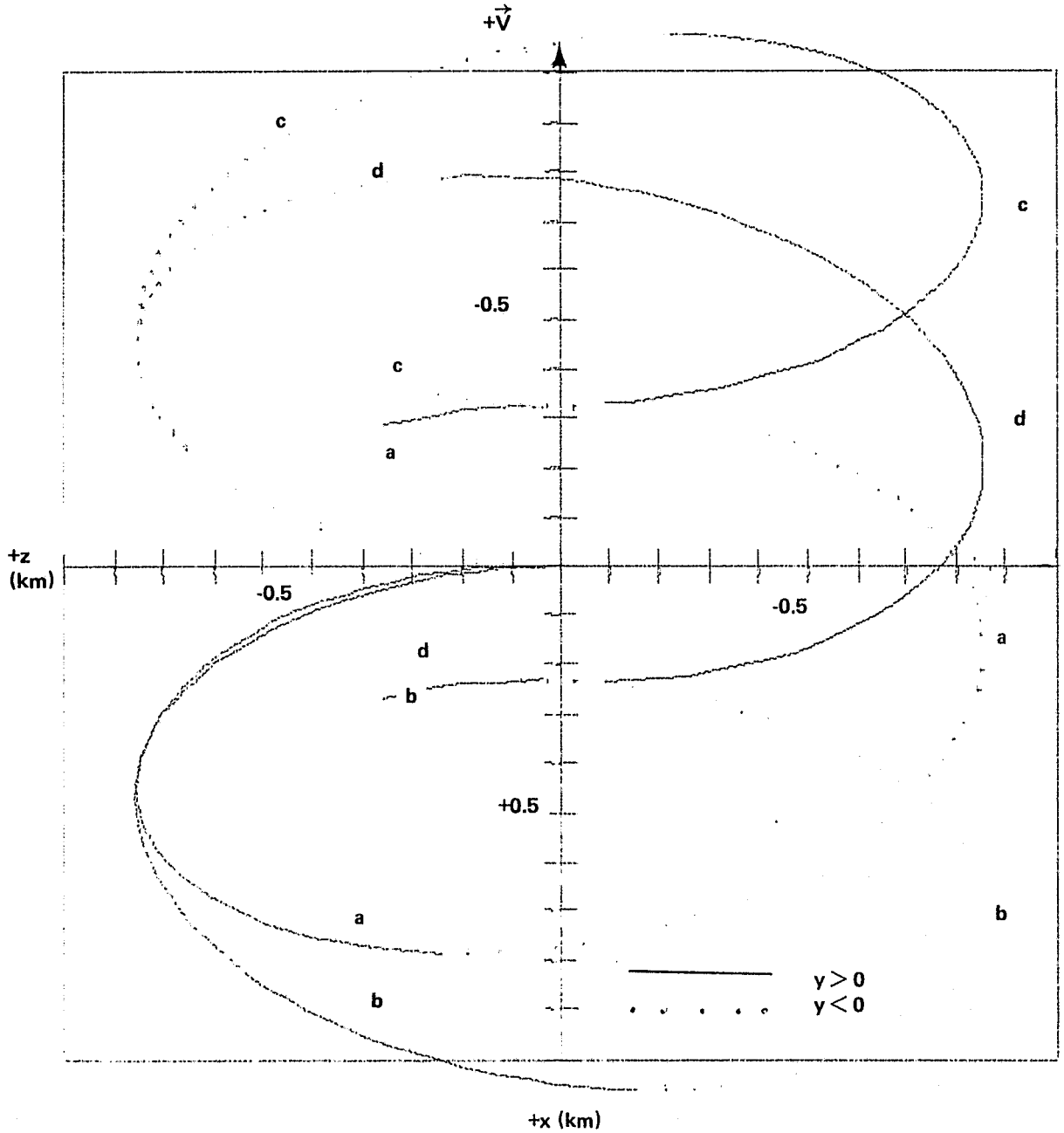

400 km CIRCULAR ORBIT $D = 1 \times 10^{-6}$ m/s^2

CASE	θ (degrees)	φ (degrees)	ΔV (m/s)
a	+15	+1	1
b	+15	-1	1
c	-15	+1	1
d	-15	-1	1

DOTS ARE SEPARATED BY 1 min IN TIME.

Figure 25. The x-z projection of the relative motion.

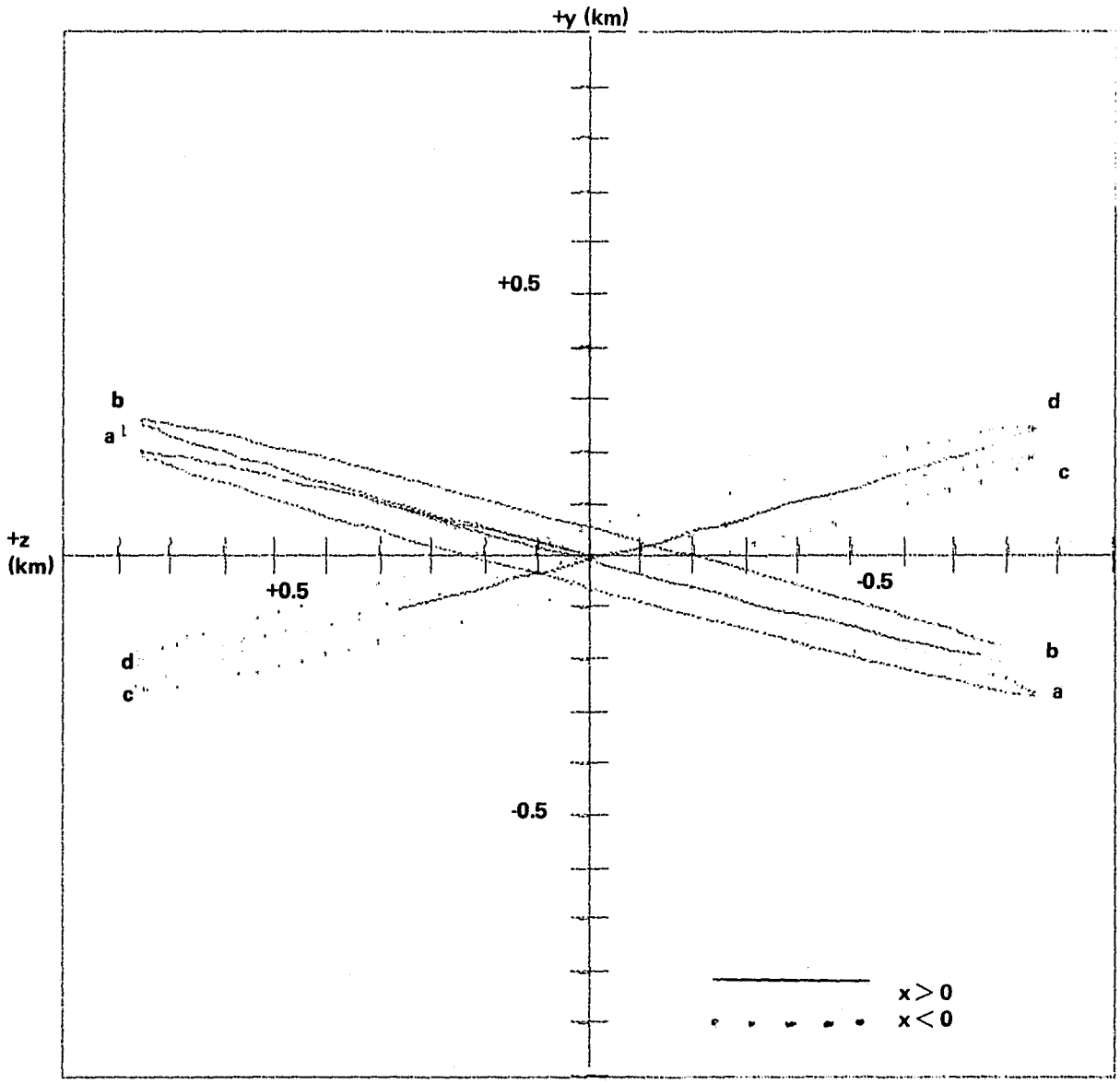

400 km CIRCULAR ORBIT $D = 1 \times 10^{-6}$ m/s^2

CASE	θ (degrees)	φ (degrees)	ΔV (m/s)
a	+15	+1	1
b	+15	-1	1
c	-15	+1	1
d	-15	-1	1

DOTS ARE SEPARATED BY 1 min IN TIME. ORBITAL VELOCITY VECTOR INTO PAGE.

Figure 26. The y-z projection of the relative motion.

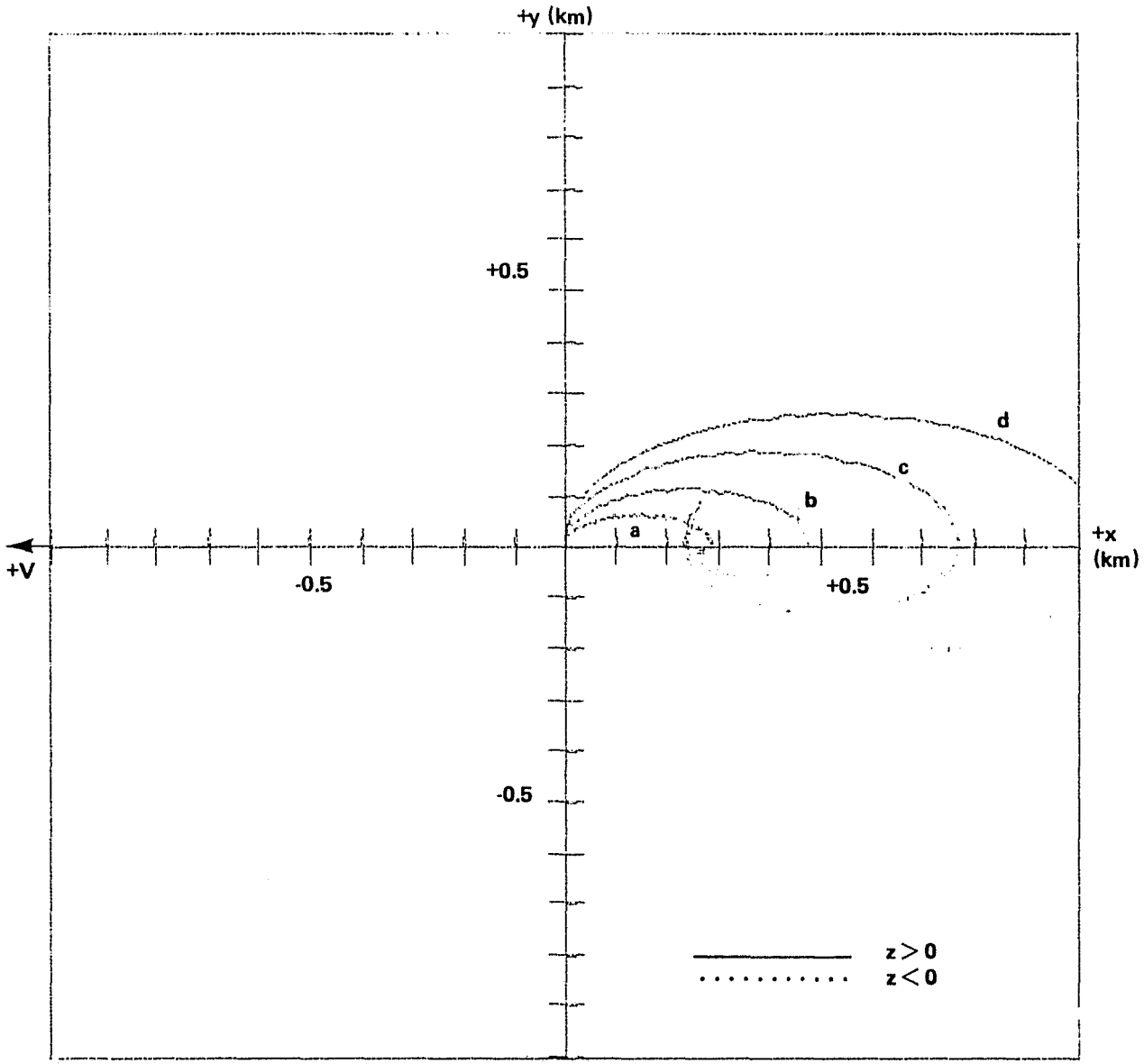

400 km CIRCULAR ORBIT $D = 1 \times 10^{-6}$ m/s

CASE	θ (degrees)	φ (degrees)	ΔV (m/s)
a	1	-1	1
b	5	-1	1
c	10	-1	1
d	15	-1	1

DOTS ARE SEPARATED BY 1 min IN TIME.

Figure 27. The x-y projection of the relative motion.

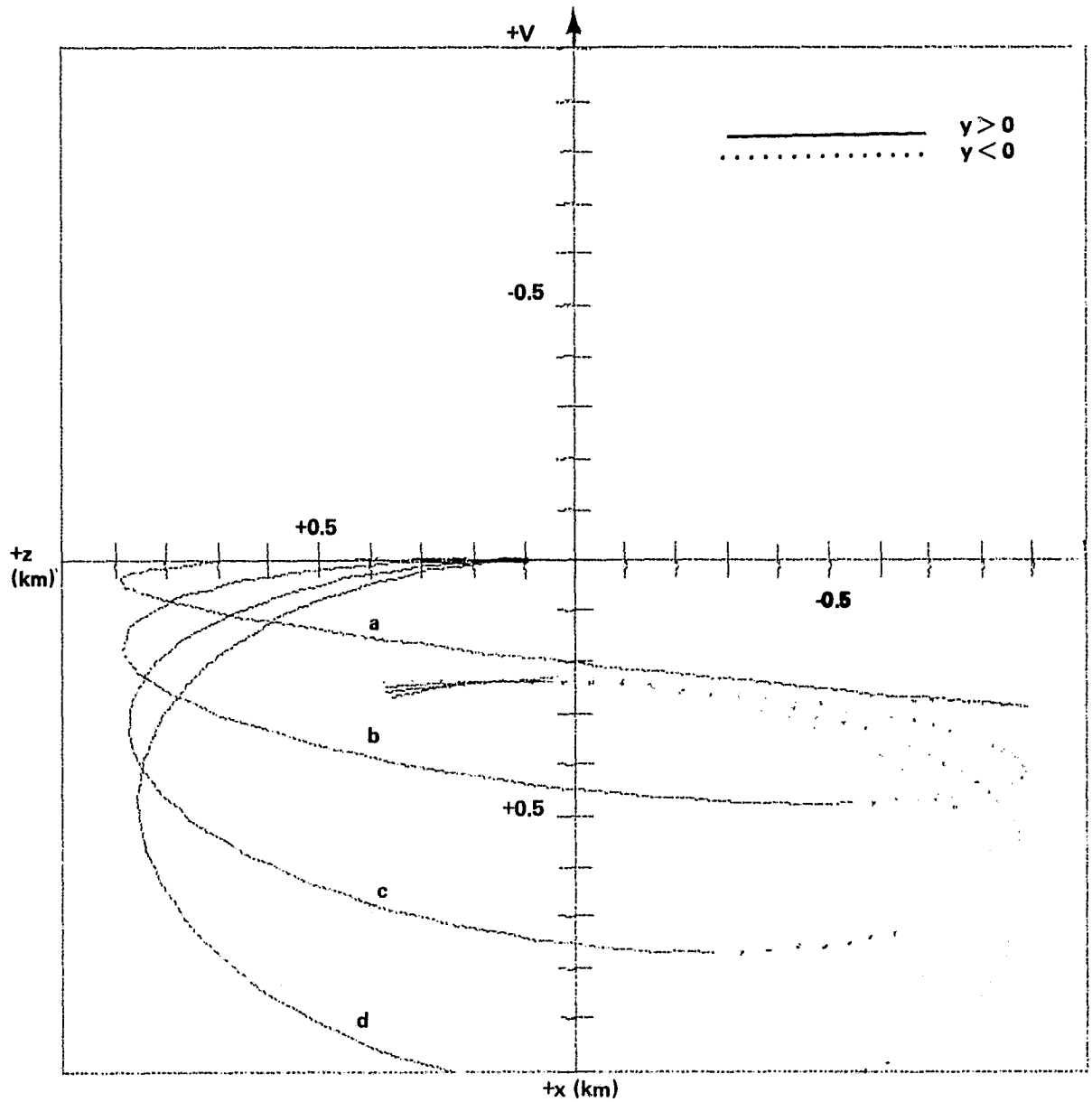

400 km CIRCULAR ORBIT $D = 1 \times 10^{-6}$ m/s^2

CASE	θ (degrees)	φ (degrees)	ΔV (m/s)
a	1	-1	1
b	5	-1	1
c	10	-1	1
d	15	-1	1

DOTS ARE SEPARATED BY 1 min IN TIME.

Figure 28. The x-z projection of the relative motion.

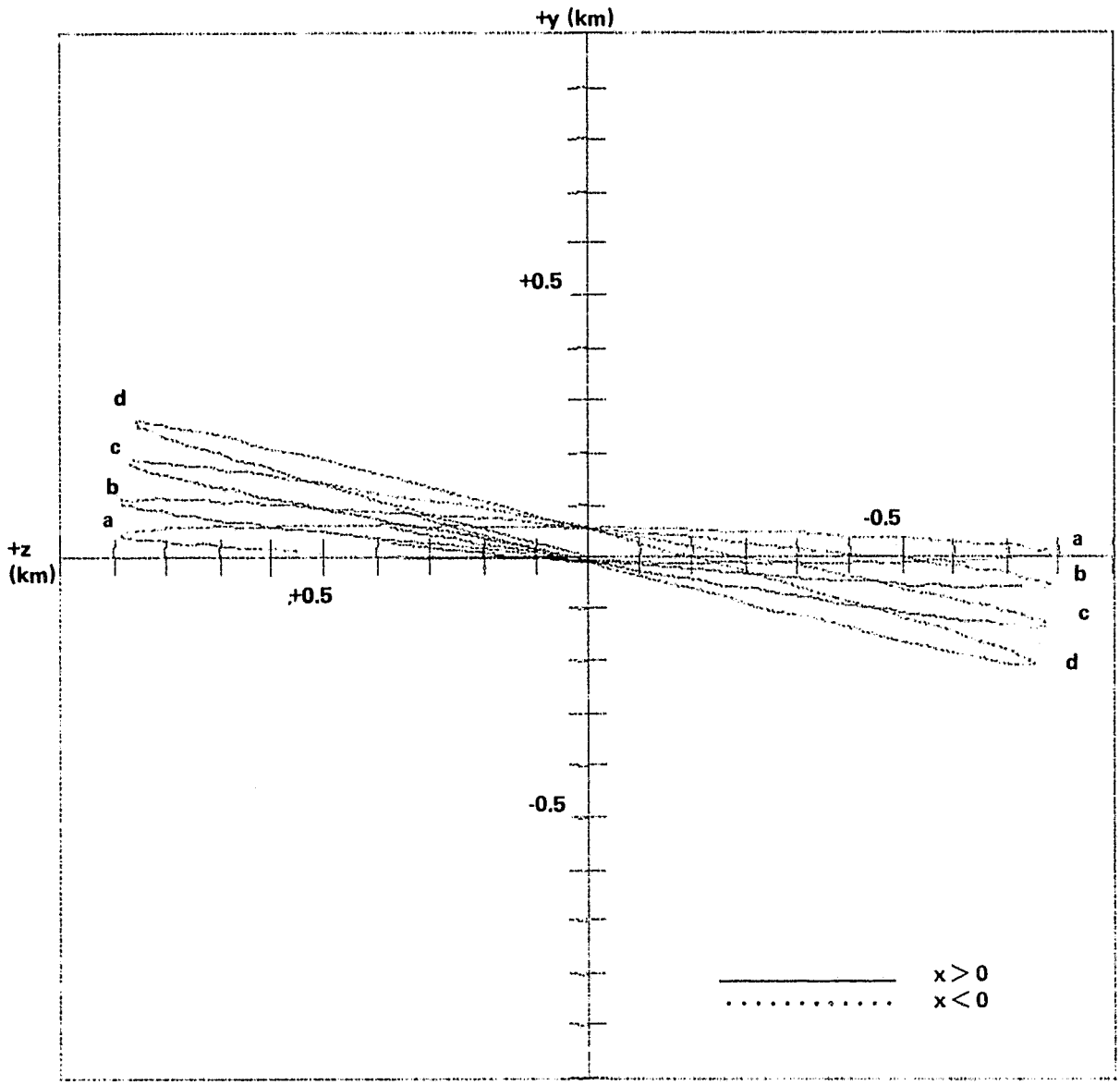

400 km CIRCULAR ORBIT $D = 1 \times 10^{-6}$ m/s

CASE	θ (degrees)	φ (degrees)	ΔV (m/s)
a	1	-1	1
b	5	-1	1
c	10	-1	1
d	15	-1	1

ORBITAL VELOCITY VECTOR INTO PAGE.

Figure 29. The y-z projection of the relative motion.

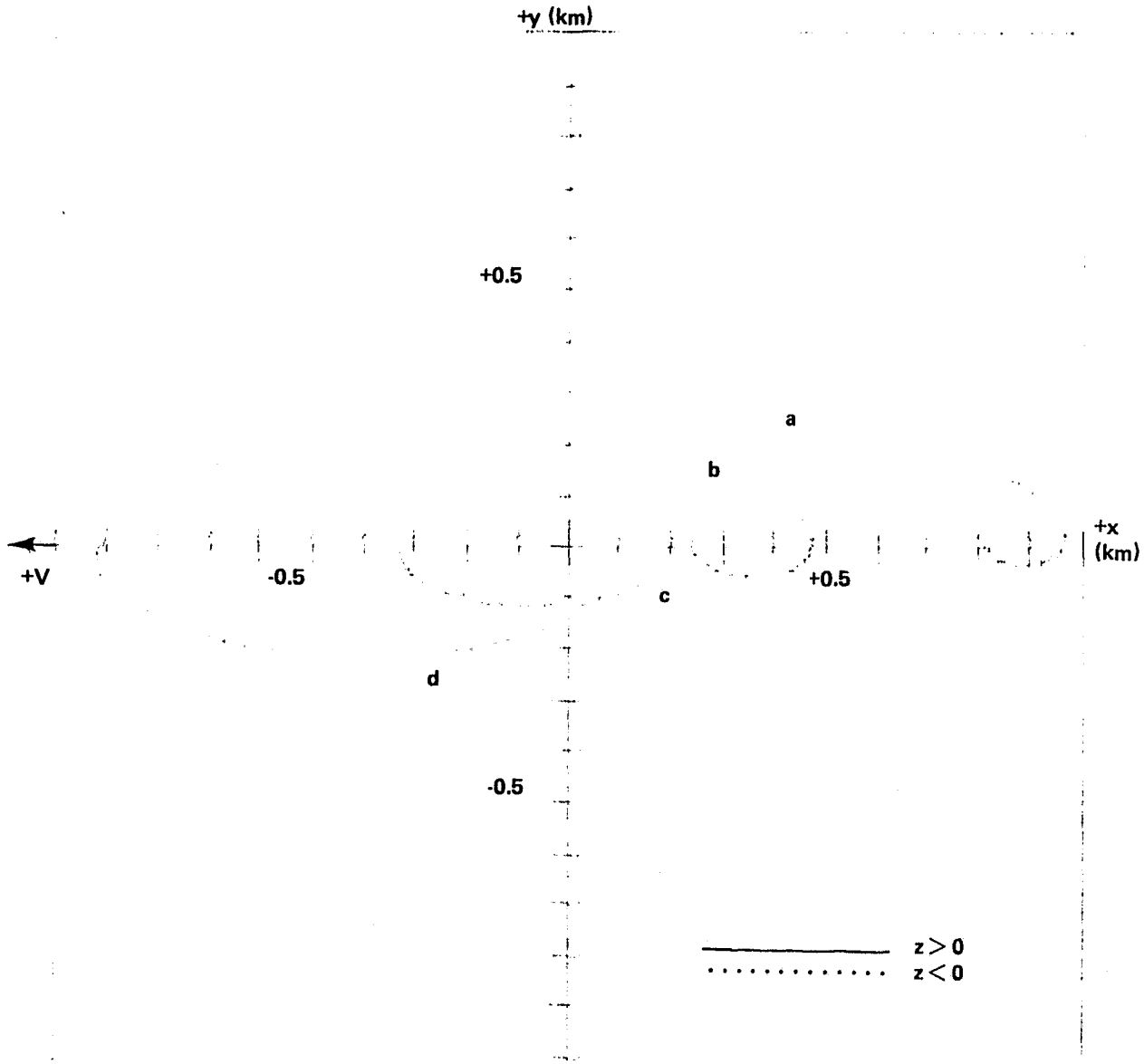

400 km CIRCULAR ORBIT D = 1 × 10^{-6} m/s

CASE	θ (degrees)	φ (degrees)	ΔV (m/s)
a	+5	-3	1
b	+5	-1	1
c	+5	+1	1
d	+5	+3	1

DOTS ARE SEPARATED BY 1 min IN TIME

Figure 30. The x-y projection of the relative motion.

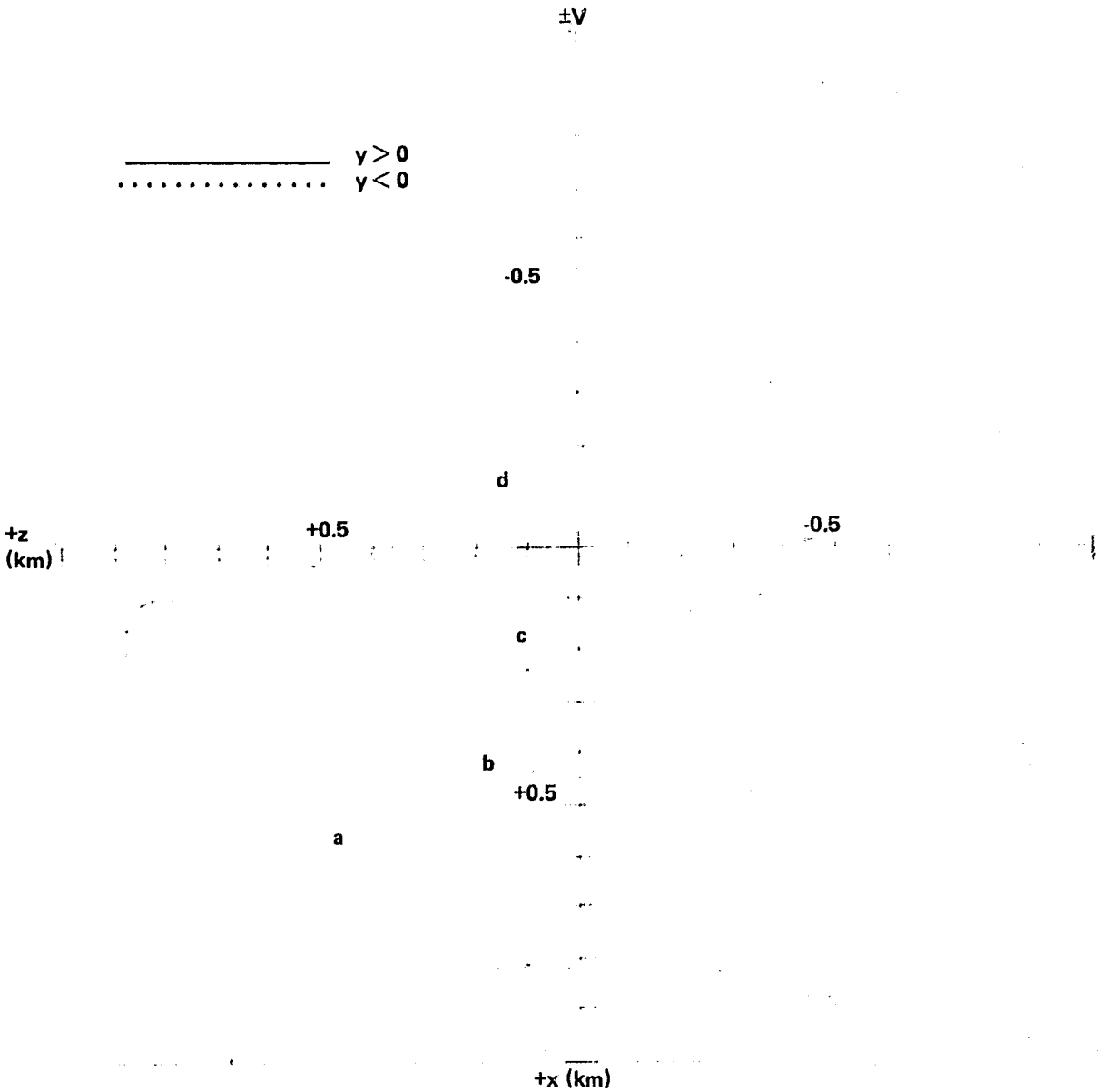

400 km CIRCULAR ORBIT $D = 1 \times 10^{-6}$ m/s

CASE	θ (degrees)	φ (degrees)	ΔV (m/s)
a	+5	-3	1
b	+5	-1	1
c	+5	+1	1
d	+5	+3	1

DOTS ARE SEPARATED BY 1 min IN TIME.

Figure 31. The x-z projection of the relative motion.

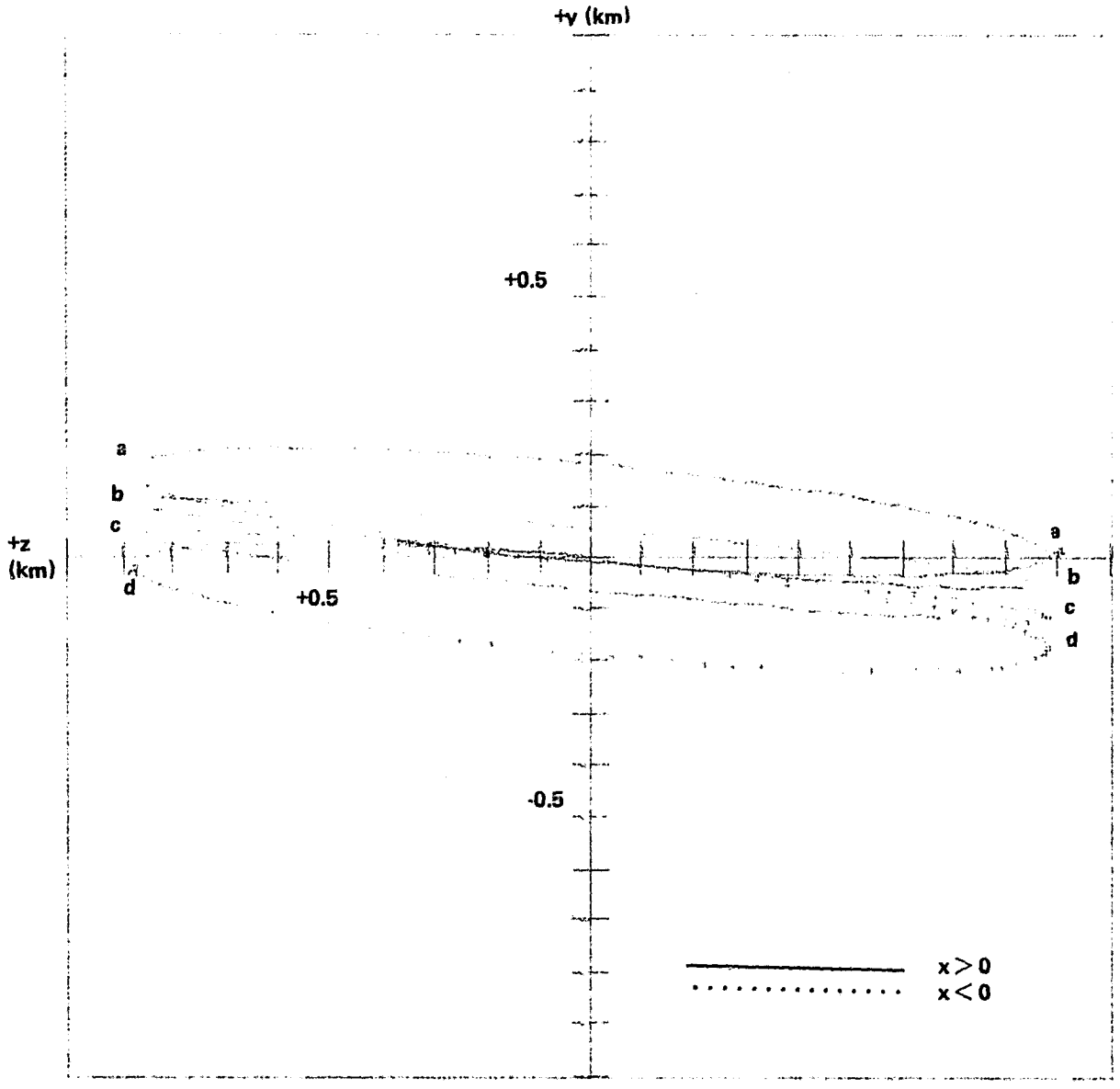

400 km CIRCULAR ORBIT $D = 1 \times 10^{-6}$ m/s

CASE	θ (degrees)	φ (degrees)	ΔV (m/s)
a	+5	-3	1
b	+5	-1	1
c	+5	+1	1
d	+5	+3	1

DOTS ARE SEPARATED BY 1 min IN TIME. ORBITAL VELOCITY VECTOR INTO PAGE.

Figure 32. The y-z projection of the relative motion.

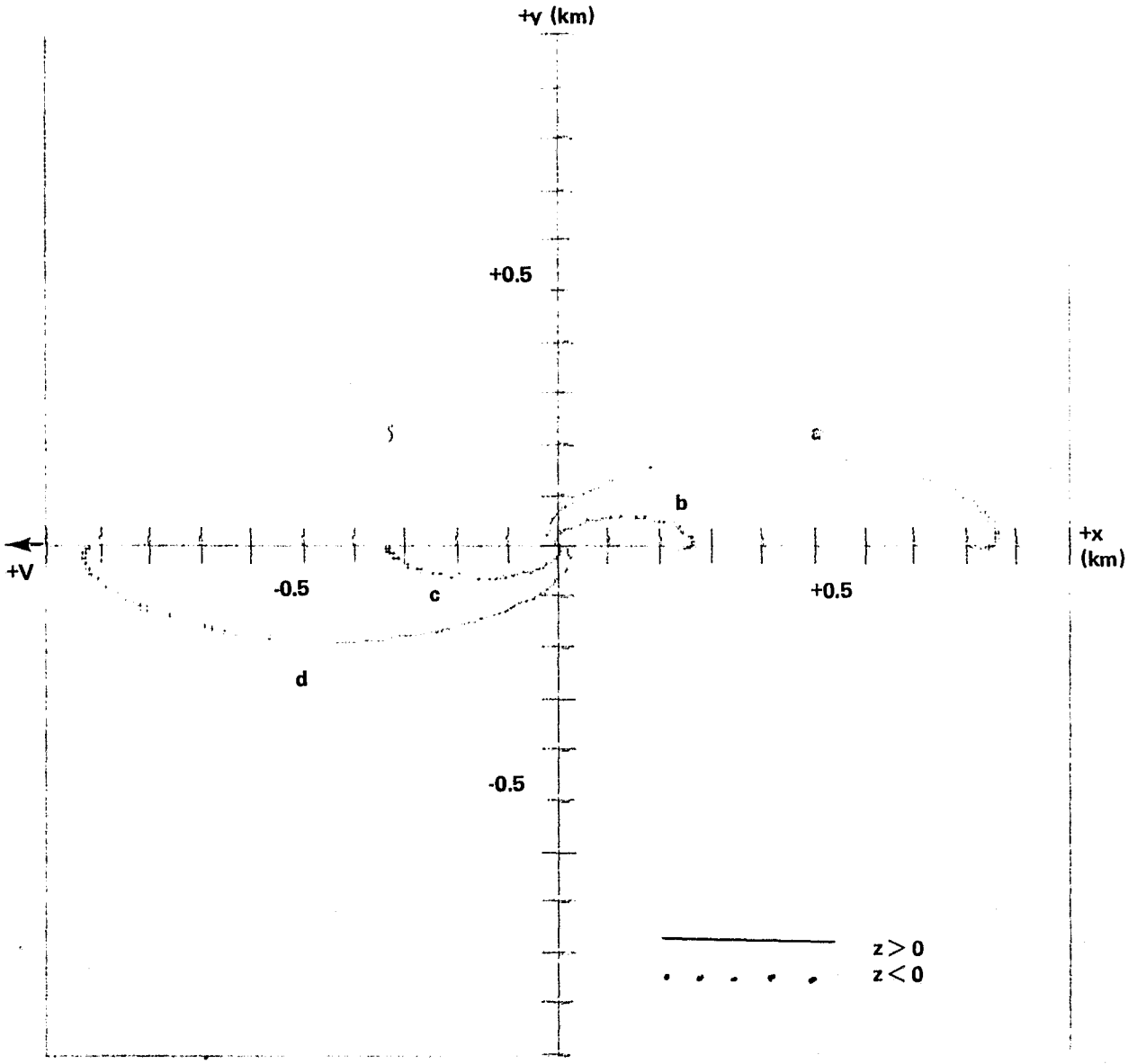

400 km CIRCULAR ORBIT $D = 1 \times 10^{-6}$ m/s^2

CASE	θ (degrees)	φ (degrees)	ΔV (m/s)
a	0	-3	1
b	0	-1	1
c	0	+1	1
d	0	+3	1

DOTS ARE SEPARATED BY 1 min IN TIME.

Figure 33. The x-y projection of the relative motion.

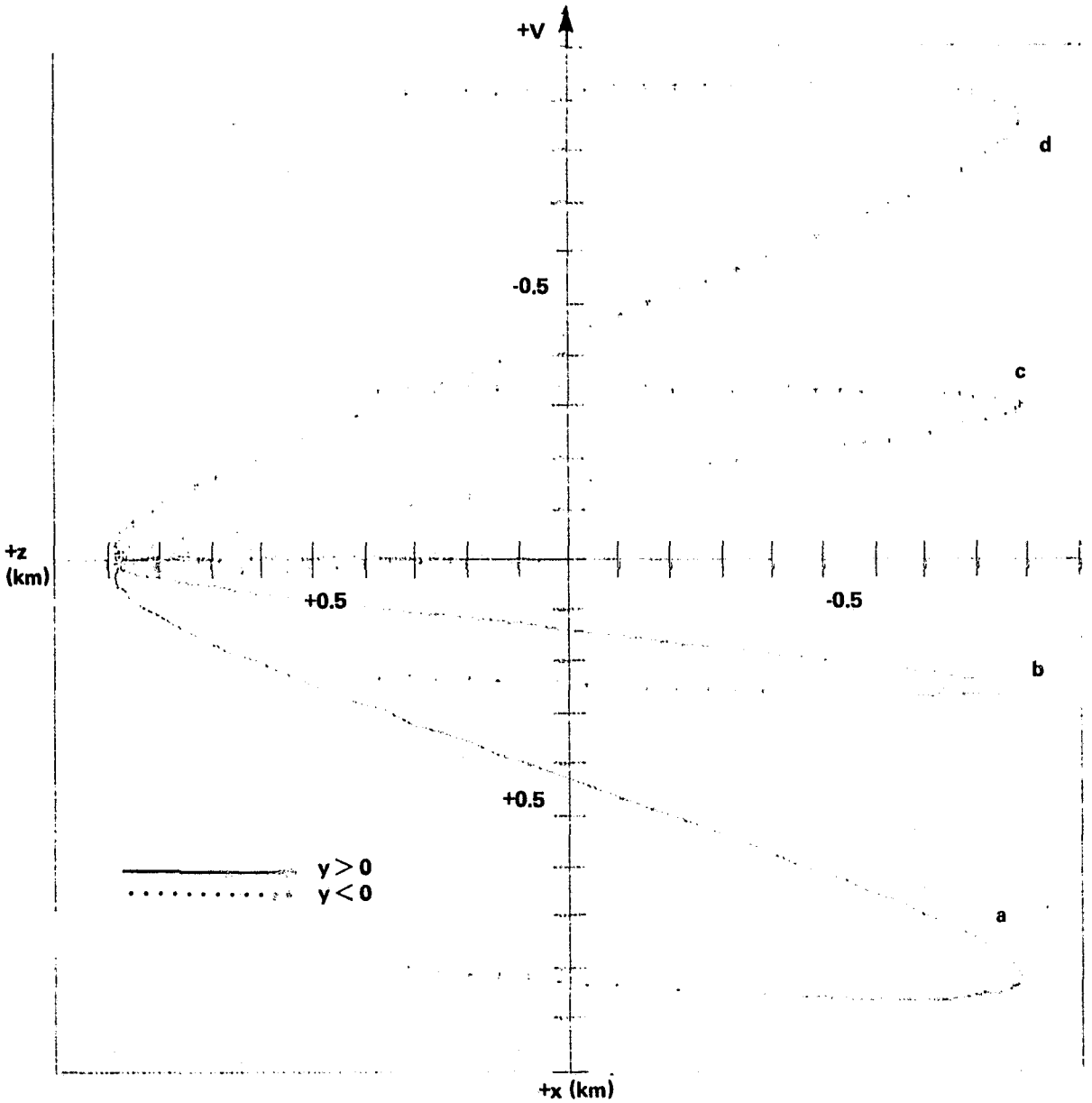

400 km CIRCULAR ORBIT $D = 1 \times 10^{-6}$ m/s^2

CASE	θ (degrees)	φ (degrees)	ΔV (m/s)
a	0	-3	1
b	0	-1	1
c	0	+1	1
d	0	+3	1

DOTS ARE SEPARATED BY 1 min IN TIME.

Figure 34. The x-z projection of the relative motion.

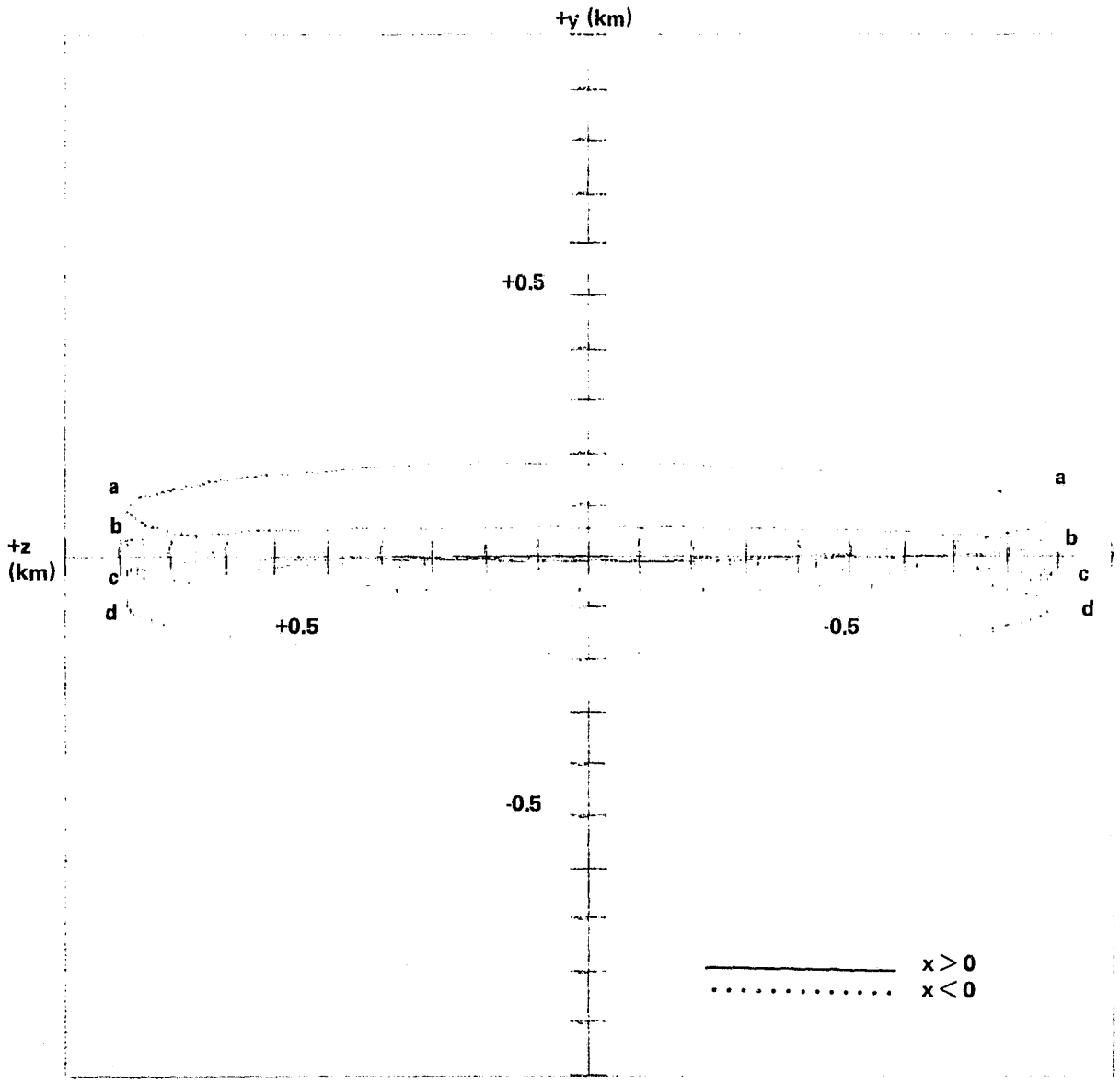

400 km CIRCULAR ORBIT $D = 1 \times 10^{-6}$ m/s^2

CASE	θ (degrees)	φ (degrees)	ΔV (m/s)
a	0	-3	1
b	0	-1	1
c	0	+1	1
d	0	+3	1

DOTS ARE SEPARATED BY 1 min IN TIME. ORBITAL VELOCITY VECTOR INTO PAGE.

Figure 35. The y-z projection of the relative motion.

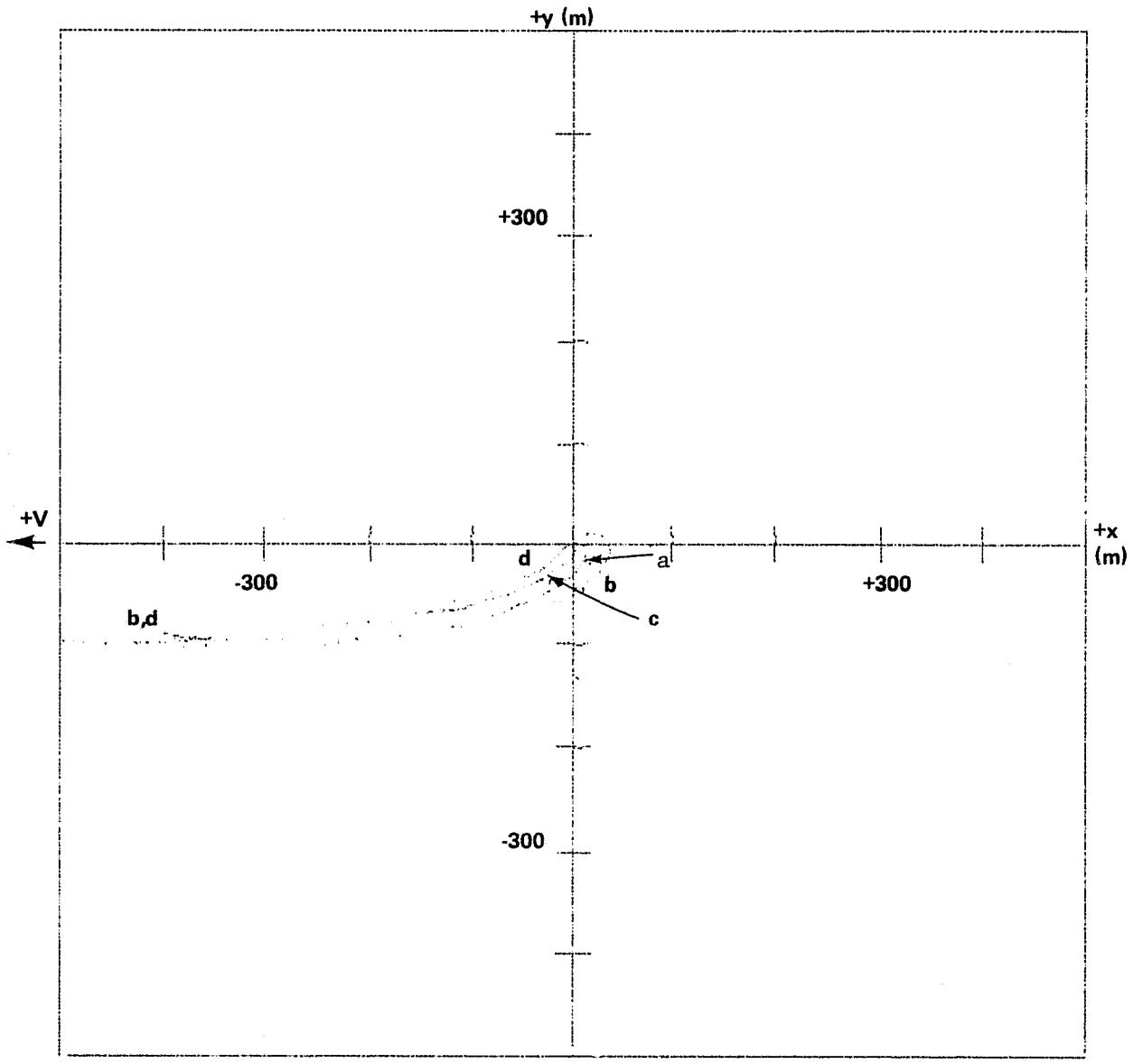

300 km CIRCULAR ORBIT $D = 1 \times 10^{-5}$ m/s^2

CASE	θ (degrees)	φ (degrees)	ΔV (m/s)
a	+5	+3.5	0.1
b	+5	-3.5	0.1
c	-5	+3.5	0.1
d	-5	-3.5	0.1

Figure 36. The x-y projection of the relative motion.

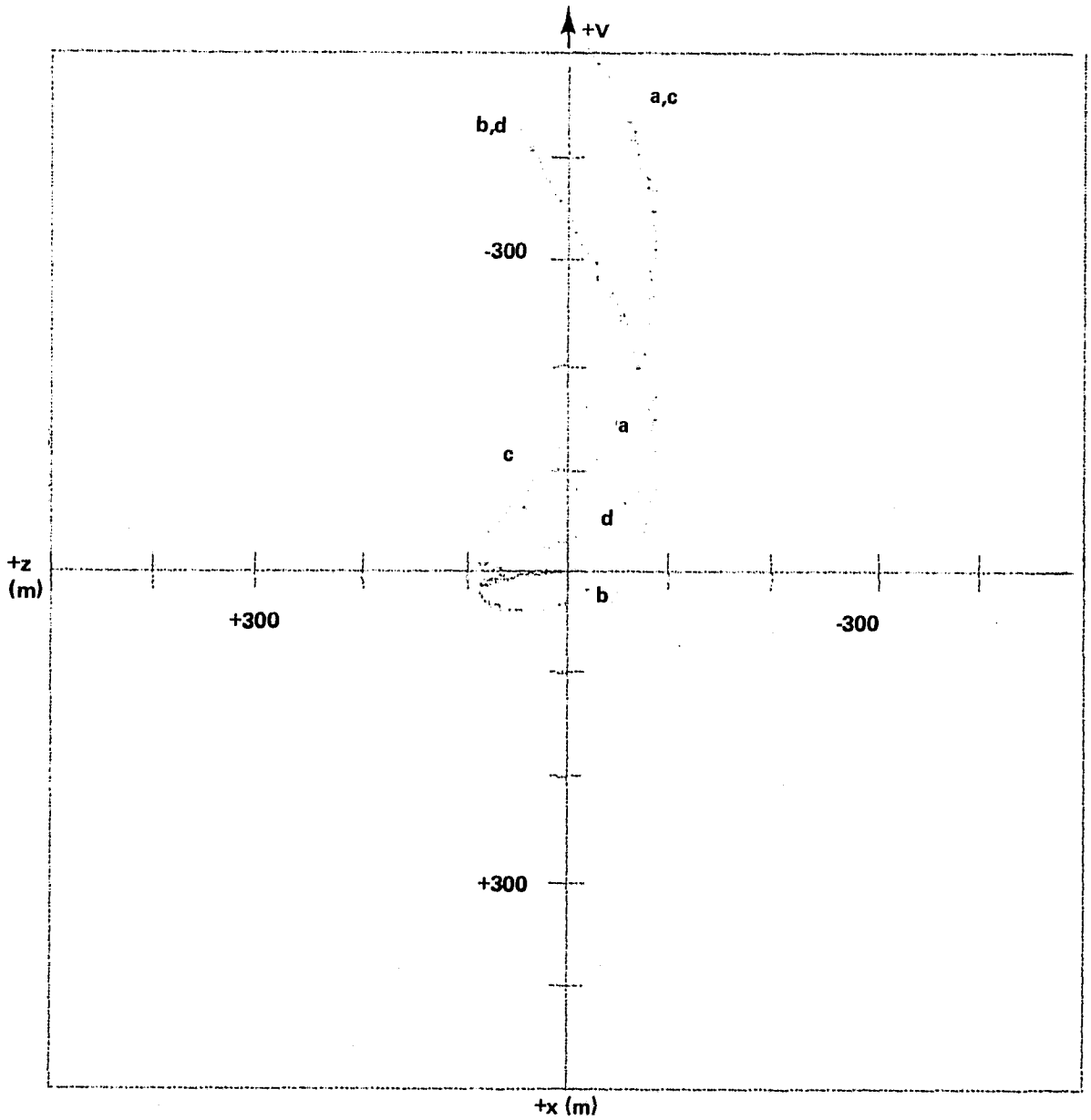

300 km CIRCULAR ORBIT $D = 1 \times 10^{-5}$ m/s^2

CASE	θ (degrees)	φ (degrees)	ΔV (m/s)
a	+5	+3.5	0.1
b	+5	-3.5	0.1
c	-5	+3.5	0.1
d	-5	-3.5	0.1

Figure 37. The x-z projection of the relative motion.

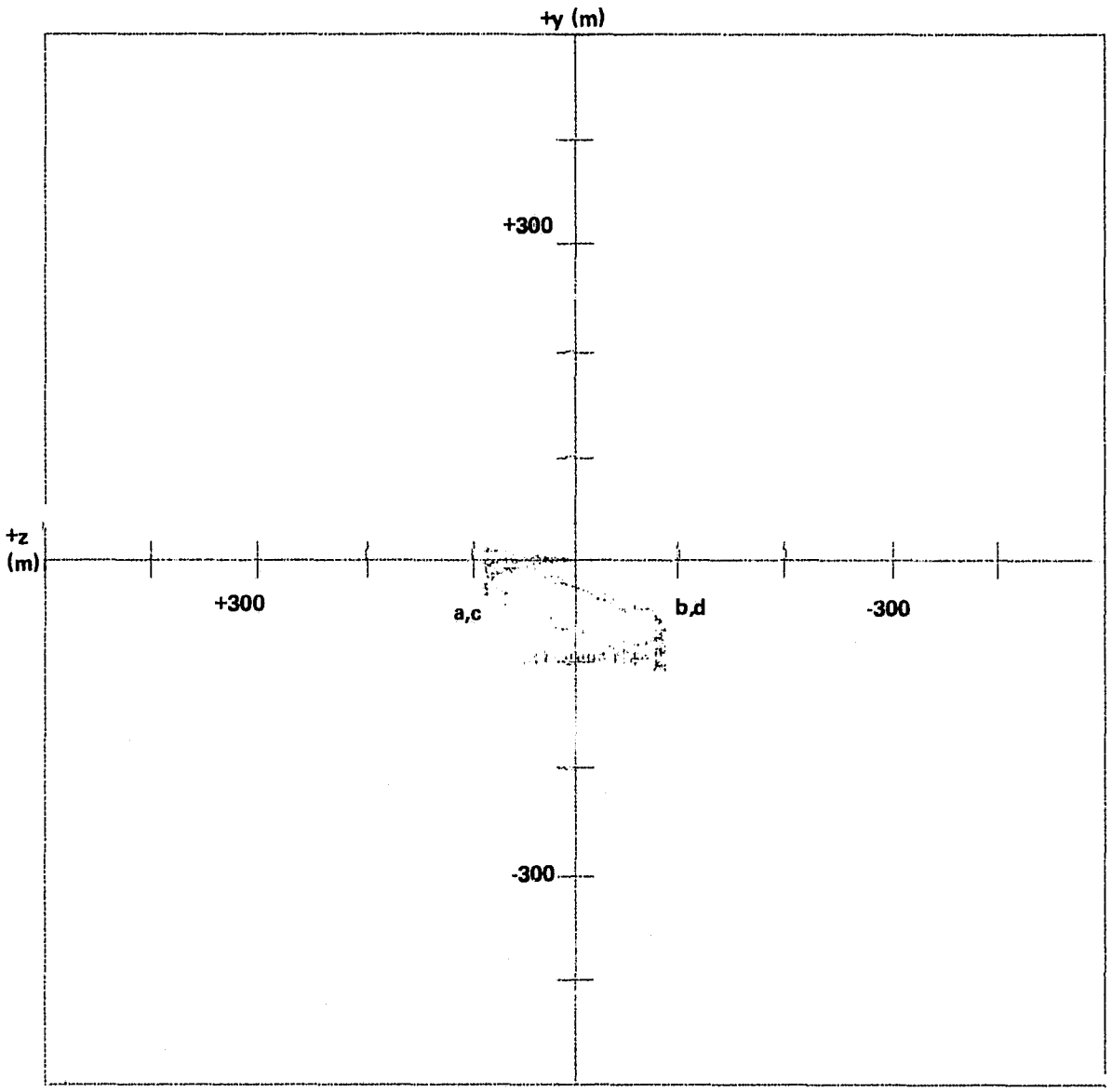

300 km CIRCULAR ORBIT $D = 1 \times 10^{-5}$ m/s^2

CASE	θ (degrees)	φ (degrees)	ΔV (m/s)
a	+5	+3.5	0.1
b	+5	-3.5	0.1
c	-5	+3.5	0.1
d	-5	-3.5	0.1

ORBITAL VELOCITY VECTOR INTO PAGE.

Figure 38. The y-z projection of the relative motion.

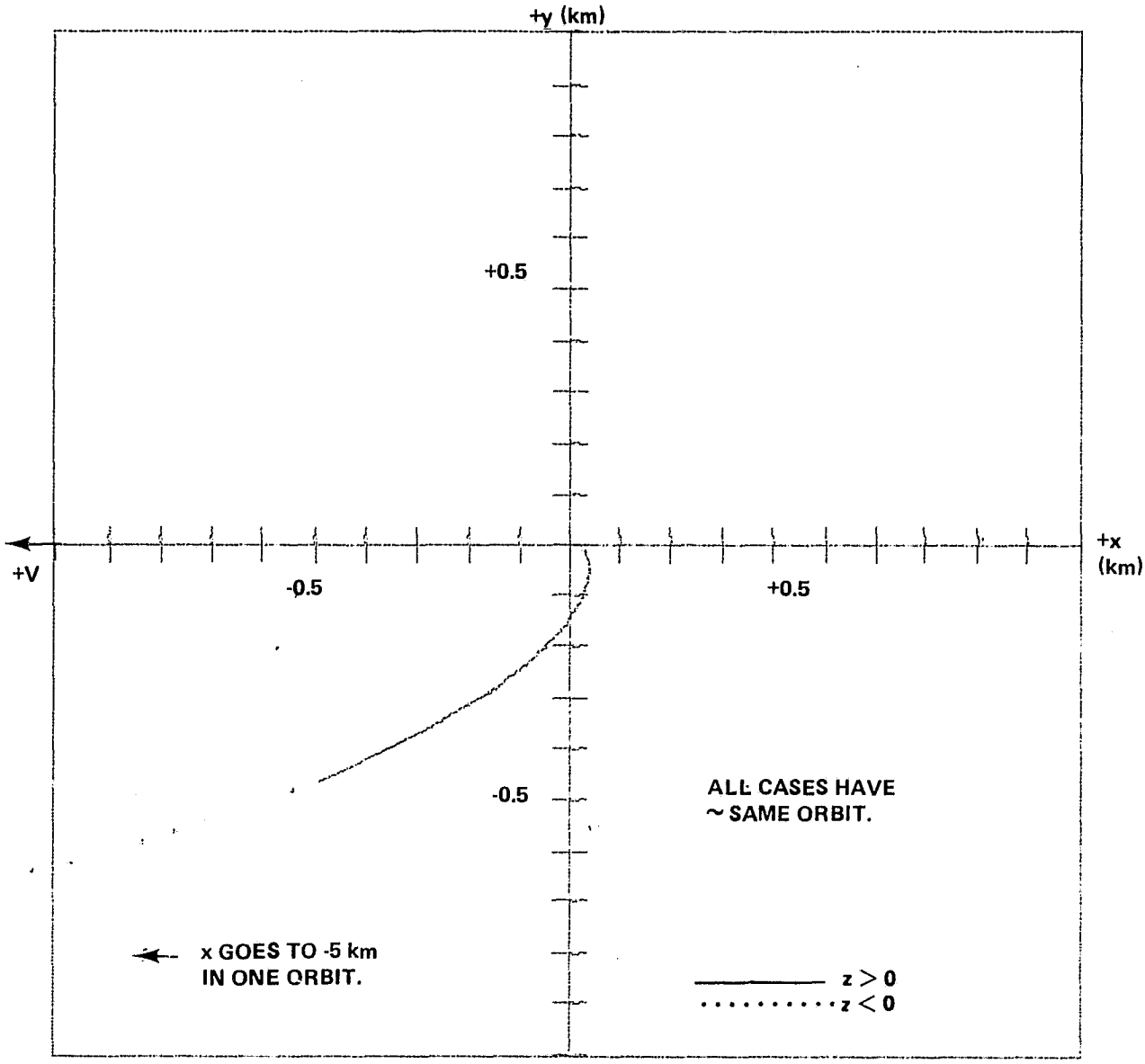

200 km CIRCULAR ORBIT $D = 1 \times 10^{-4}$ m/s^2

CASE	θ (degrees)	φ (degrees)	ΔV (m/s)
a	+5	+3.5	0.1
b	+5	-3.5	0.1
c	-5	+3.5	0.1
d	-5	-3.5	0.1

Figure 39. The x-y projection of the relative motion.

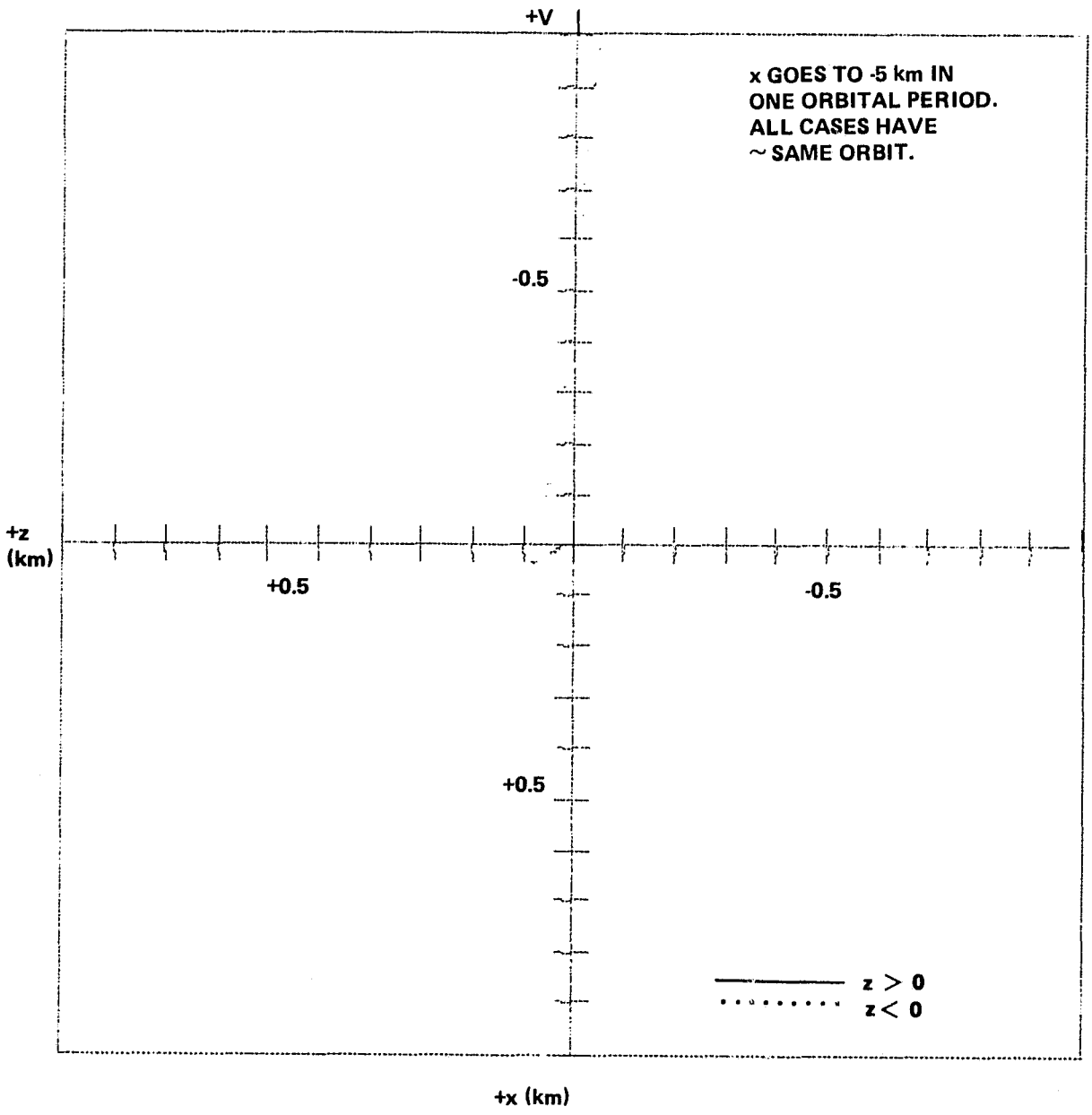

200 km CIRCULAR ORBIT $D = 1 \times 10^{-4}$ m/s^2

CASE	θ (degrees)	φ (degrees)	ΔV (m/s)
a	+5	+3.5	0.1
b	+5	-3.5	0.1
c	-5	+3.5	0.1
d	-5	-3.5	0.1

Figure 40. The x-z projection of the relative motion.

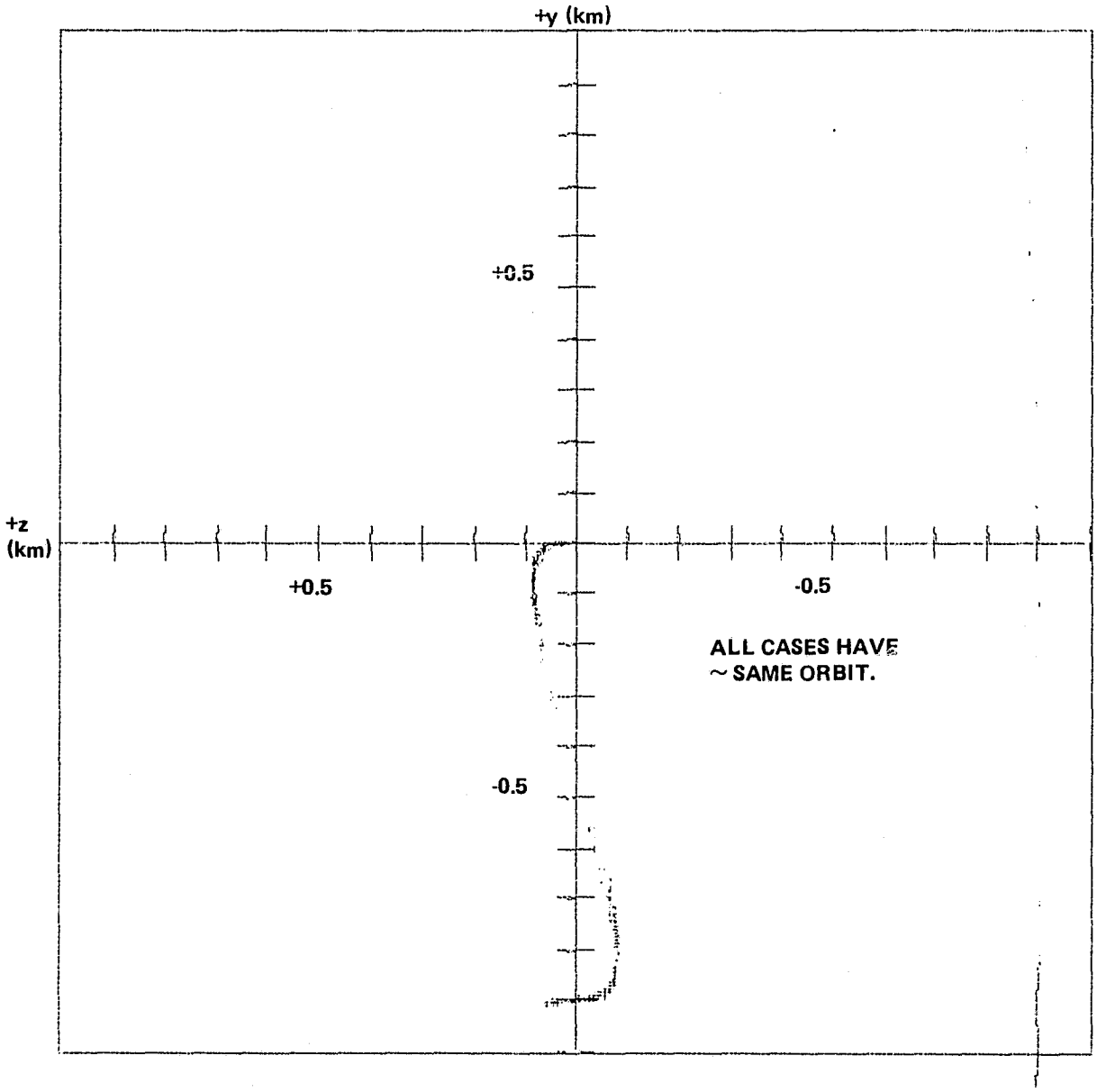

200 km CIRCULAR ORBIT $D = 1 \times 10^{-4}$ m/s

CASE	θ (degrees)	φ (degrees)	ΔV (m/s)
a	+5	+3.5	0.1
b	+5	-3.5	0.1
c	-5	+3.5	0.1
d	-5	-3.5	0.1

ORBITAL VELOCITY VECTOR INTO PAGE.

Figure 41. The y-z projection of the relative motion.

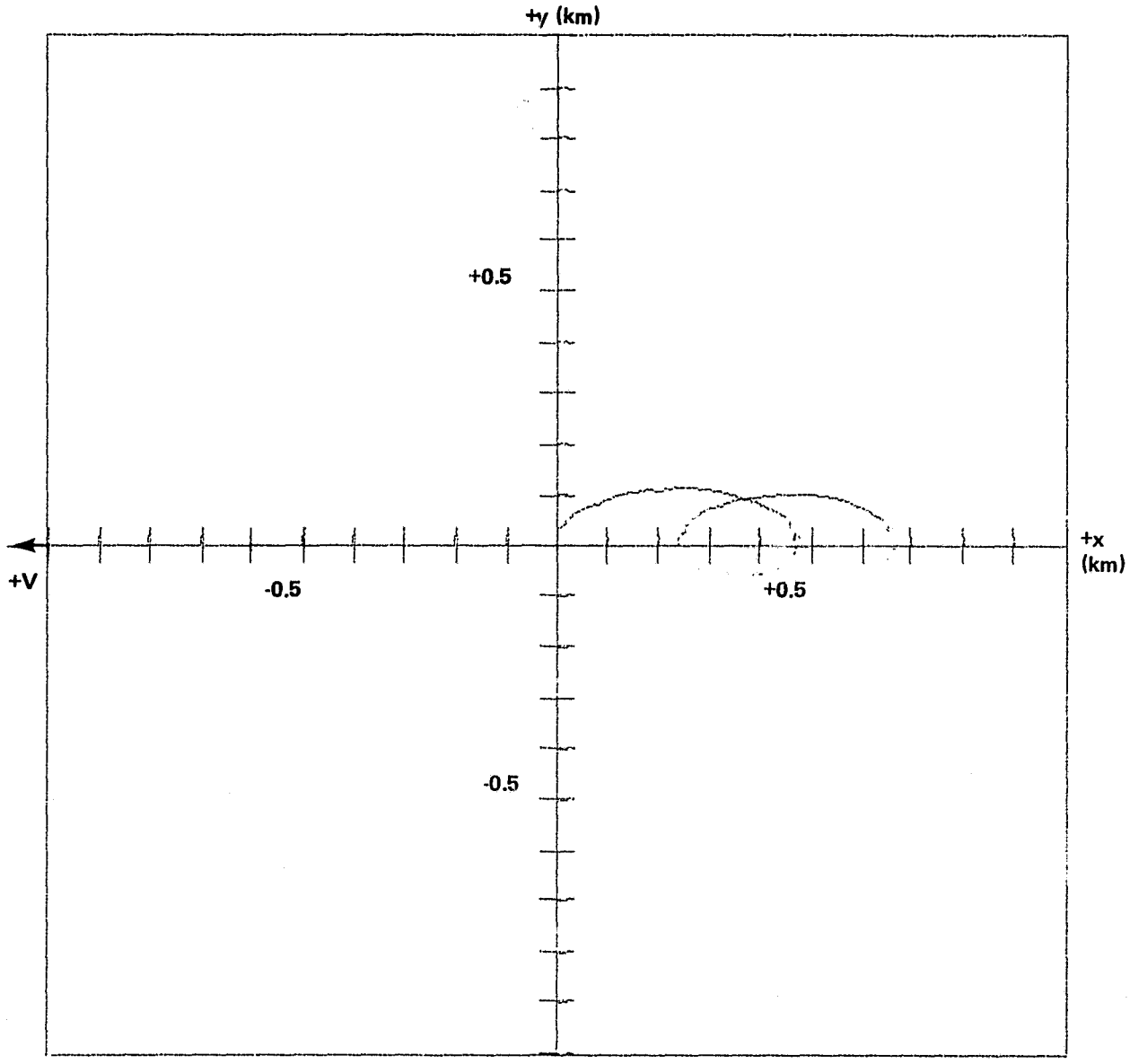

400 km CIRCULAR ORBIT $D = 1 \times 10^{-6}$ m/s^2

$\Delta V = 1$ m/s, $\theta = +5°$, $\varphi = -1°$

TWO ORBITAL PERIODS. DOTS ARE SEPARATED BY 2 min IN TIME.

Figure 42. The x-y projection of the relative motion.

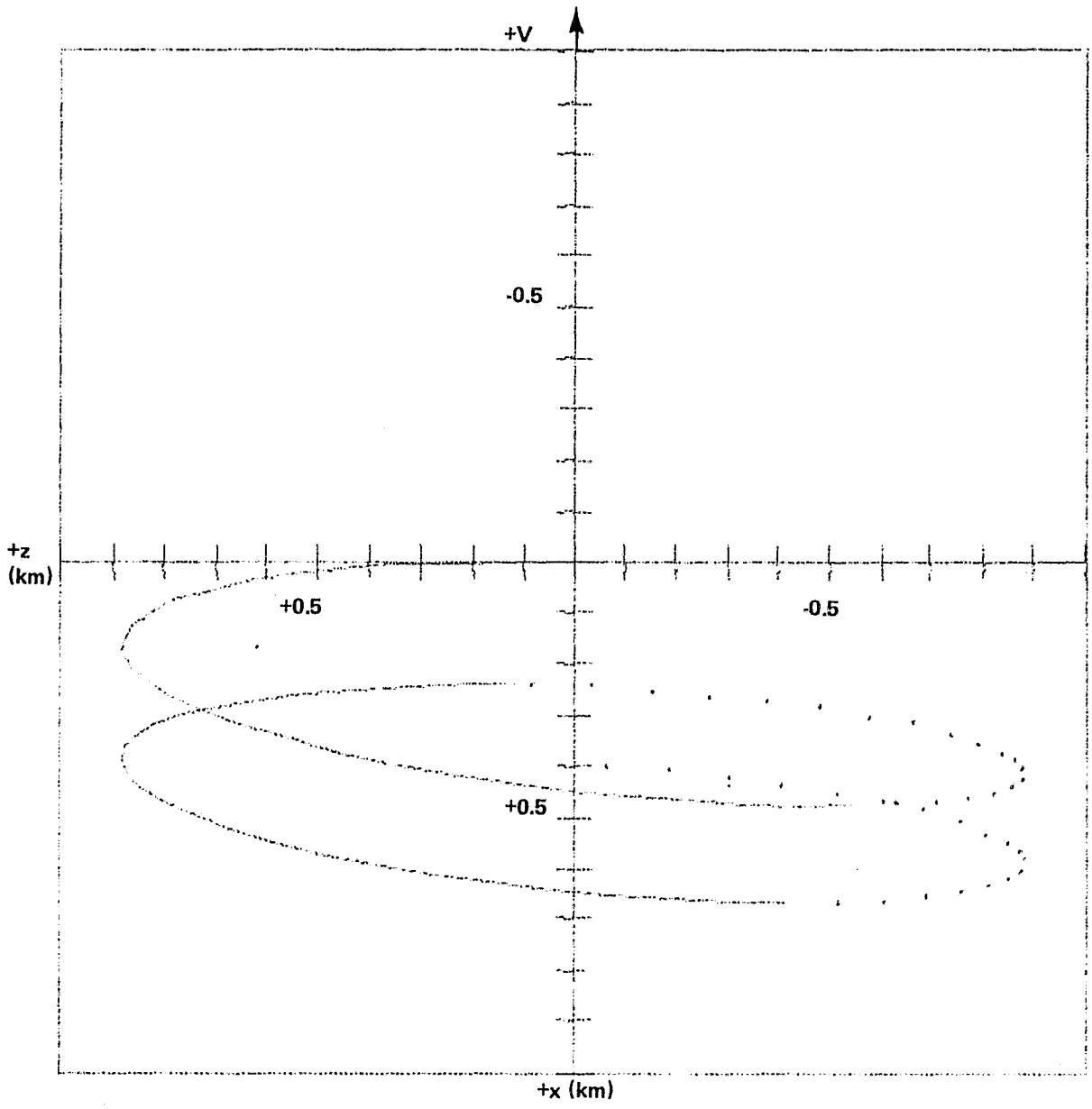

400 km CIRCULAR ORBIT $D = 1 \times 10^{-6}$ m/s^2

$\Delta V = 1$ m/s, $\theta = +5°$, $\varphi = -1°$

TWO ORBITAL PERIODS. DOTS ARE SEPARATED BY 2 min IN TIME.

Figure 43. The x-z projection of the relative motion.

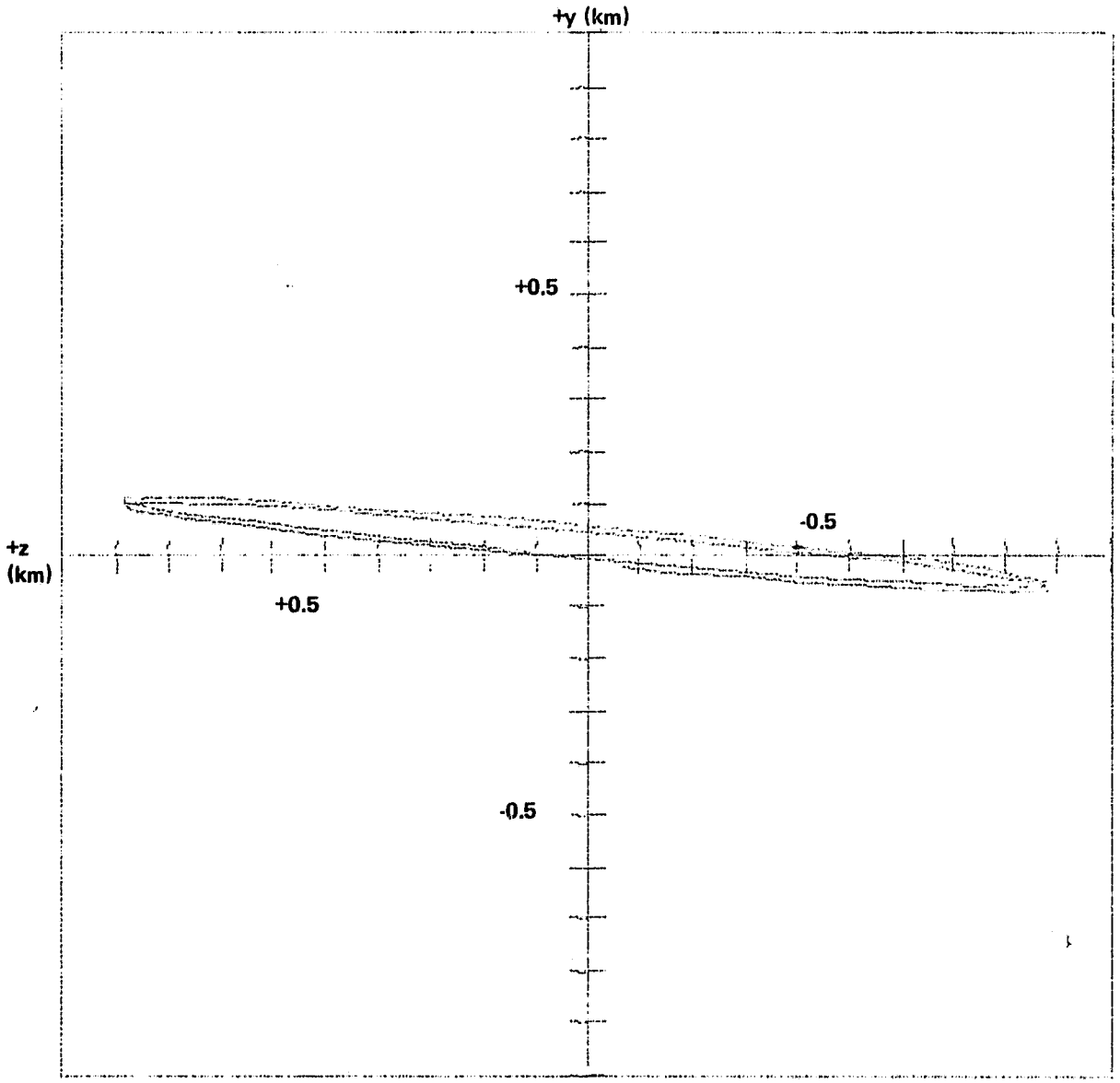

400 km CIRCULAR ORBIT $D = 1 \times 10^{-6}$ m/s^2

$\Delta V = 1$ m/s, $\theta = +5°$, $\varphi = -1°$

TWO ORBITAL PERIODS. ORBITAL VELOCITY VECTOR INTO PAGE.

Figure 44. The y-z projection of the relative motion.

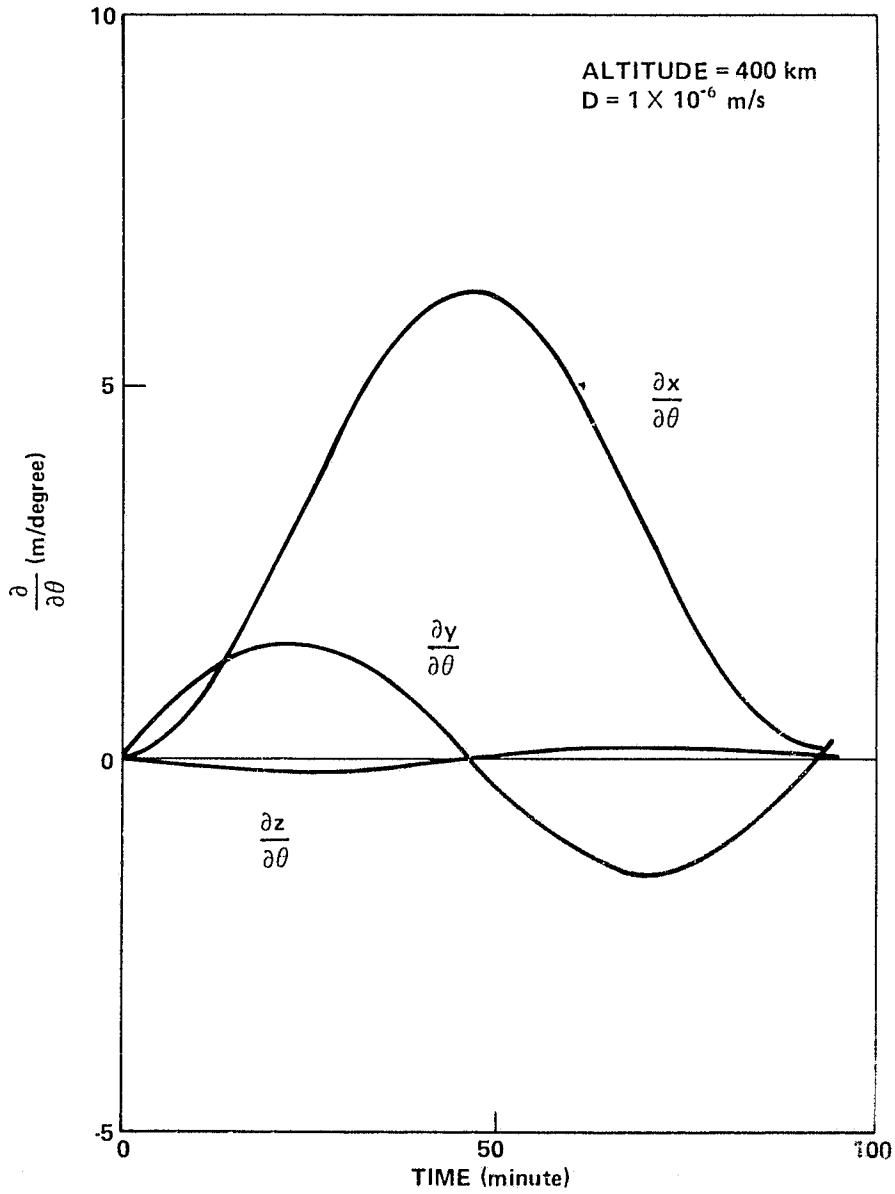

Figure 45. Partials of the coordinates with respect to the initial angle θ versus time for the nominal case (θ = +5 degrees, φ = +3.5 degrees, ΔV = 0.1 m/s).

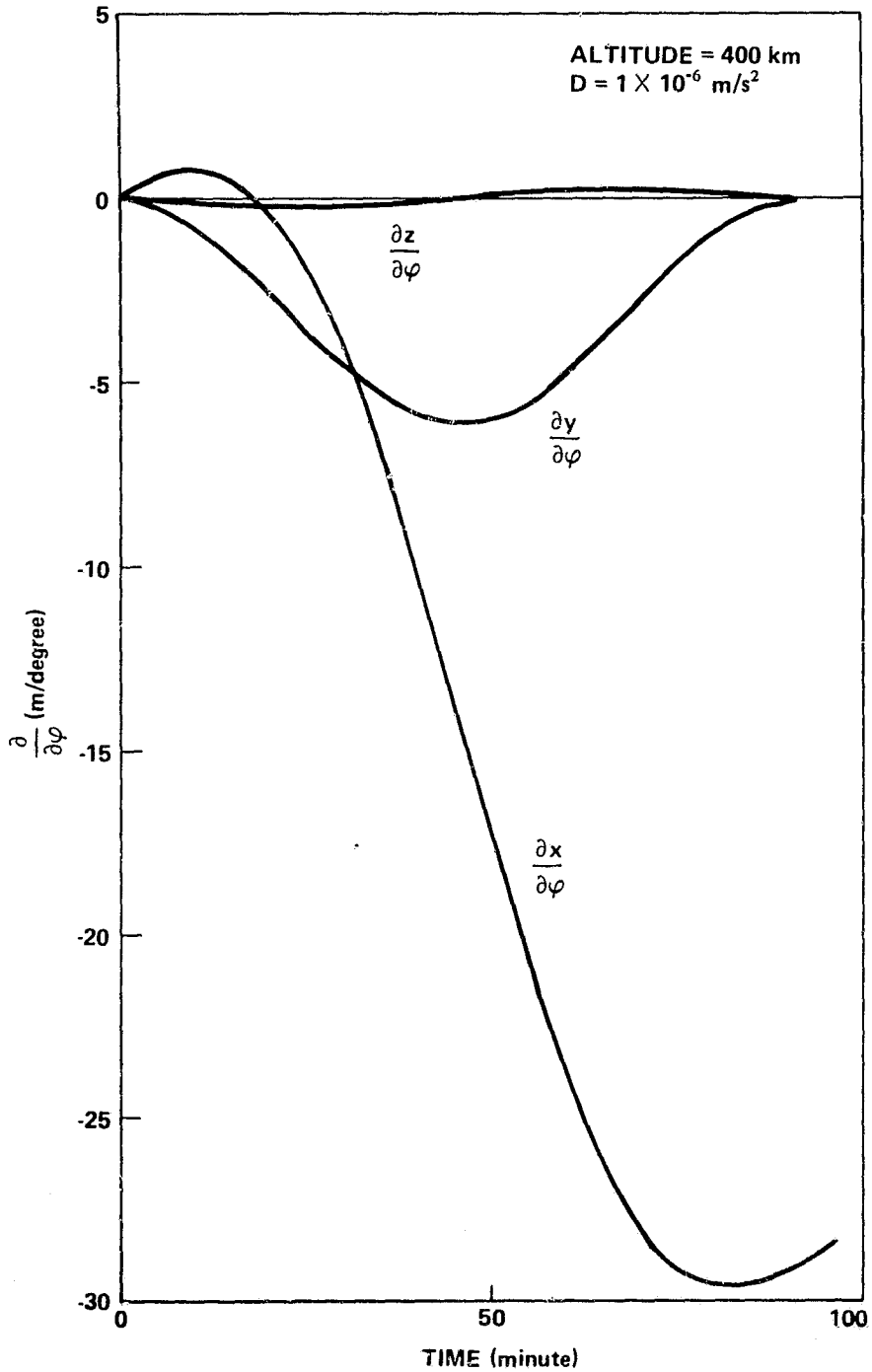

Figure 46. Partials of the coordinates with respect to the initial angle φ versus time for the nominal case (θ = +5 degrees, φ = +3.5 degrees, ΔV = 0.1 m/s).

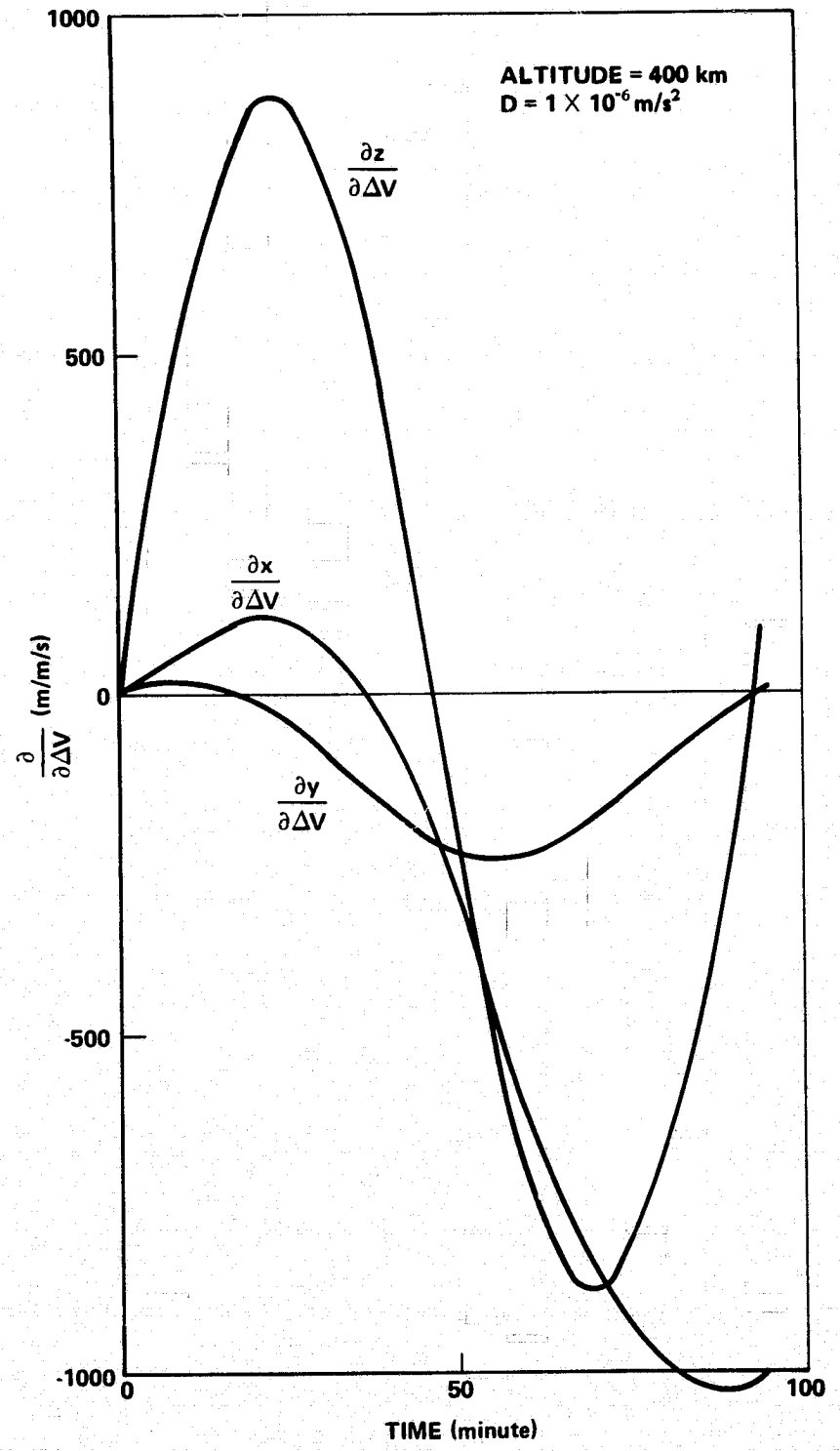

Figure 47. Partials of the coordinates with respect to the initial impulse ΔV versus time for the nominal case (θ = +5 degrees, φ = +3.5 degrees, ΔV = 0.1 m/s).

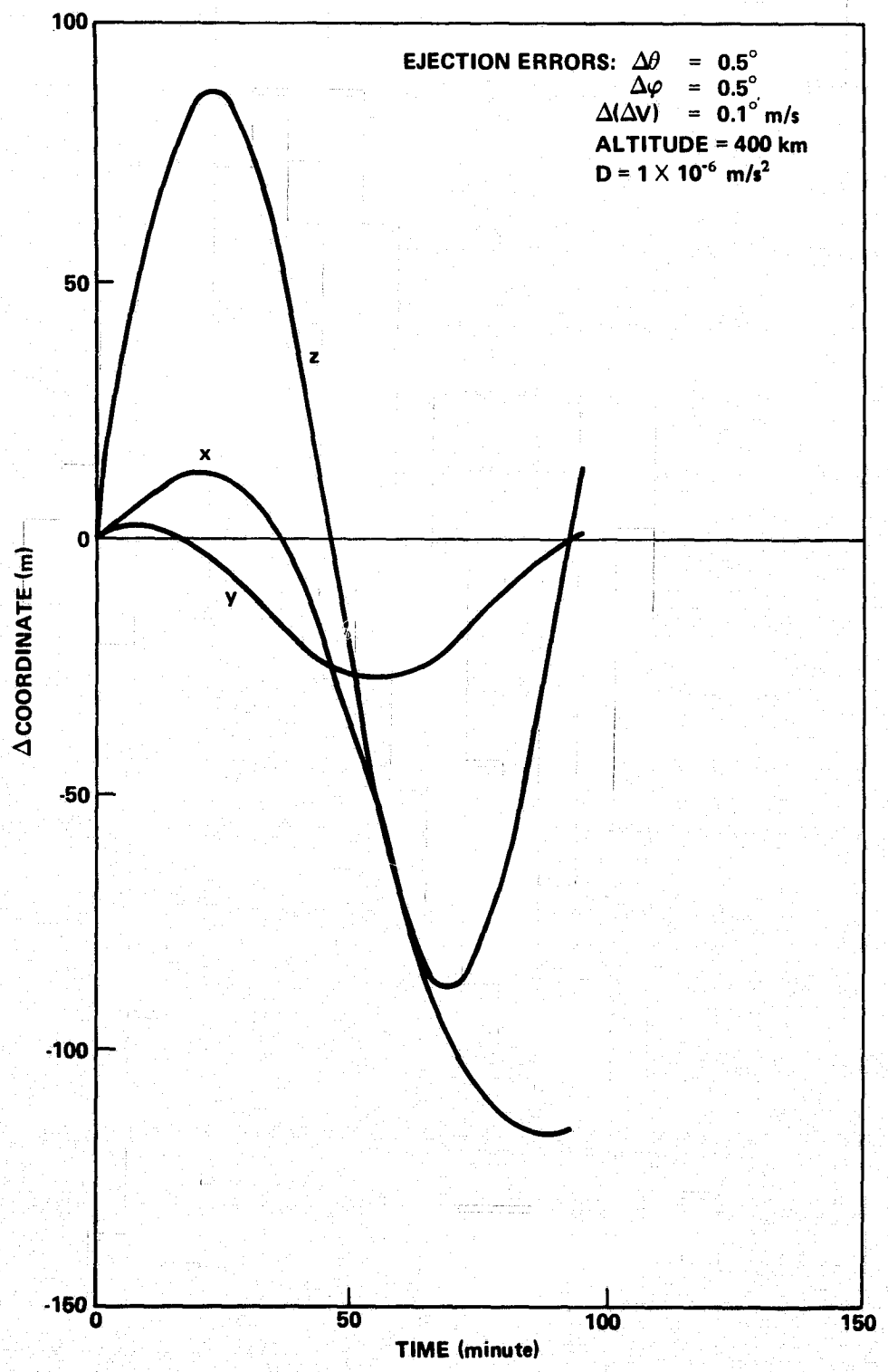

Figure 48. Errors in the coordinates versus time due to errors in the ejection conditions for the nominal case (θ = +5 degrees, φ = +3.5 degrees, ΔV = 0.1 m/s).

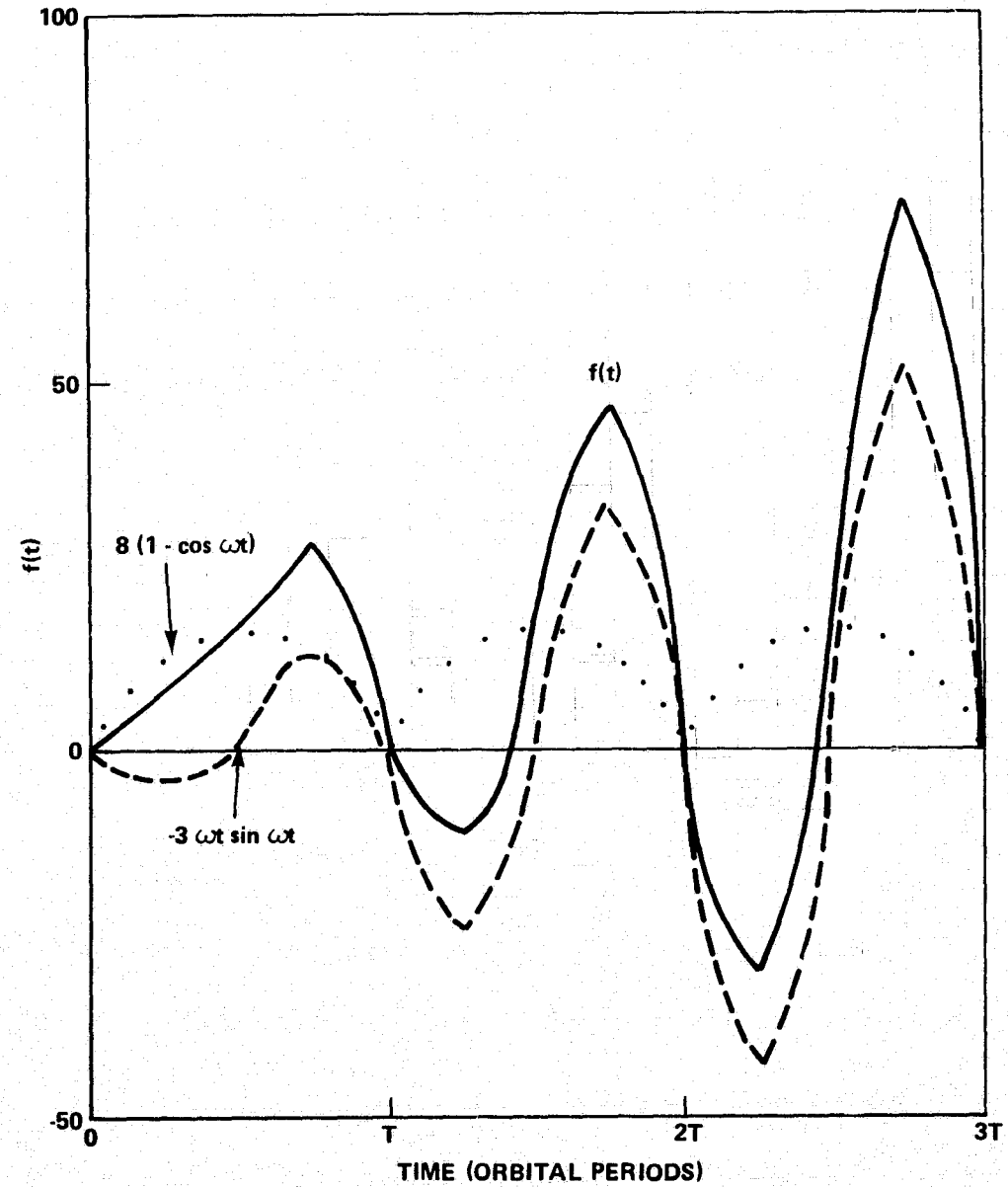

Figure 49. A plot of the function $f(t) = -3\omega t \sin \omega t + 8(1 - \cos \omega t)$ versus time for three orbital periods.

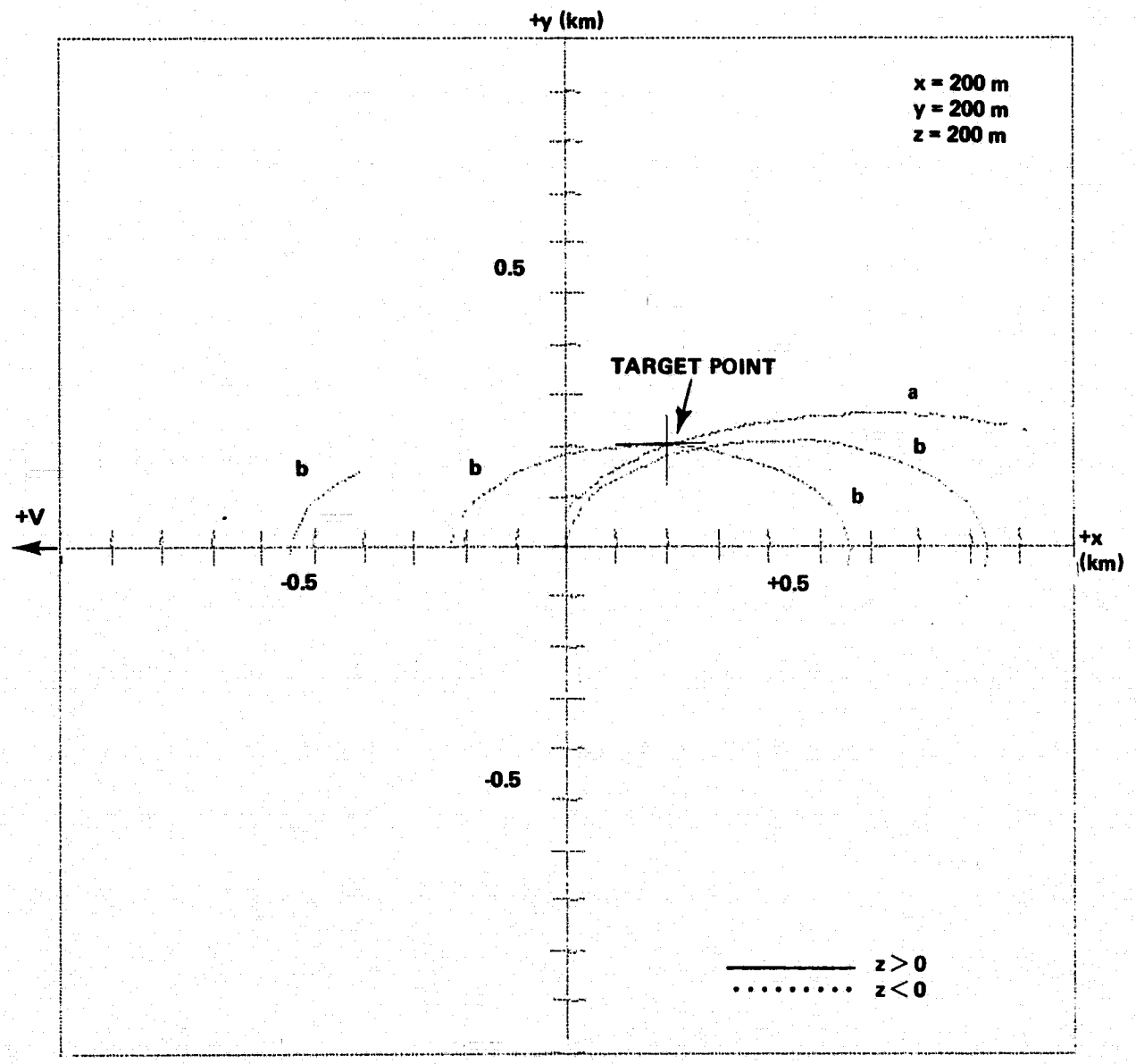

400 km CIRCULAR ORBIT $D = 1 \times 10^{-6}$ m/s^2

CASE	θ (degrees)	φ (degrees)	ΔV (m/s)
a	20.926	-16.830	0.253
b	48.943	2.743	0.345

CASE a SHOWN FOR ONE ORBITAL PERIOD
CASE b SHOWN FOR TWO ORBITAL PERIODS

Figure 50. The x-y projection of the relative motion. [two sample cases targeting to the point in (a) one-fourth T and (b) one and one-fourth T].

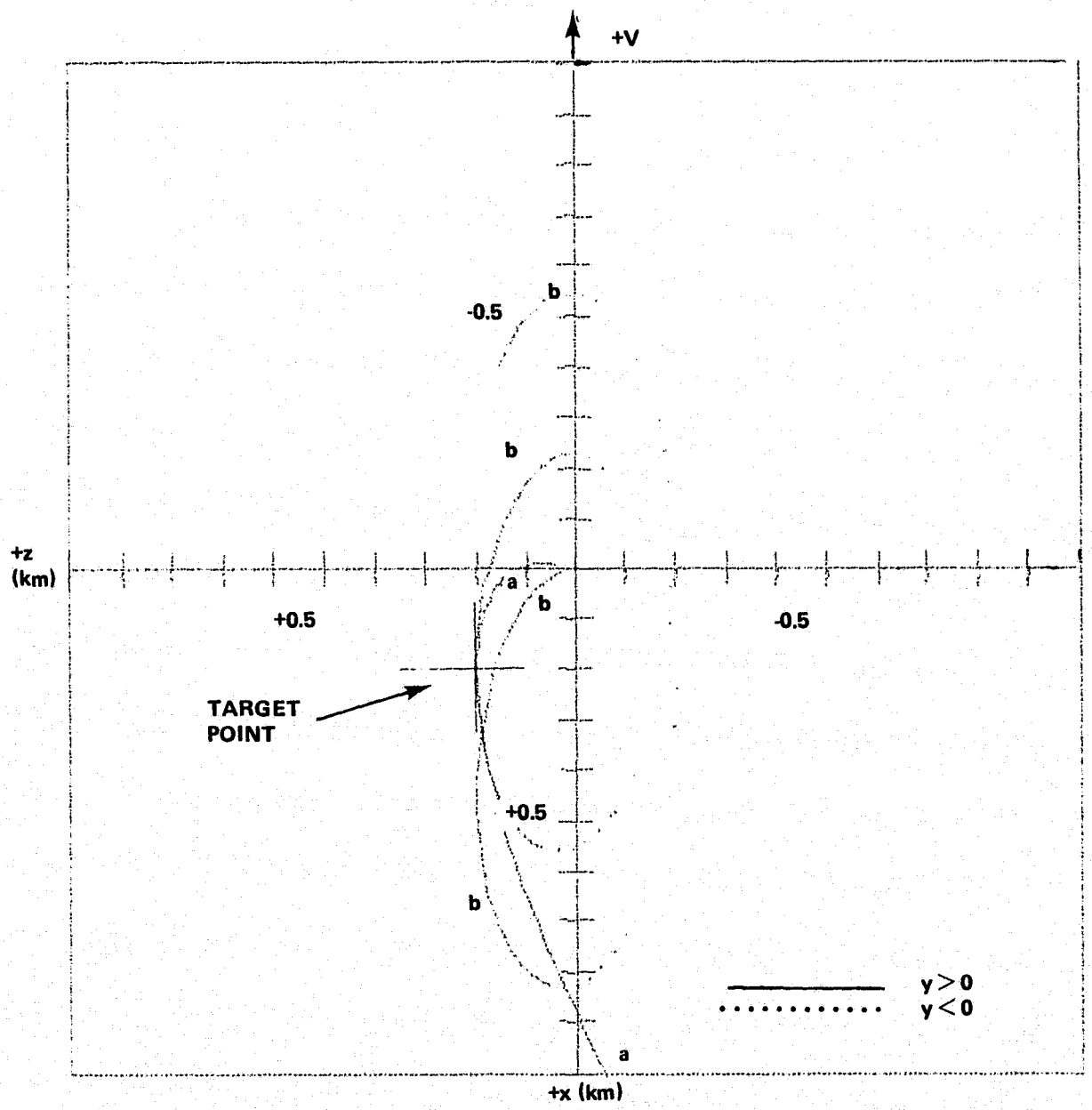

400 km CIRCULAR ORBIT $D = 1 \times 10^{-6}$ m/s^2

CASE	θ (degrees)	φ (degrees)	ΔV (m/s)
a	20.926	-16.830	0.253
b	48.943	2.743	0.345

CASE a SHOWN FOR ONE ORBITAL PERIOD
CASE b SHOWN FOR TWO ORBITAL PERIODS

Figure 51. The x-z projection of the relative motion [two sample cases targeting to the point in (a) one-fourth T and (b) one and one-fourth T].

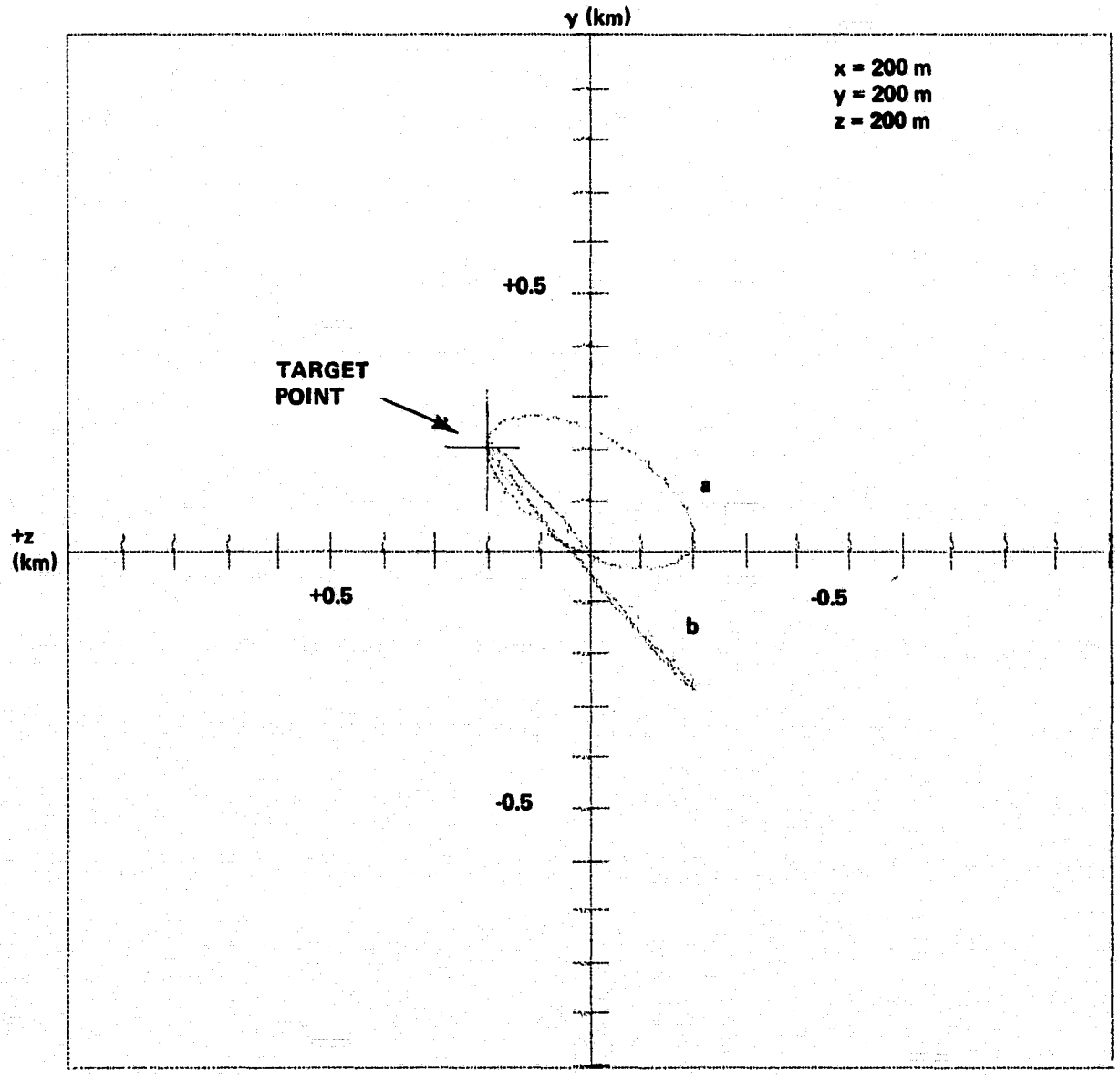

400 km CIRCULAR ORBIT $D = 1 \times 10^{-6}$ m/s^2

CASE	θ (degrees)	φ (degrees)	ΔV (m/s)
a	20.926	-16.830	0.253
b	48.943	2.743	0.345

CASE a SHOWN FOR ONE ORBITAL PERIOD
CASE b SHOWN FOR TWO ORBITAL PERIODS

ORBITAL VELOCITY VECTOR INTO PAGE

Figure 52. The y-z projection of the relative motion [two sample cases targeting to the point in (a) one-fourth T and (b) one and one-fourth T].

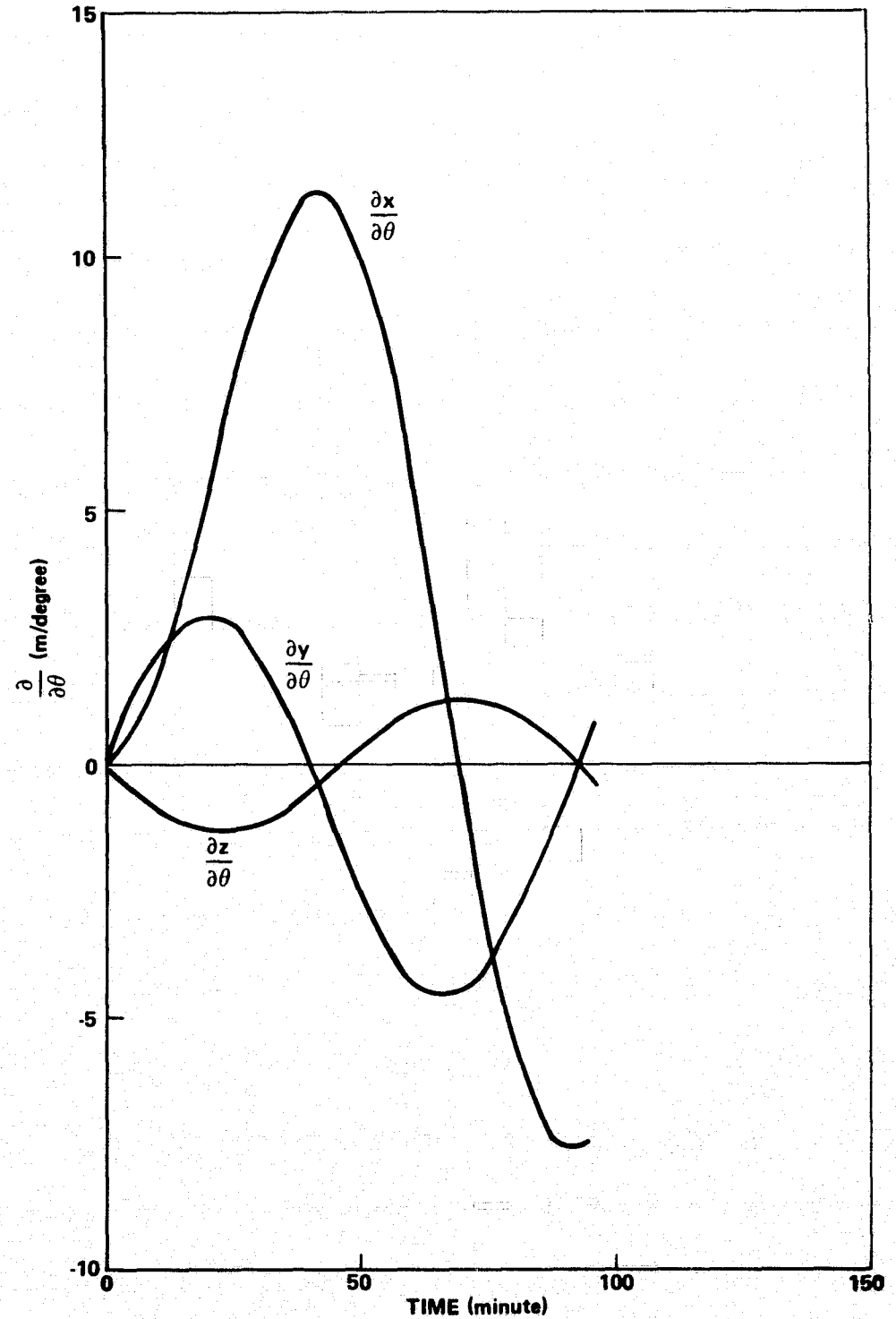

Figure 53. The partials of the coordinates with respect to the initial angle θ versus time for the nominal case (θ = 20.926 degrees, φ = -16.829 degrees, ΔV = 0.253 m/s).

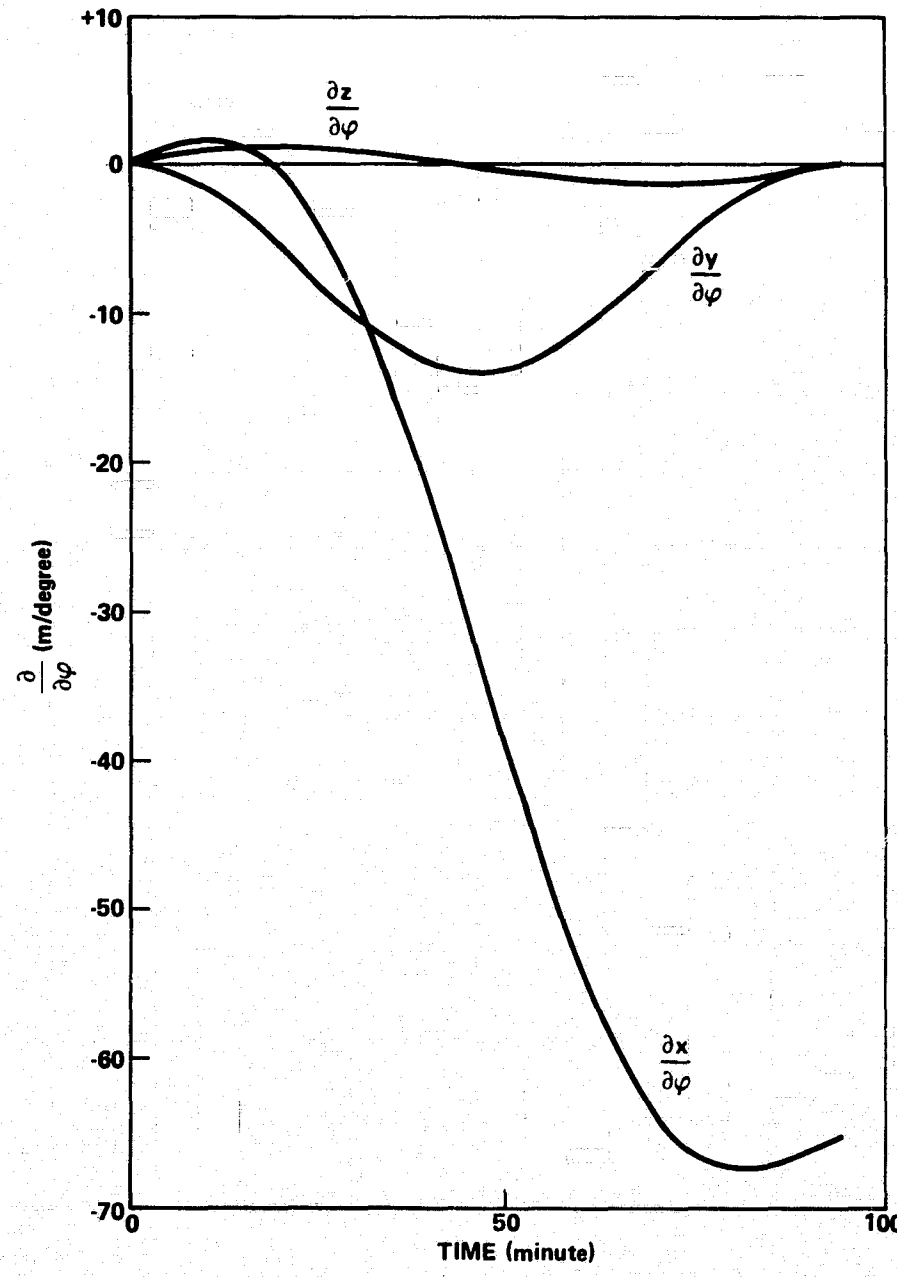

Figure 54. The partials of the coordinates with respect to the initial angle φ versus time for the nominal case (θ = 20.926 degrees, φ = -16.829 degrees, ΔV = 0.253 m/s).

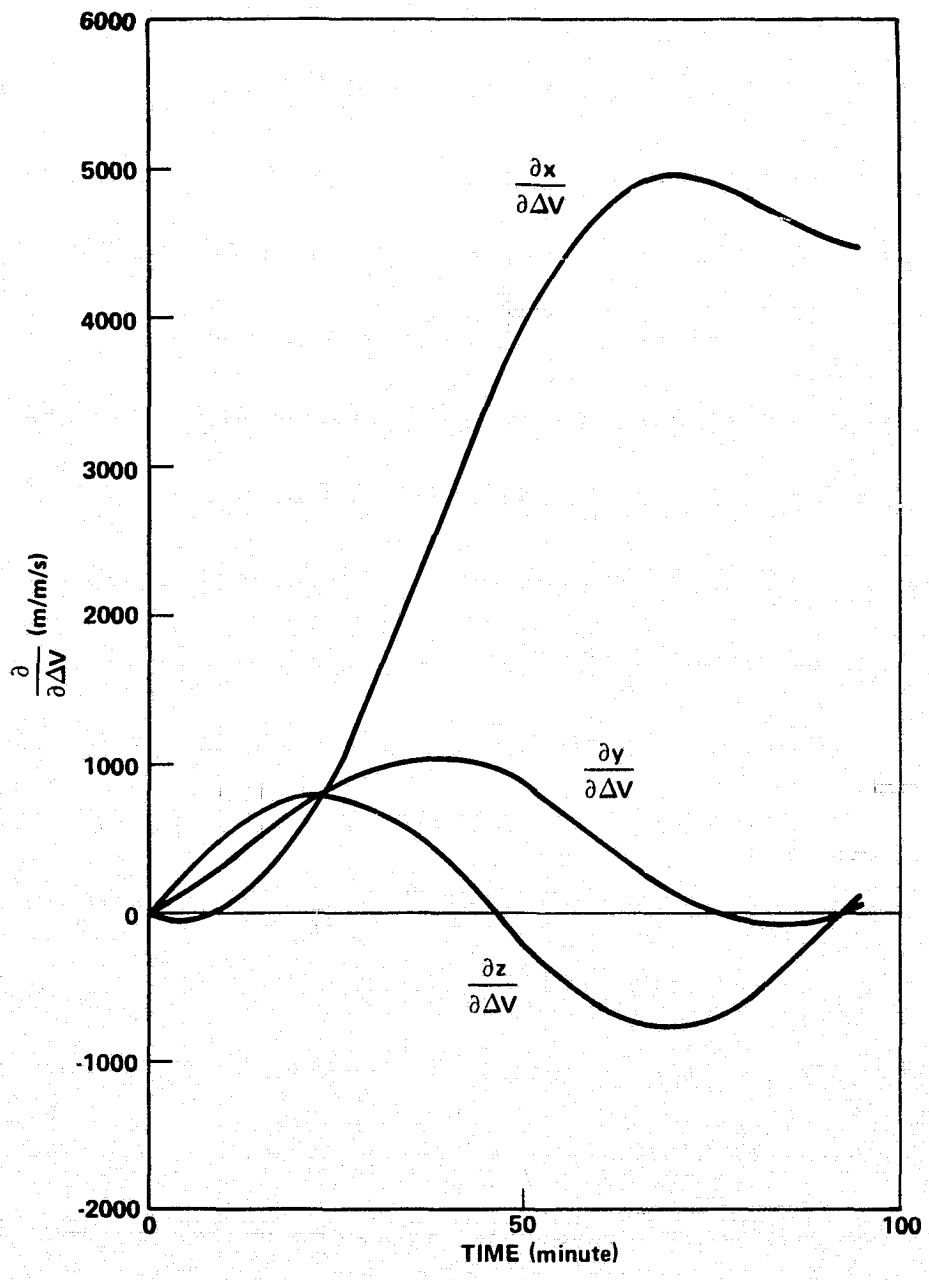

Figure 55. The partials of the coordinates with respect to the initial impulse ΔV versus time for the nominal case (θ = 20.926 degrees, φ = -16.829 degrees, ΔV = 0.253 m/s).

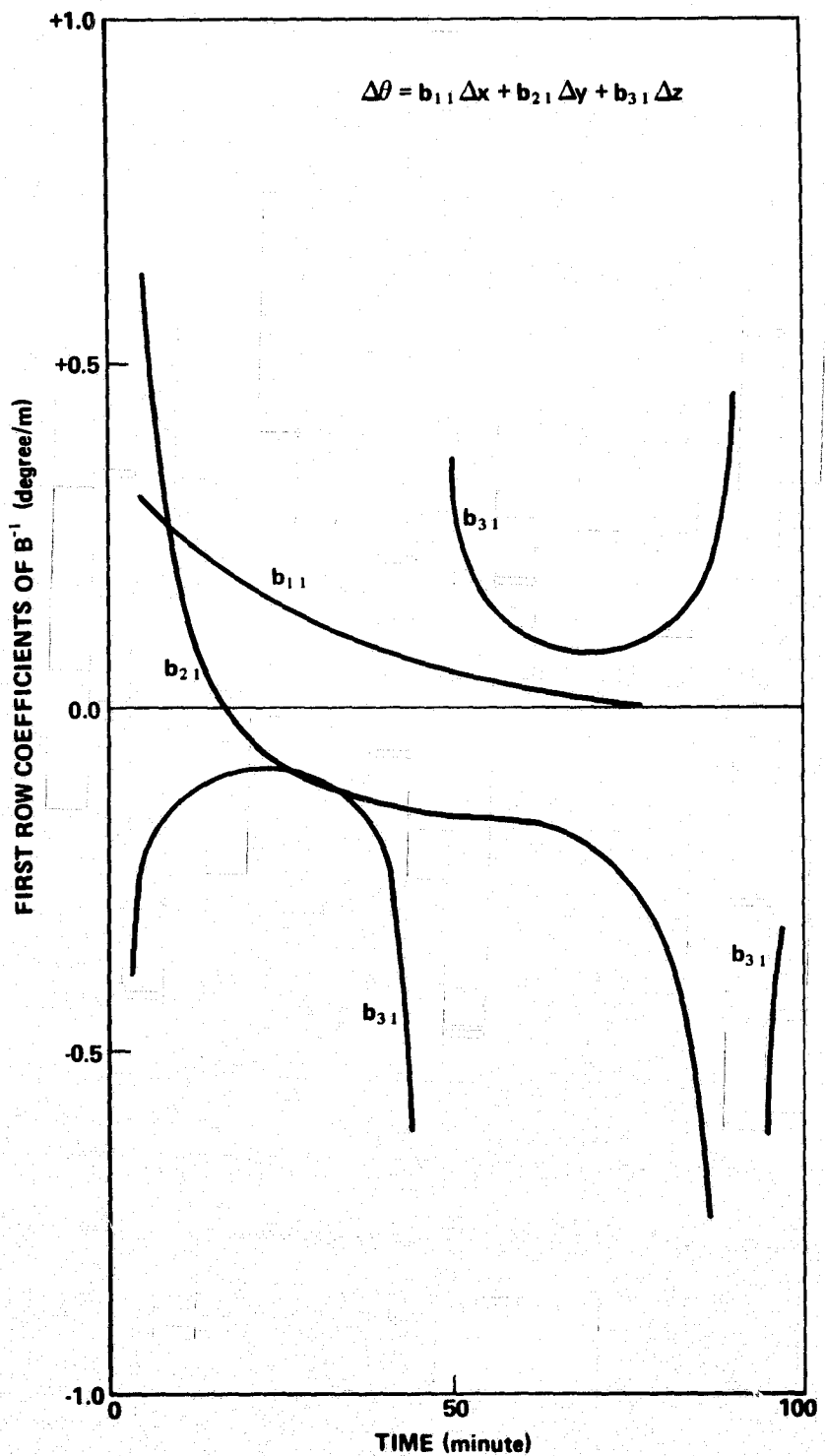

Figure 56. Coefficients determining allowable error in the ejection angle θ for a specified allowable error in the position versus time for the nominal case (θ = 20.926 degrees, φ = -16.829 degrees, ΔV = 0.253 m/s).

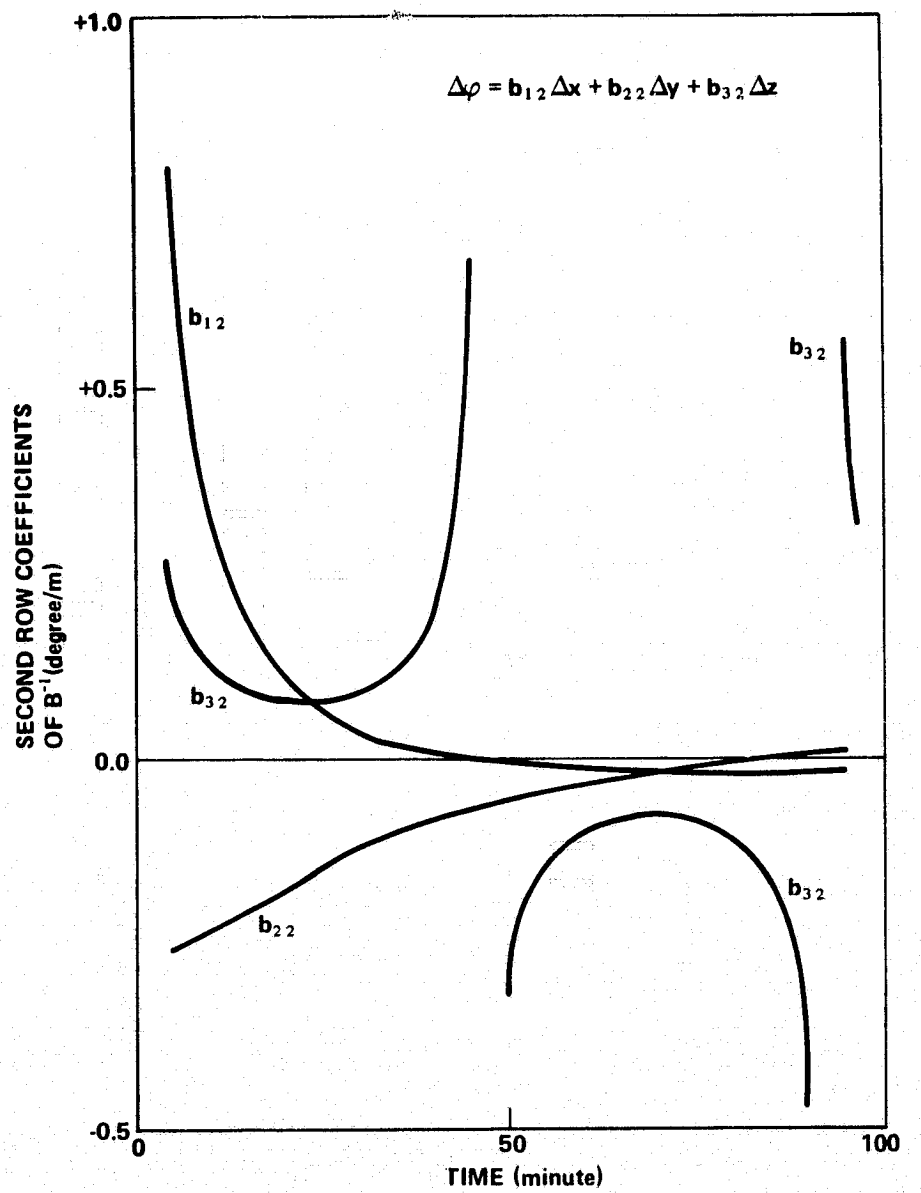

Figure 57. Coefficients determining allowable error in the ejection angle φ for a specified allowable error in the position versus time for the nominal case (θ = 20.926 degrees, φ = -16.829 degrees, ΔV = 0.253 m/s).

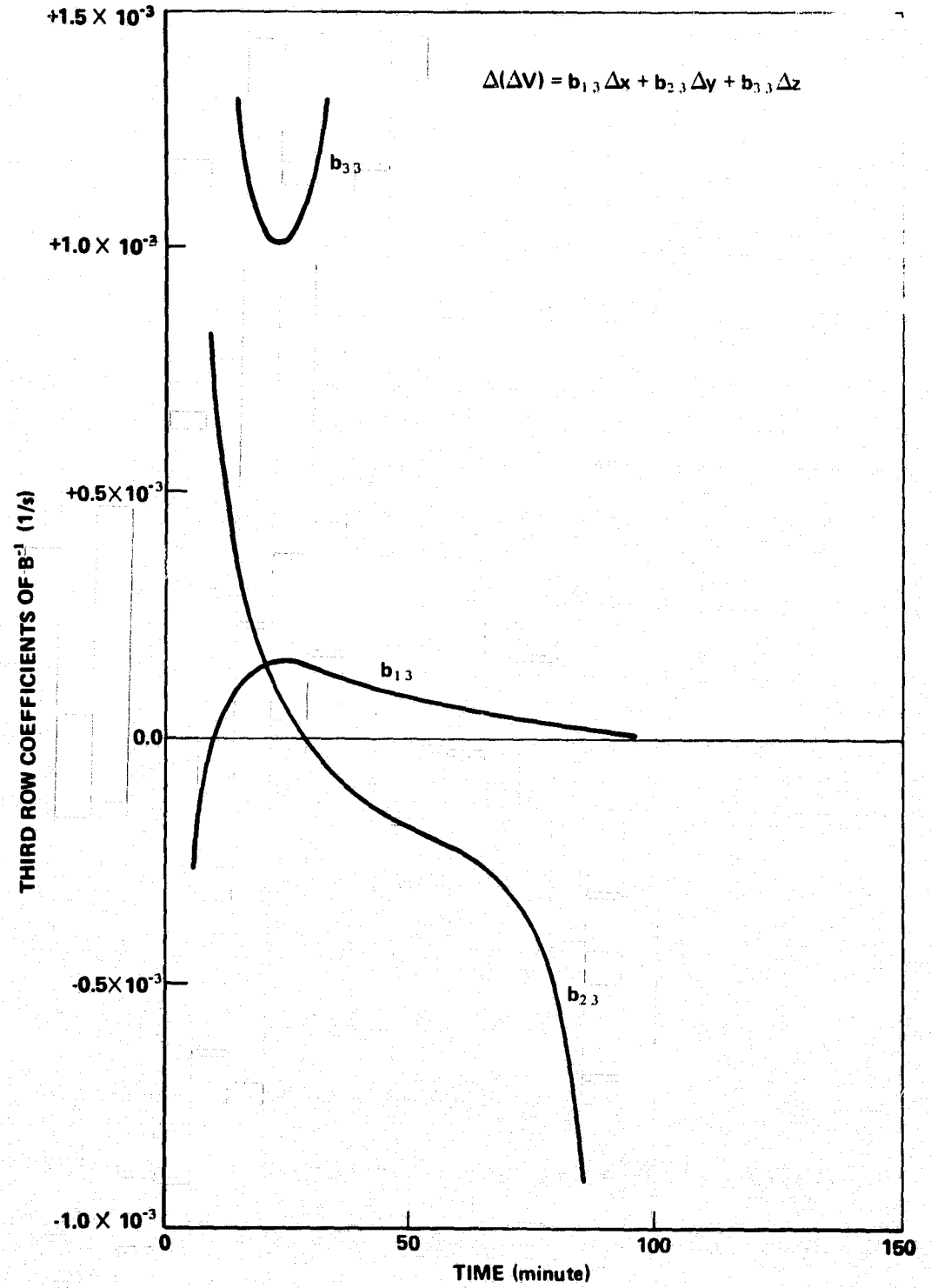

Figure 58. Coefficients determining allowable error in the ejection impulse ΔV for a specified allowable error in the position versus time for the nominal case (θ = 20.926 degrees, φ = -16.829 degrees, ΔV = 0.253 m/s).

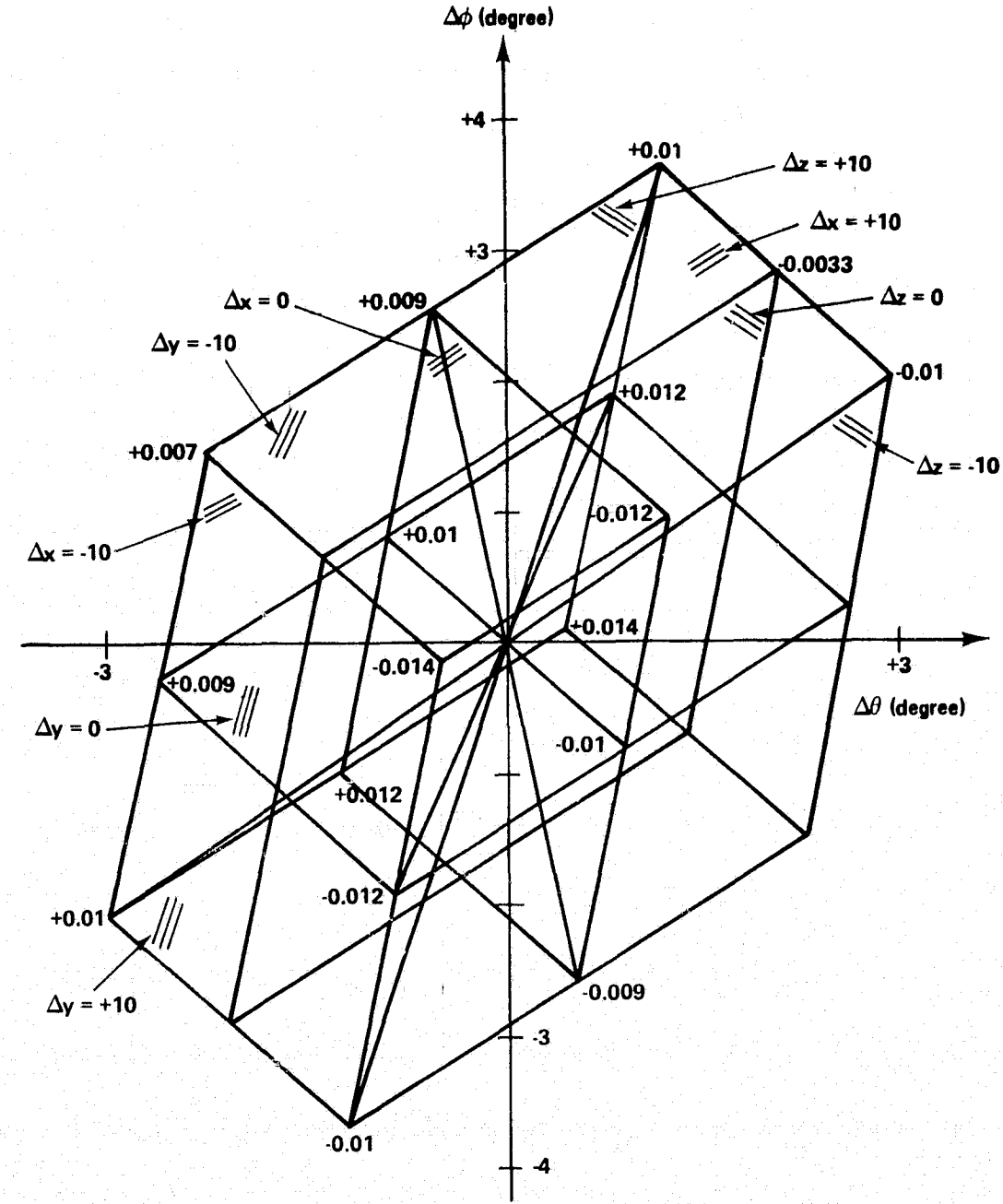

Figure 59. The allowed ejection error box for a cube of allowed position errors of sides 20 m about the nominal point at 20 min for the nominal case (θ = 20.926 degrees, φ = -16.830 degrees, ΔV = 0.253 m/s).

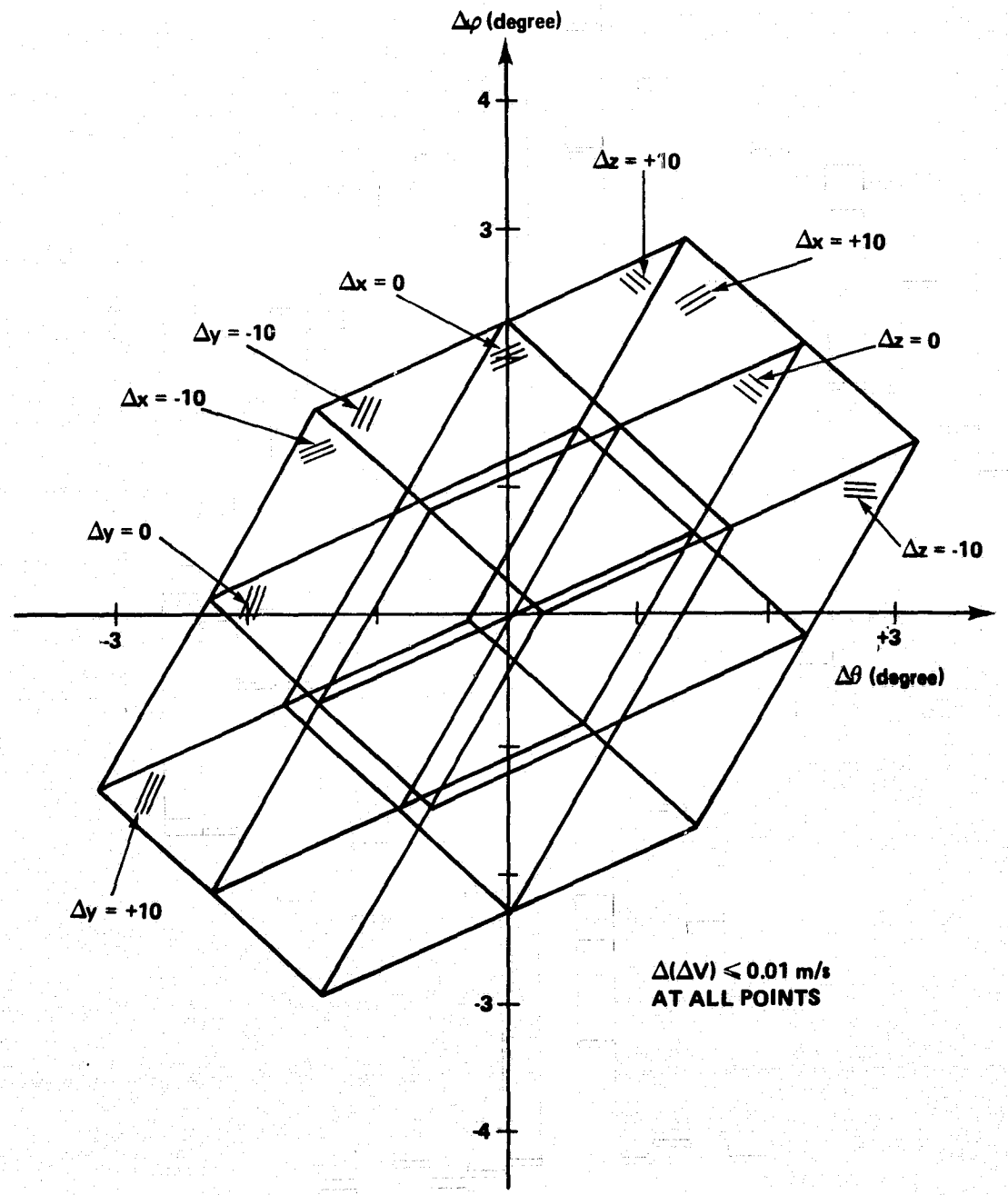

Figure 60. The allowed ejection error box for a cube of allowed position errors of sides 20 m about the nominal point at 25 min for the nominal case (θ = 20.926 degrees, φ = -16.830 degrees, ΔV = 0.253 m/s).

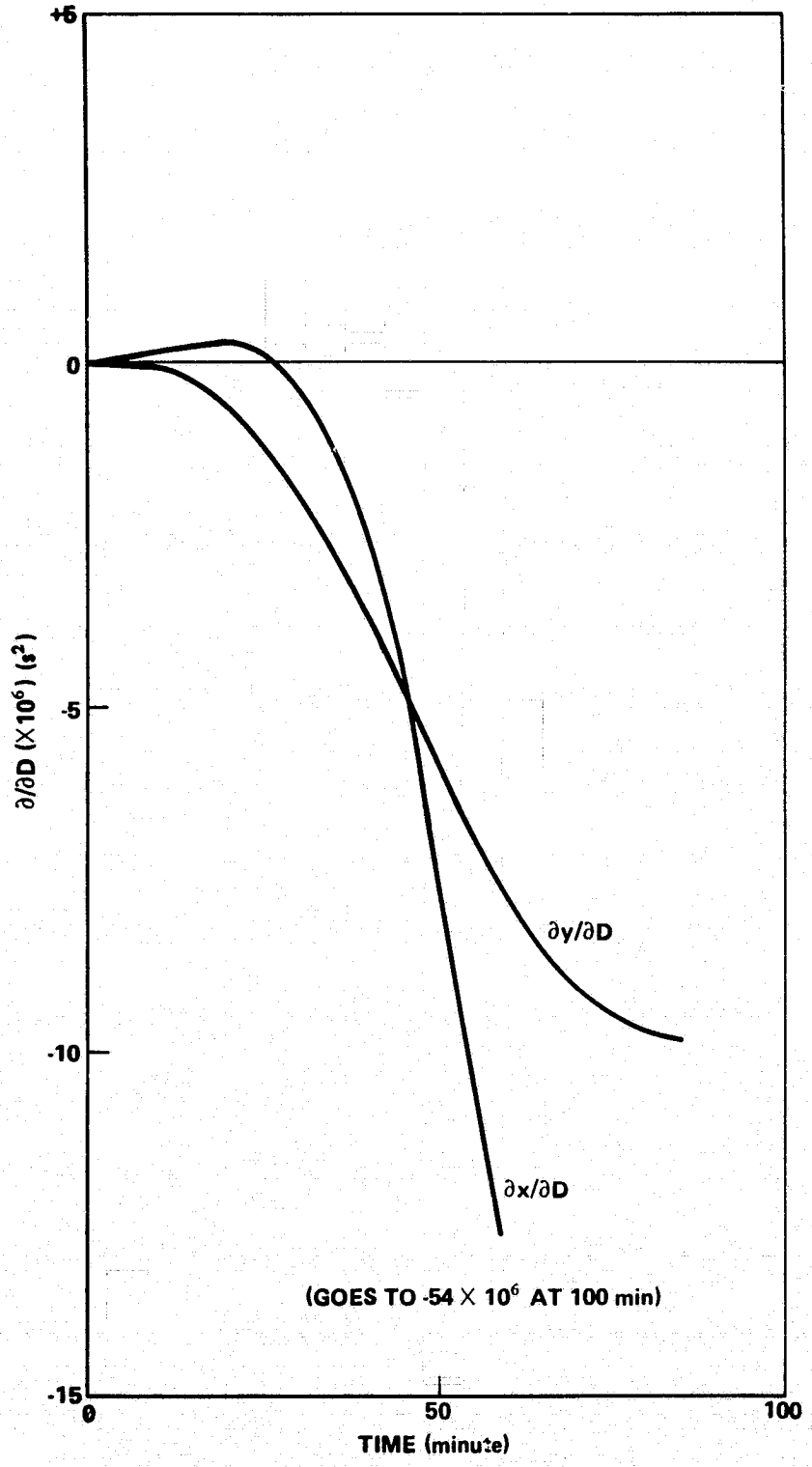

Figure 61. The partial derivatives of x and y with respect to differential drag for one orbital period.

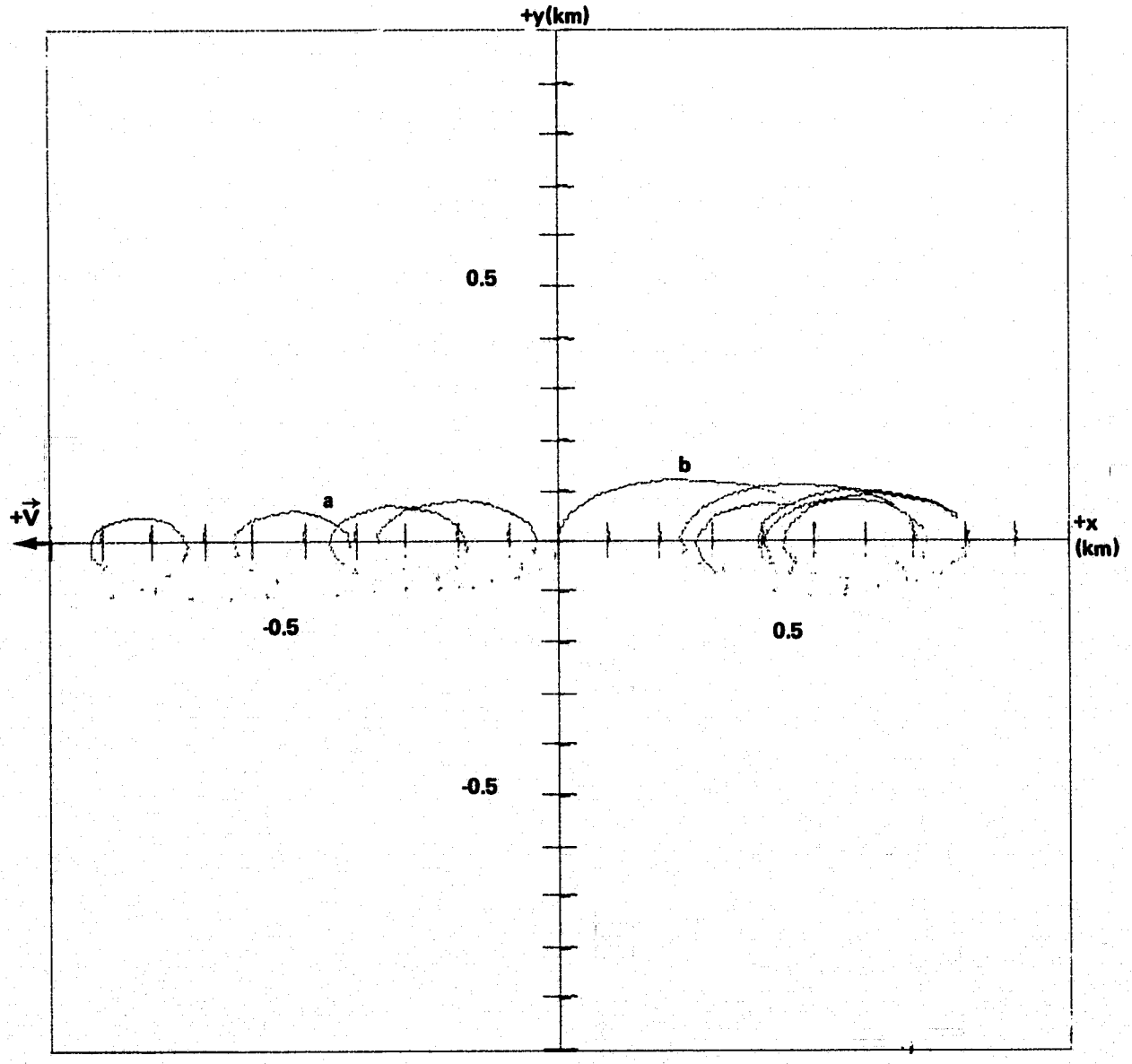

400 km CIRCULAR ORBIT $D = 1 \times 10^{-6}$ m/s^2

CASE	θ (degrees)	φ (degrees)	ΔV (m/s)
a	270	90	0.1
b	100	90	0.1

EACH CASE SHOWN FOR APPROXIMATELY FIVE ORBITS
DOTS ARE SEPARATED BY 5 min IN TIME
ALL MOTION IN THE ORBITAL PLANE (x-y) FOR THESE CASES

Figure 62. The x-y projection of the relative motion.

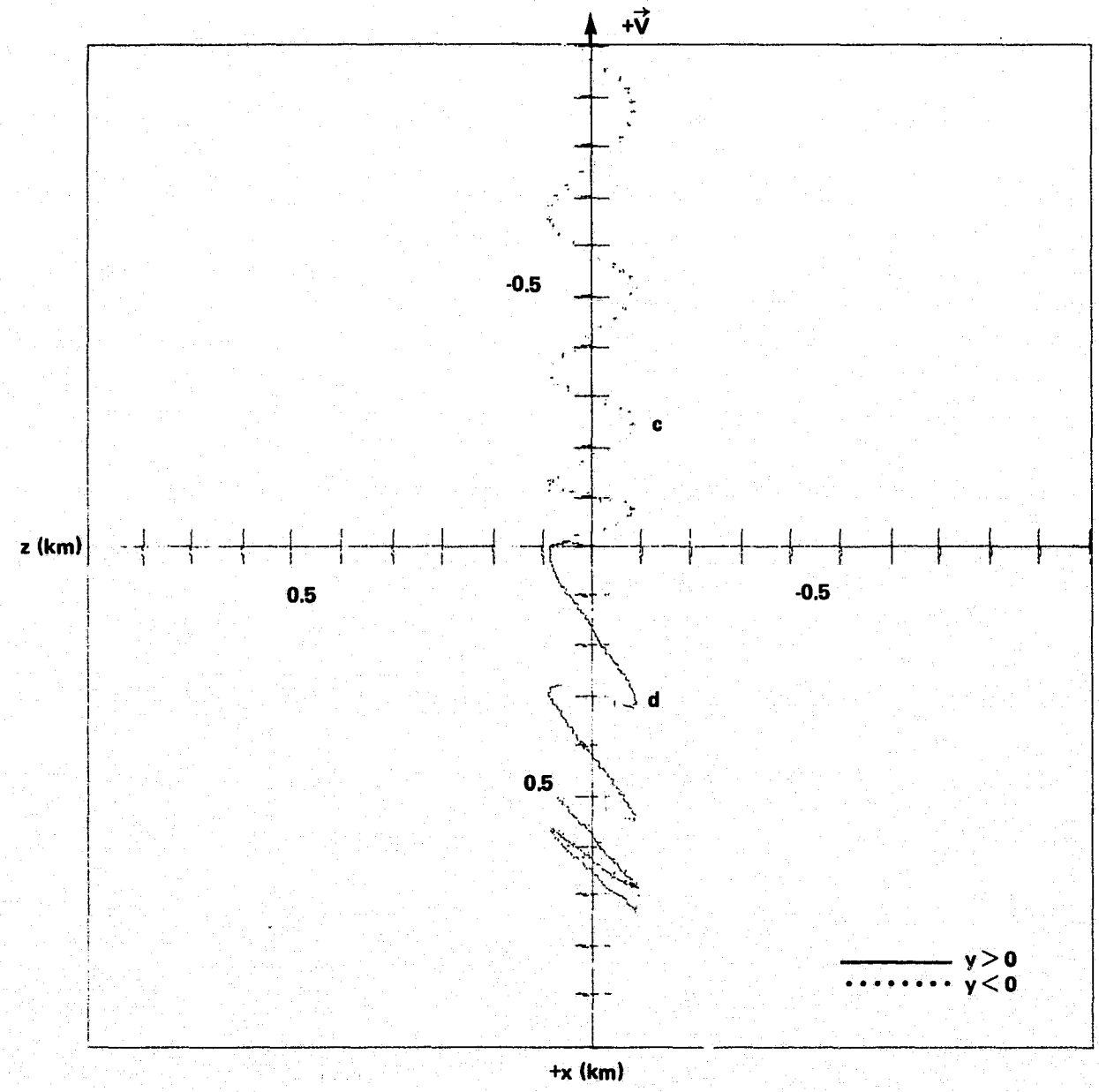

400 km CIRCULAR ORBIT $D = 1 \times 10^{-6}$ m/s^2

CASE	θ (degrees)	φ (degrees)	ΔV (m/s)
c	0	2	0.1
d	0	-12	0.1

EACH CASE SHOWN FOR APPROXIMATELY FIVE ORBITS
DOTS ARE SEPARATED BY 5 min IN TIME

Figure 63. The x-z projection of the relative motion.

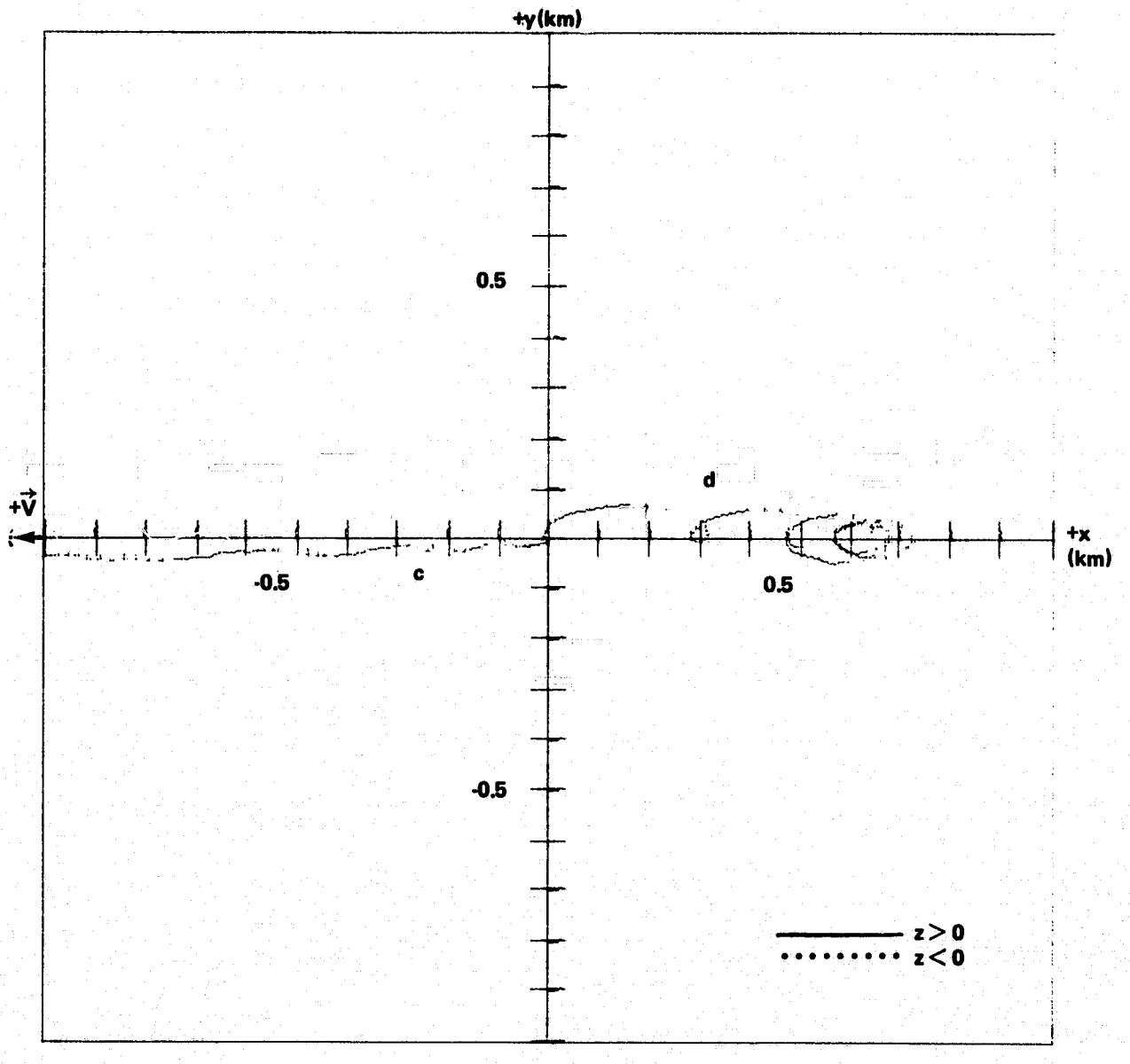

400 km CIRCULAR ORBIT $D = 1 \times 10^{-6}$ m/s^2

CASE	θ (degrees)	φ (degrees)	ΔV (m/s)
c	0	2	0.1
d	0	-12	0.1

EACH CASE SHOWN FOR APPROXIMATELY FIVE ORBITS
DOTS ARE SEPARATED BY 5 min IN TIME

Figure 64. The x-y projection of the relative motion.

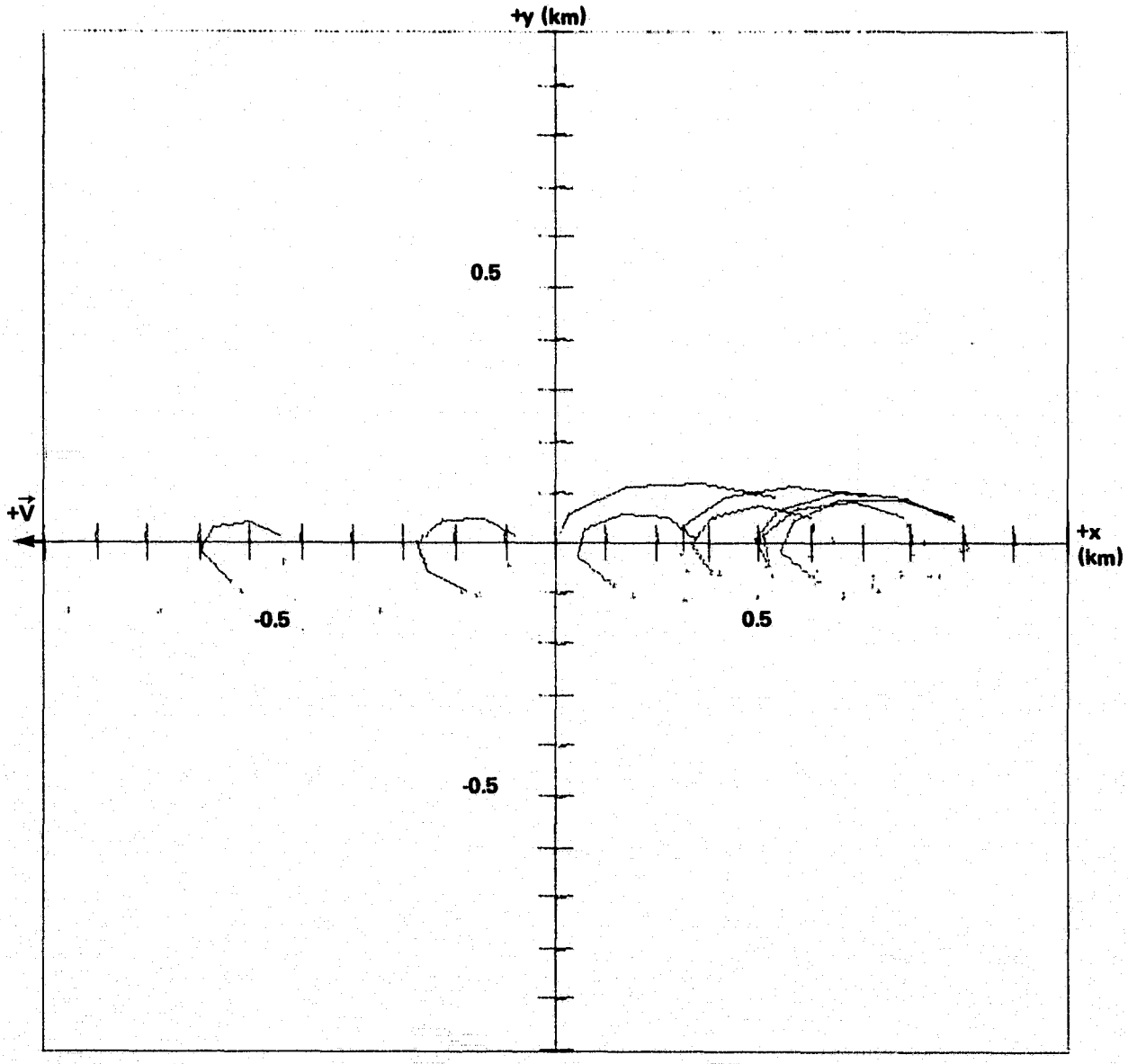

400 km CIRCULAR ORBIT $D = 1 \times 10^{-6}$ m/s^2

CASE b: $\theta = 100°$, $\varphi = 90°$, $\Delta V = 0.1$ m/s

THIS CASE SHOWN FOR APPROXIMATELY NINE ORBITS
DOTS ARE SEPARATED BY 10 min IN TIME
ALL MOTION IN THE ORBITAL PLANE (x-y) FOR THIS CASE

Figure 65. The x-y projection of the relative motion.

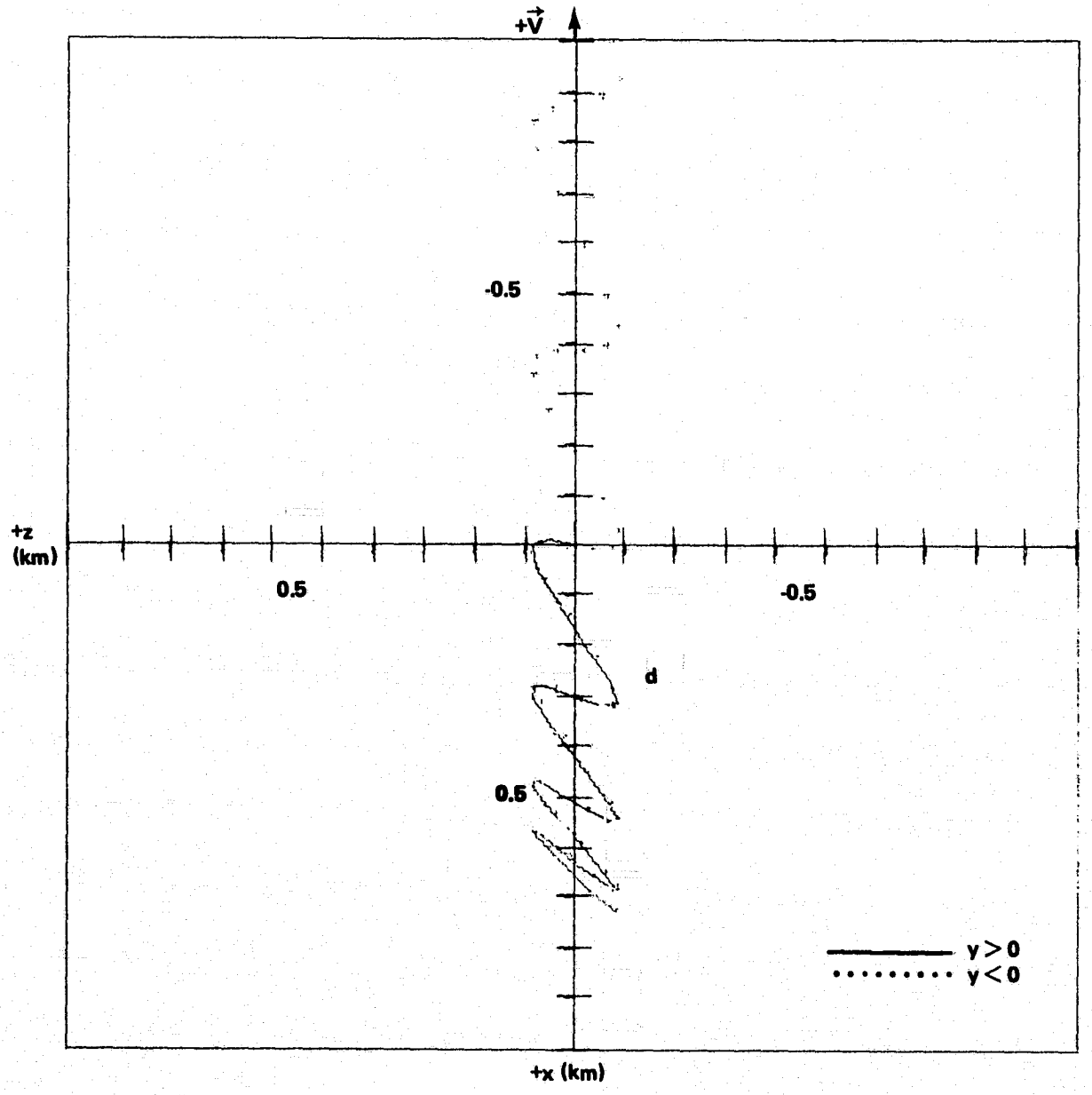

400 km CIRCULAR ORBIT $D = 1 \times 10^{-6}$ m/s^2

CASE d: $\theta = 0°$, $\varphi = -12°$, $\Delta V = 0.1$ m/s

THIS CASE SHOWN FOR APPROXIMATELY TEN ORBITS
DOTS ARE SEPARATED BY 10 min IN TIME

Figure 66. The x-z projection of the relative motion.

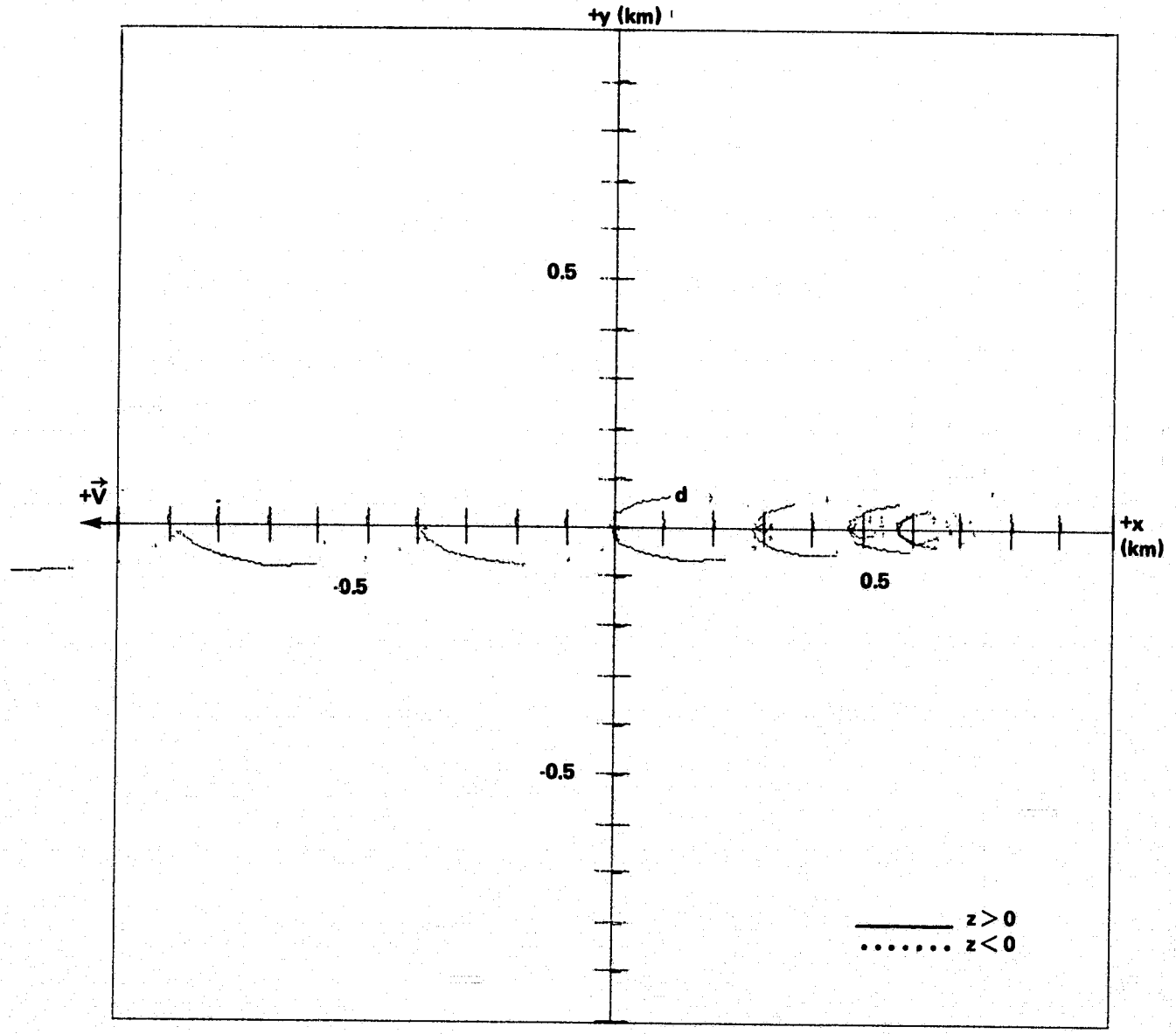

400 km CIRCULAR ORBIT $D = 1 \times 10^{-6}$ m/s^2

CASE d: $\theta = 0°$, $\varphi = -12°$, $\Delta V = 0.1$ m/s

THIS CASE SHOWN FOR APPROXIMATELY TEN ORBITS
DOTS ARE SEPARATED BY 10 min IN TIME

Figure 67. The x-y projection of the relative motion.

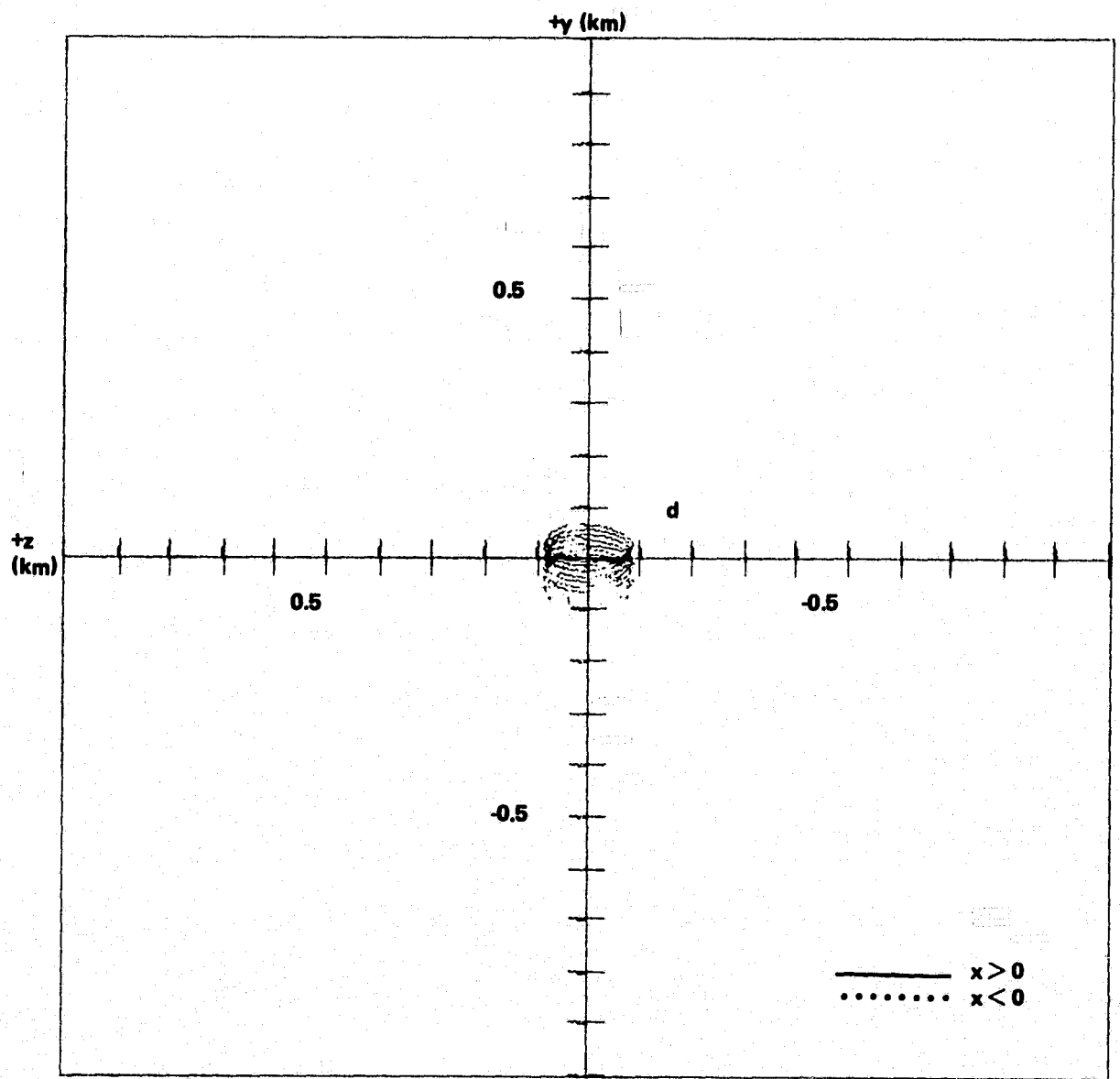

400 km CIRCULAR ORBIT $D = 1 \times 10^{-6}$ m/s^2

CASE d: $\theta = 0°$, $\varphi = -12°$, $\Delta V = 0.1$ m/s

THIS CASE SHOWN FOR APPROXIMATELY TEN ORBITS
DOTS ARE SEPARATED BY 10 min IN TIME

Figure 68. The y-z projection of the relative motion.

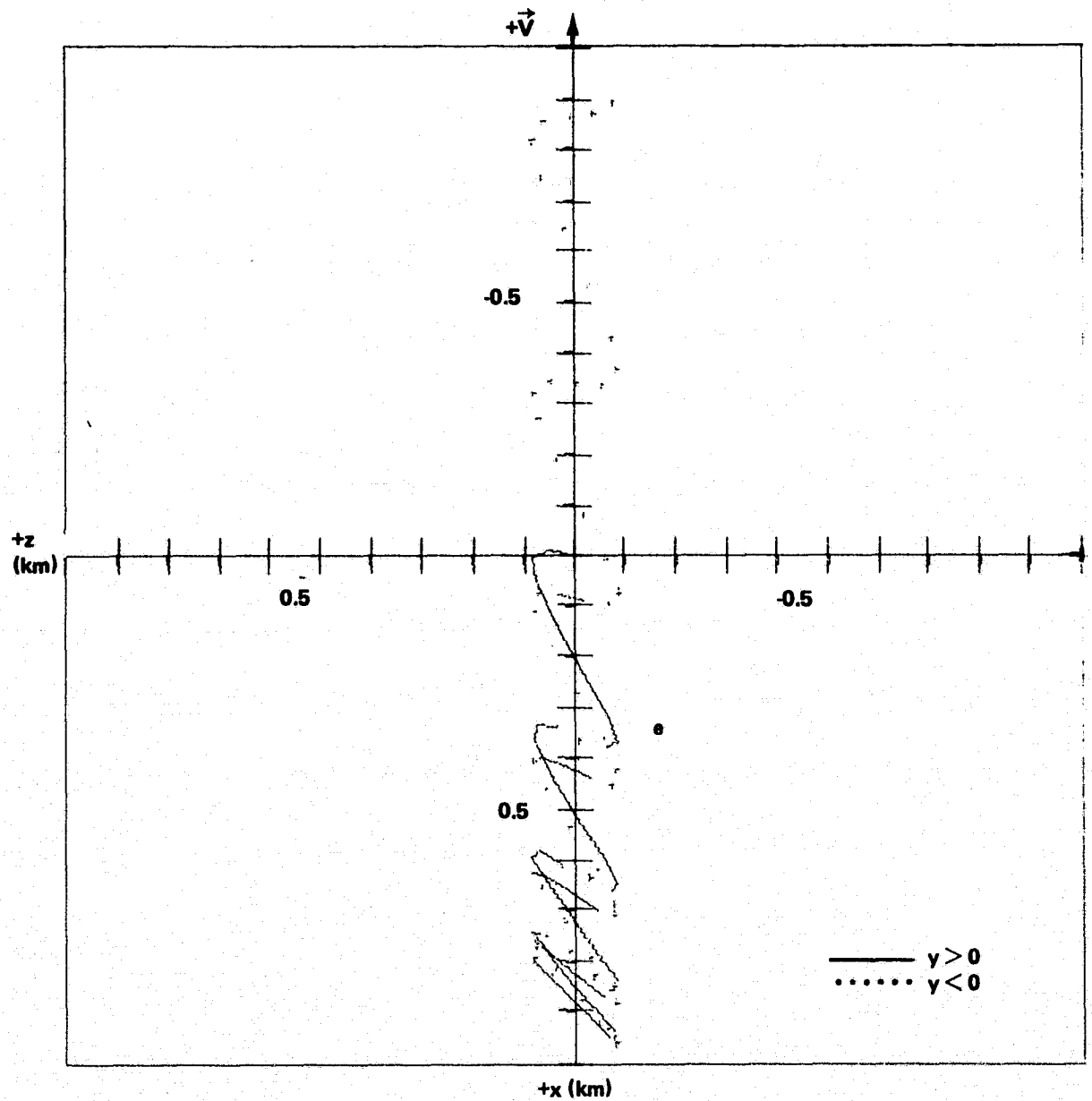

400 km CIRCULAR ORBIT $D = 1 \times 10^{-6}$ m/s^2

CASE e: $\theta = 0°$, $\varphi = -14°$, $\Delta V = 0.1$ m/s

THIS CASE SHOWN FOR APPROXIMATELY TEN ORBITS
DOTS ARE SEPARATED BY 10 min IN TIME

Figure 69. The x-z projection of the relative motion.

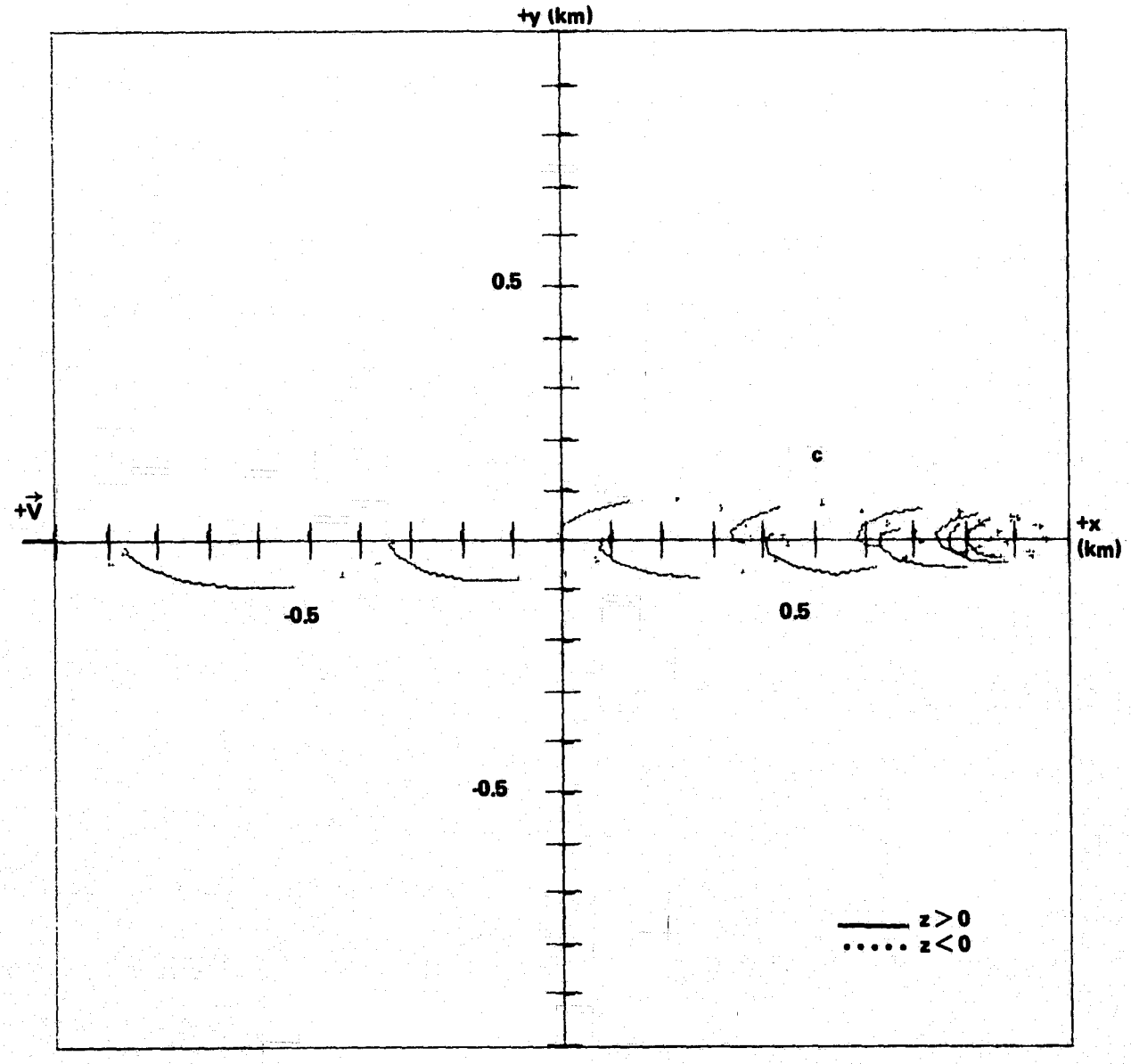

400 km CIRCULAR ORBIT $D = 1 \times 10^{-6}$ m/s^2

CASE e: $\theta = 0°$, $\varphi = -14°$, $\Delta V = 0.1$ m/s

THIS CASE SHOWN FOR APPROXIMATELY TEN ORBITS
DOTS ARE SEPARATED BY 10 min IN TIME

Figure 70. The x-y projection of the relative motion.

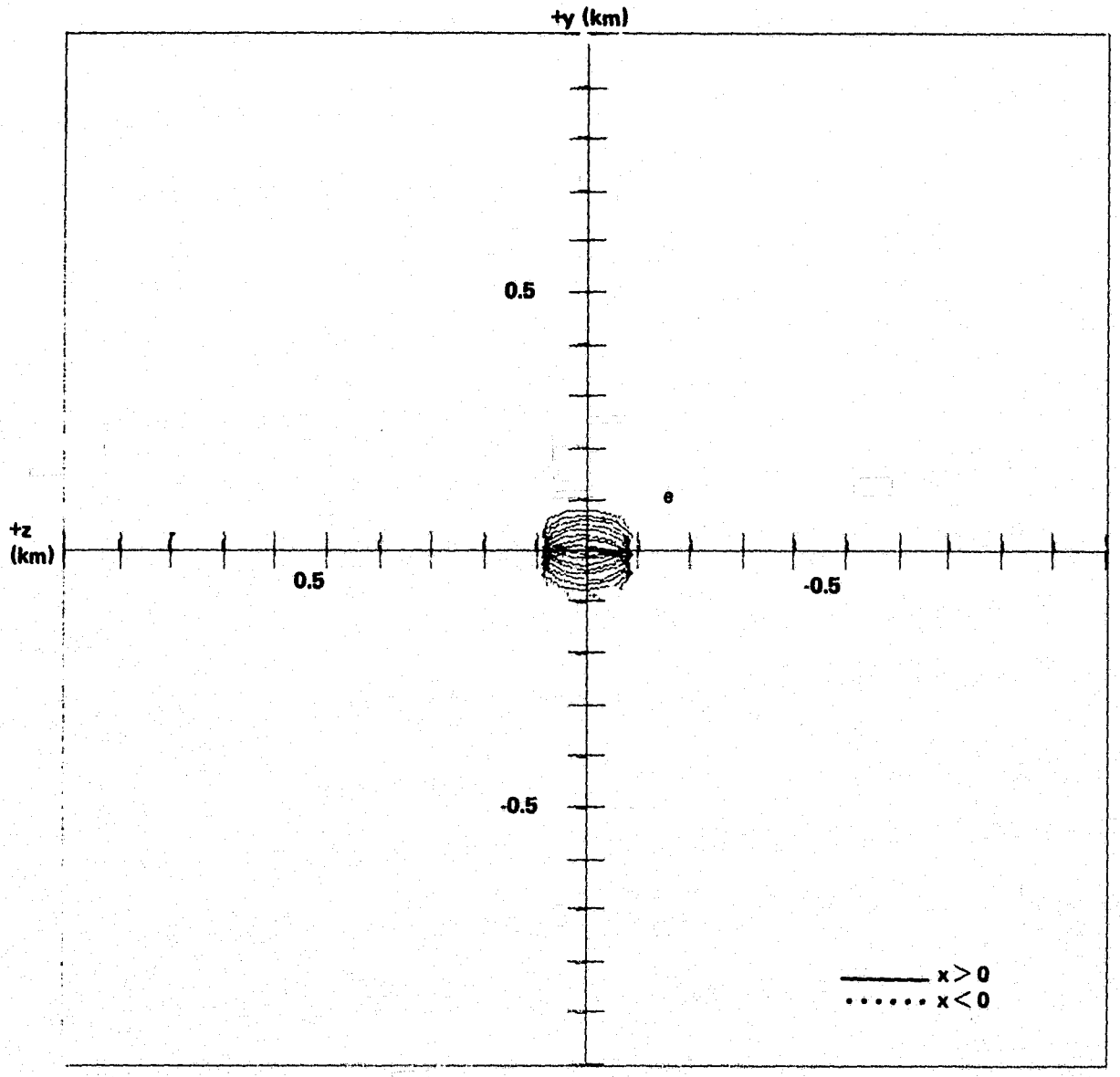

400 km CIRCULAR ORBIT $D = 1 \times 10^{-6}$ m/s^2

CASE e: $\theta = 0°$, $\varphi = -14°$, $\Delta V = 0.1$ m/s

THIS CASE SHOWN FOR APPROXIMATELY TEN ORBITS
DOTS ARE SEPARATED BY 10 min IN TIME

Figure 71. The y-z projection of the relative motion.

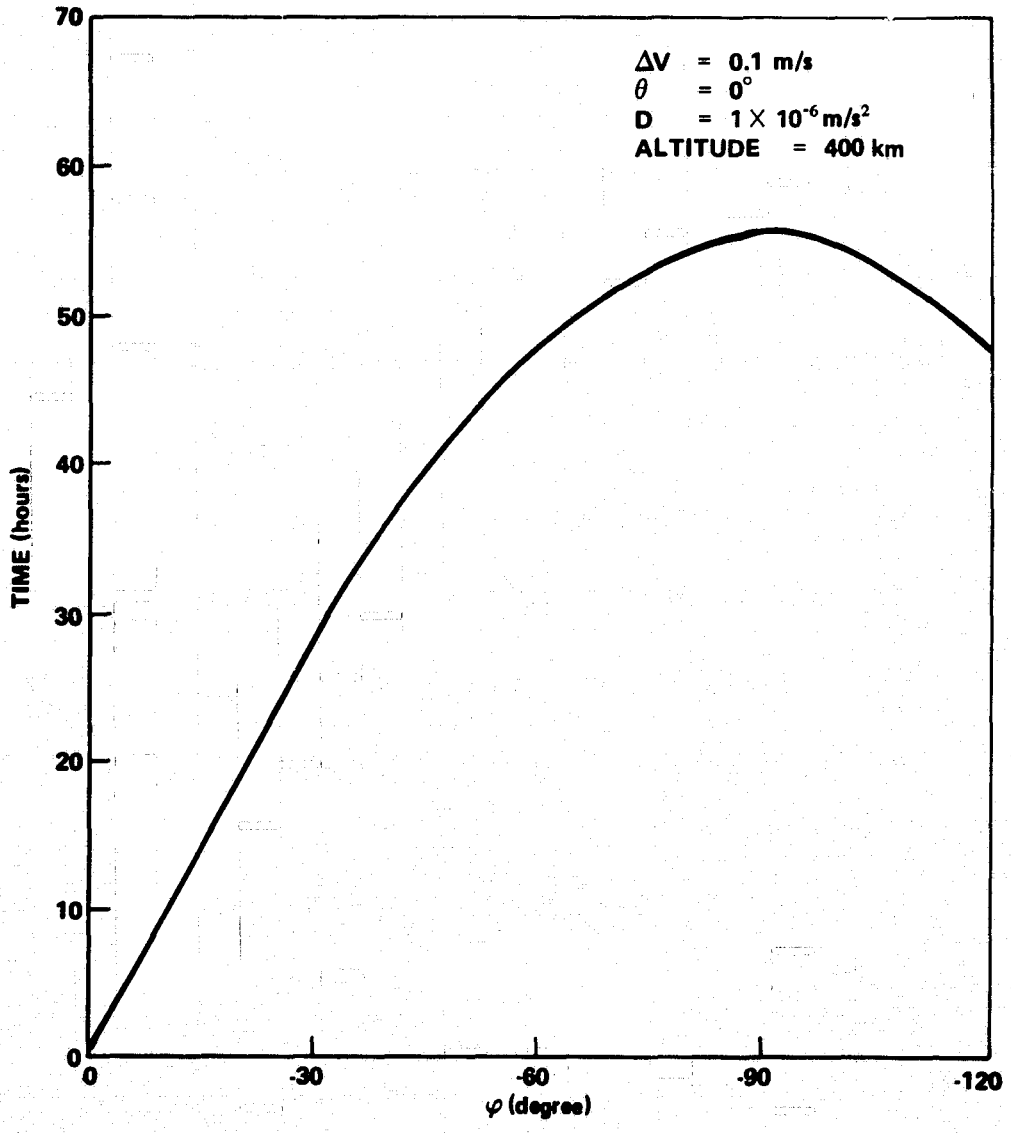

Figure 72. Time TAD stays behind the Shuttle versus the ejection angle φ.

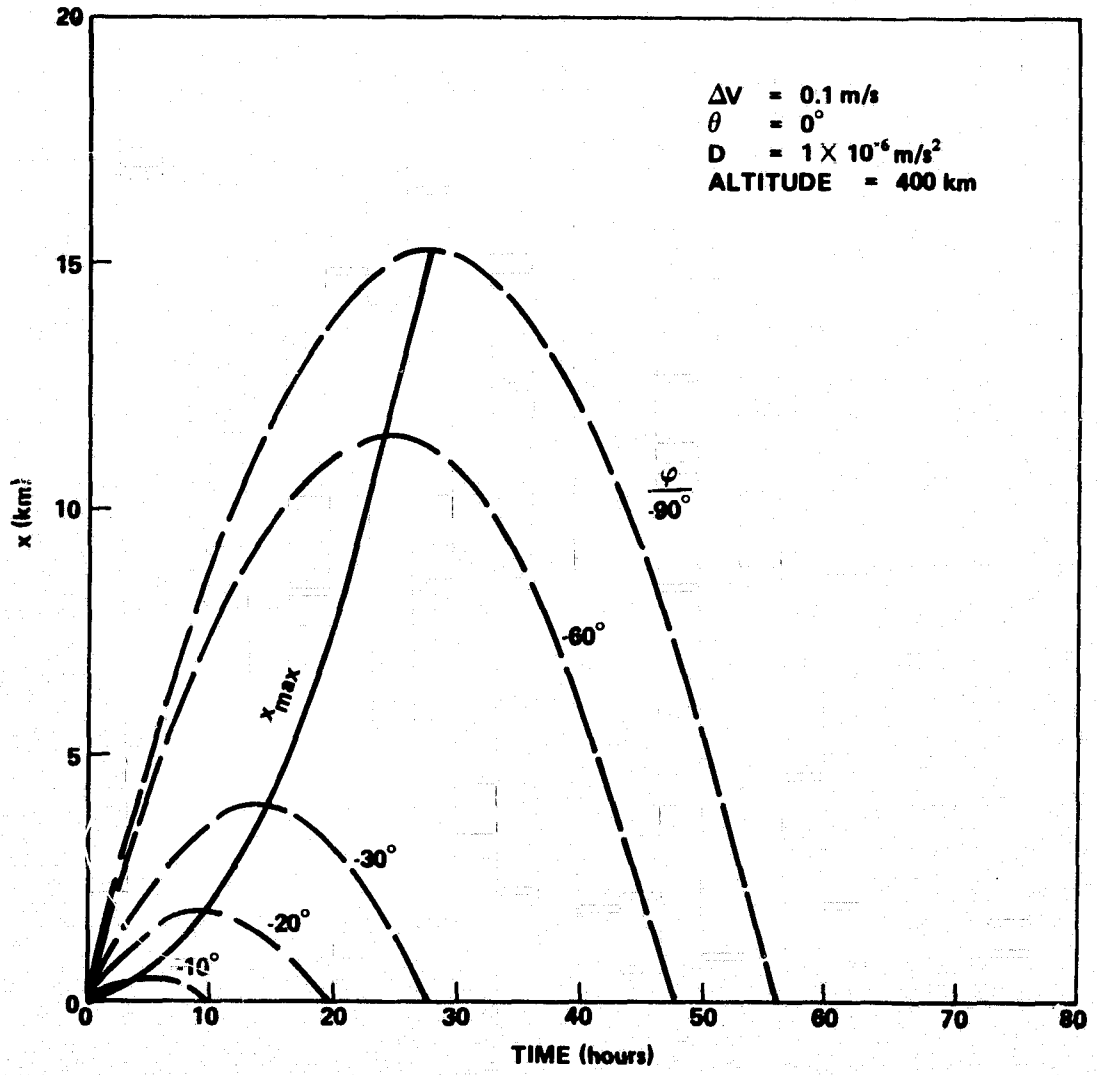

Figure 73. Distance of the TAD behind the Shuttle versus time with the ejection angle φ parameterized.

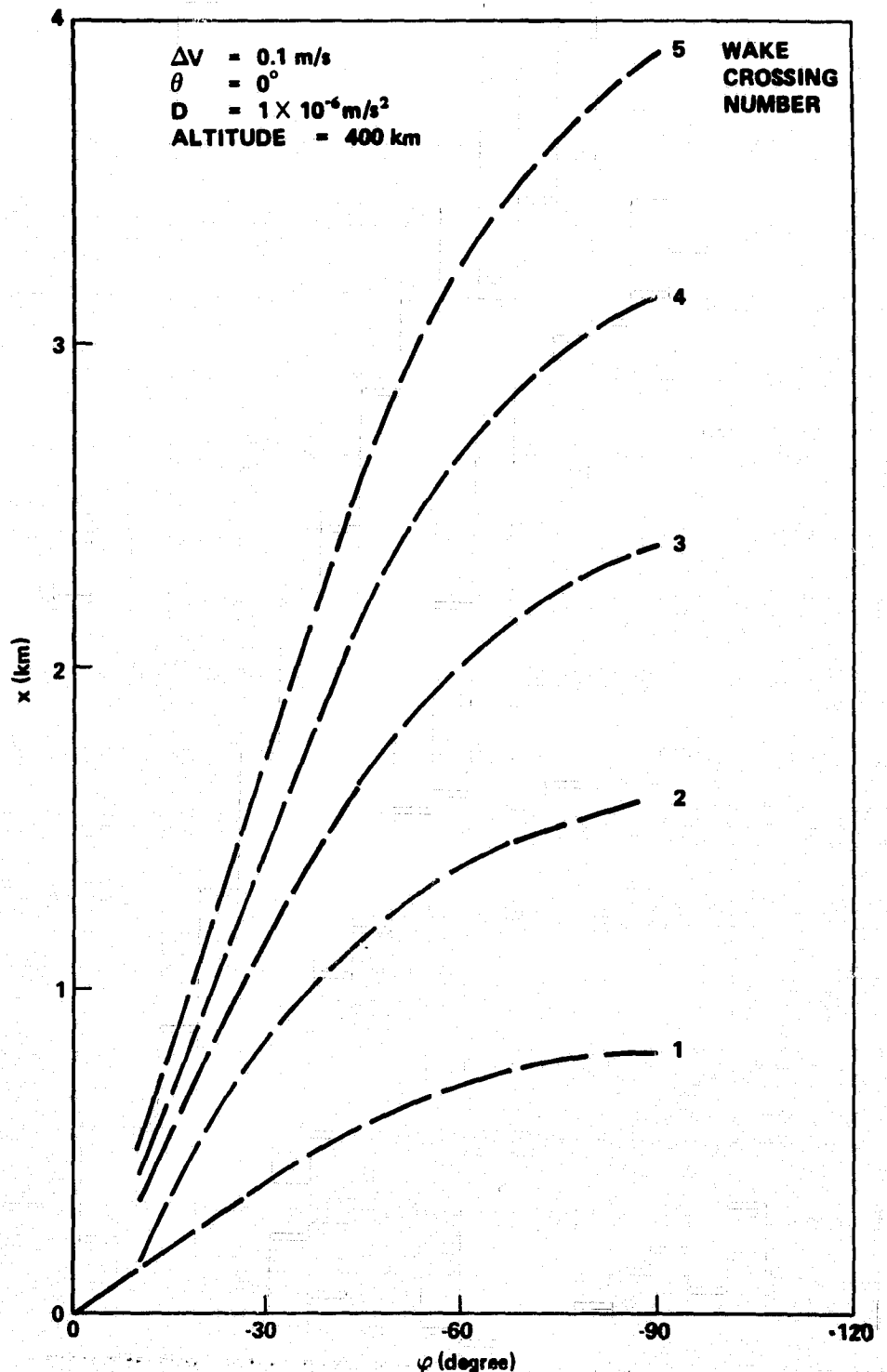

Figure 74. Distances of the first five wake crossings behind the Shuttle versus the ejection angle φ.

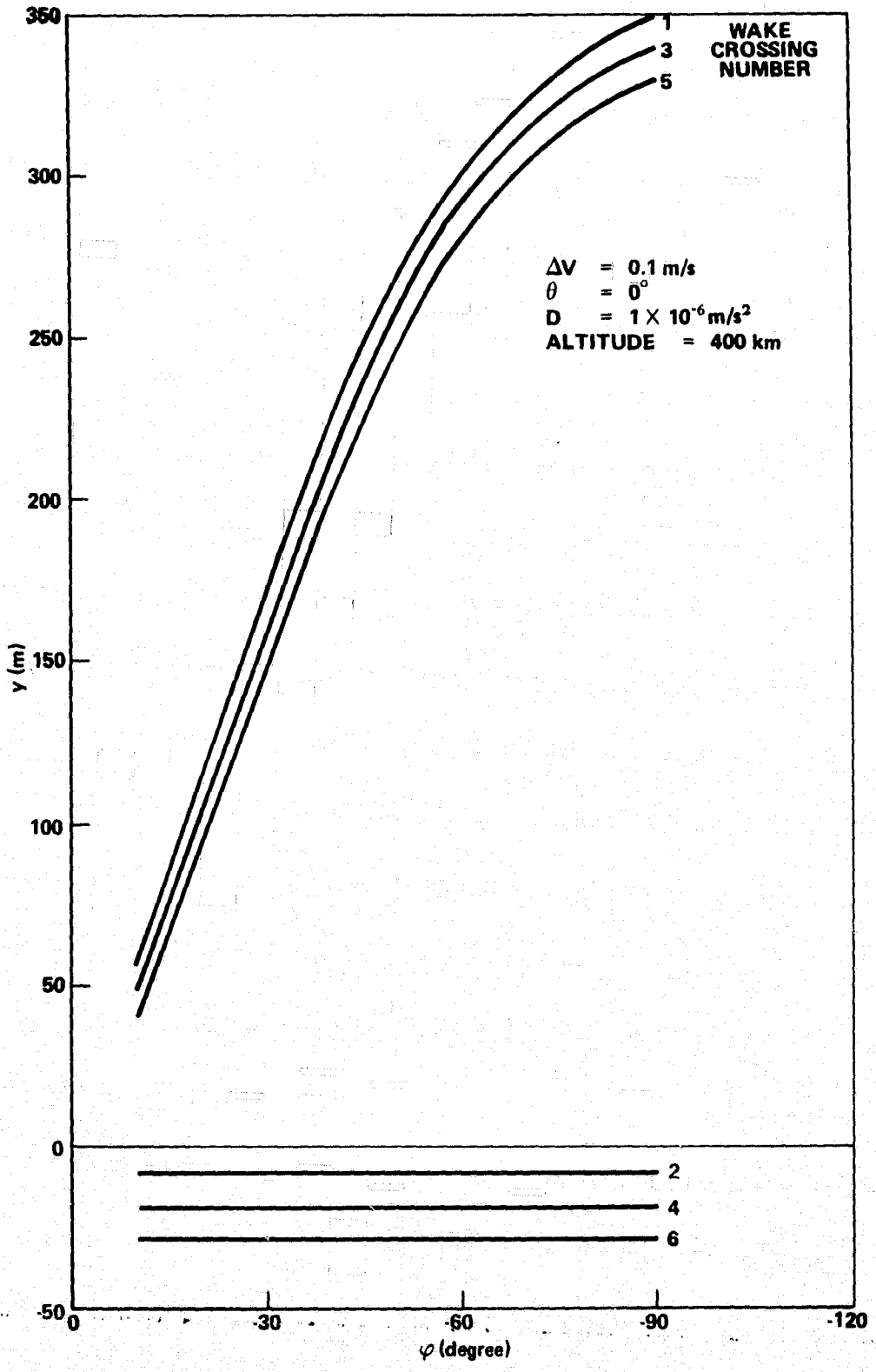

Figure 75. Altitude of the first six wake crossings behind the Shuttle versus the ejection angle φ.

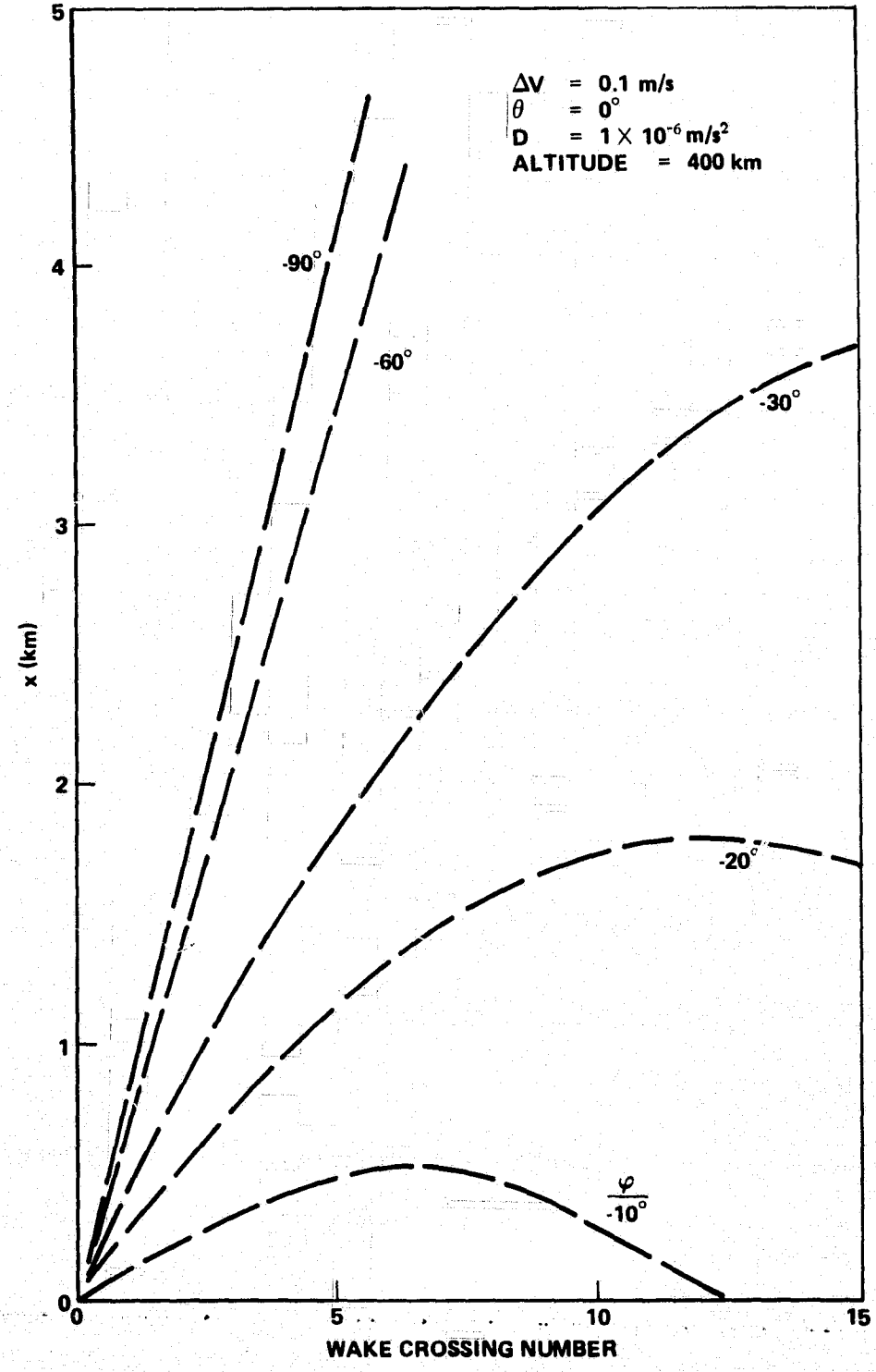

Figure 76. Distances of the wake crossings behind the Shuttle versus the wake crossing number.

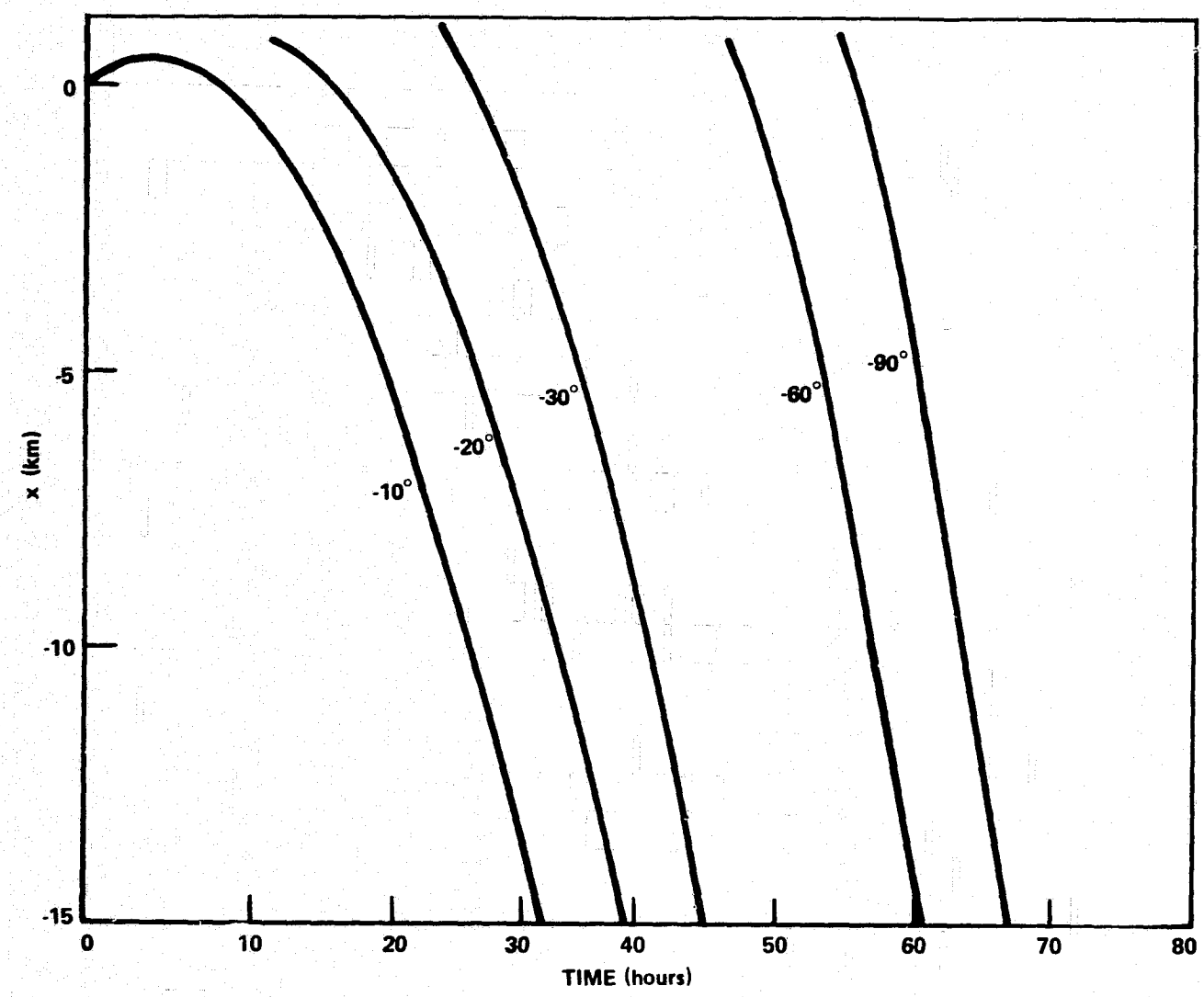

Figure 77. Distance of the TAD in front of the Shuttle versus time with the ejection angle φ parameterized.

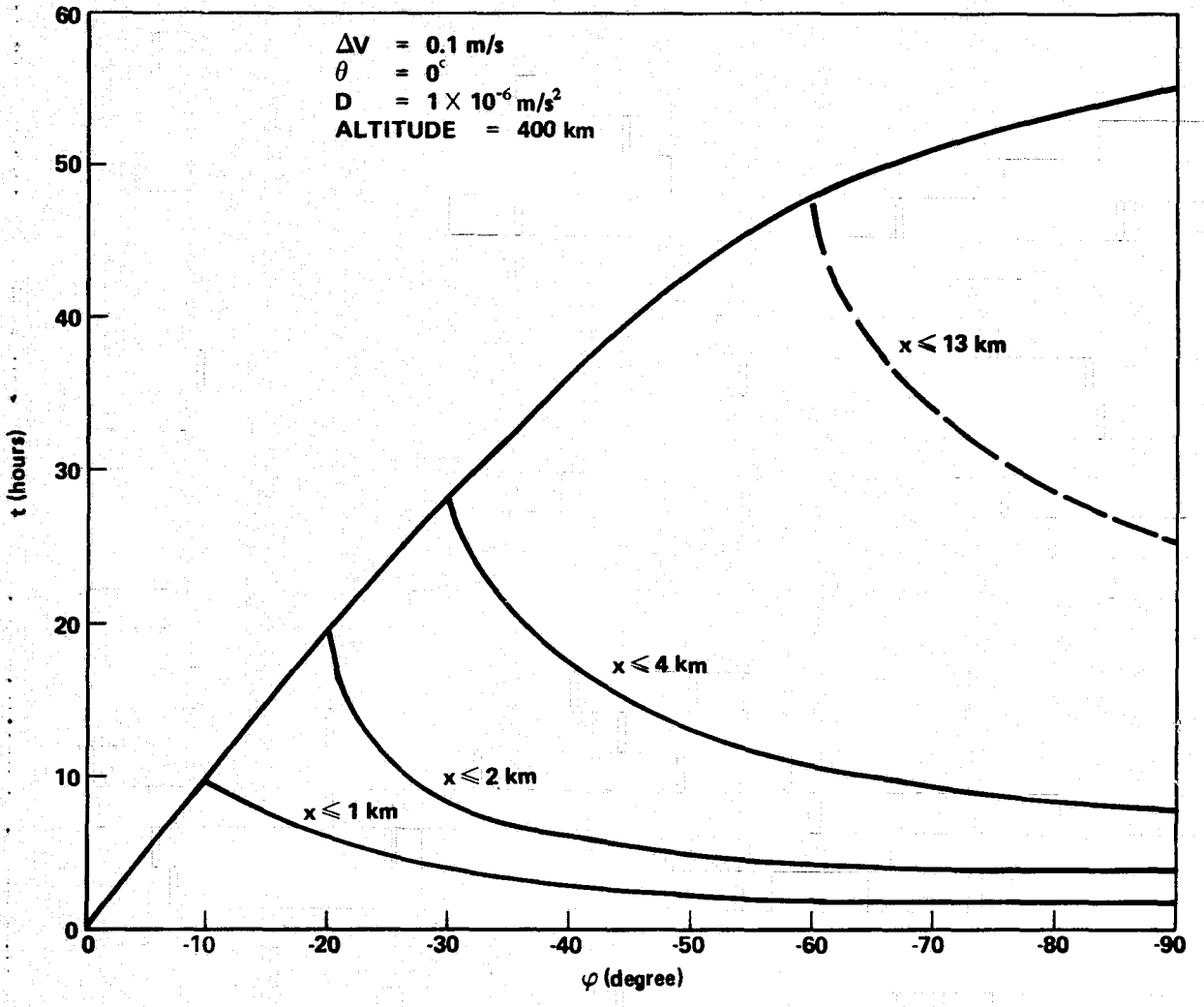

Figure 78. Time of TAD behind the Shuttle within a given distance versus the ejection angle φ.

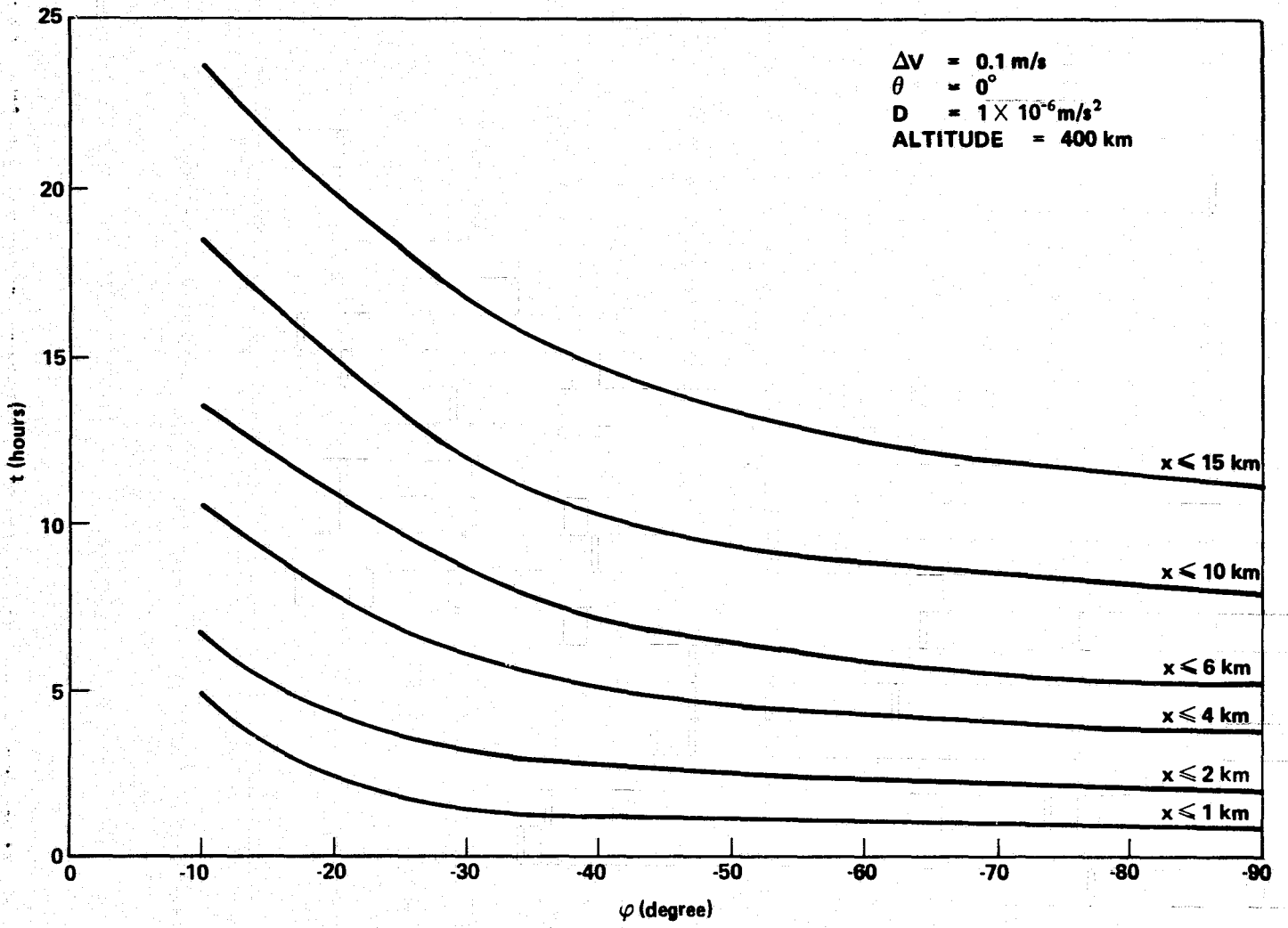

Figure 79. Time of TAD in front of the Shuttle within a given distance versus the ejection angle φ.

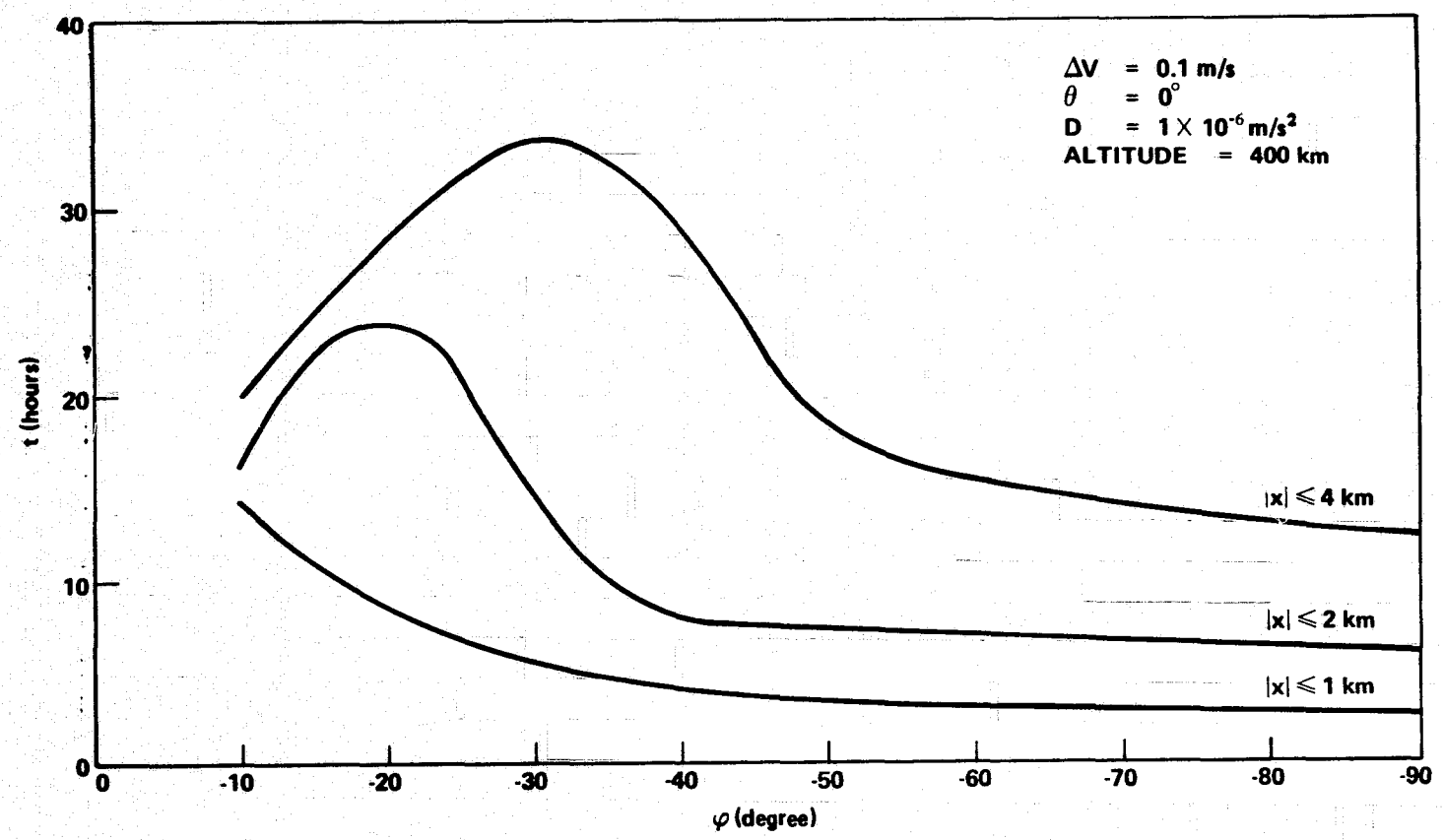

Figure 80. Time of TAD within plus or minus a given distance of the Shuttle versus the ejection angle φ.

REFERENCES

1. Clohessy, W. H.; and Wiltshire, R. S.: Terminal Guidance System for Satellite Rendezvous. J. Aerospace Science, vol. 27, 1960, pp. 653-658.

2. Fowles, G. R.: Analytical Mechanics. Holt, Rinehart and Winston, New York, 1962, p. 102.

3. Gantmacher, F. R.: The Theory of Matrices. Vol. I, Chelsea Publishing Company, New York, 1959, p. 120.

APPROVAL

THE MOTION OF THROW AWAY DETECTORS RELATIVE TO THE SPACE SHUTTLE

By Larry D. Mullins

The information in this report has been reviewed for security classification. Review of any information concerning Department of Defense or Atomic Energy Commission programs has been made by the MSFC Security Classification Officer. This report, in its entirety, has been determined to be unclassified.

This document has also been reviewed and approved for technical accuracy.

R. H. BENSON
Chief, Orbital Mechanics Branch

J. P. LINDBERG
Chief, Mission Analysis Division

H. E. THOMASON
Director, Systems Analysis and Integration Laboratory

☆ U.S. GOVERNMENT PRINTING OFFICE 1975—641-255/14 REGION NO. 4